| | |
|---|---|
| Title | Distribution of glycerol dialkyl glycerol tetraethers in Lake Biwa basin and the reconstruction of lake water pH during the last 300,000 years |
| Author(s) | 味岡, 拓 |
| Citation | 北海道大学. 博士(環境科学) 乙第6934号 |
| Issue Date | 2014-09-25 |
| DOI | 10.14943/doctoral.r6934 |
| Doc URL | http://hdl.handle.net/2115/57145 |
| Type | theses (doctoral) |
| File Information | Taku_Ajioka.pdf |

博士論文

# Distribution of glycerol dialkyl glycerol tetraethers in Lake Biwa basin and the reconstruction of lake water pH during the last 300,000 years

# 琵琶湖集水域系における GDGT の分布と過去 30 万年間の湖水 pH の復元


Division of Earth System Science, Graduate School of Environmental Science, Hokkaido University

北海道大学大学院環境科学院地球圏科学専攻

Taku Ajioka

味岡　拓


August 2014

## Abstract

We investigated glycerol dialkyl glycerol tetraether (GDGT) distributions in soils and river/lake sediments in the Lake Biwa basin of central Japan, in order to understand their source and fate in a terrestrial environment. GDGTs analyzed in 16 soil profiles exhibited significant depth variation at each site. Branched GDGTs were generally most abundant in the surface litter layer (O layer) and decreased with depth, while the maximum concentration of crenarcheol appeared in the upper soil layer (A layer), above the maximum concentration of the other isoprenoid GDGTs. This finding is consistent with different microbial communities contribution to these GDGT pools the subsurface soil sequences. The relationship between methylation index of branched tetraethers/cyclization ratio of branched tetraethers (MBT′/CBT) and pH/MAAT in Lake Biwa basin soils was consistent with those of a previous report for global soils. The GDGT distributions in surface sediments from the lake differed from those of soils and river sediments in the watershed, suggesting that the GDGTs were produced in the lake water rather than supplied from the land. The CBT for lake sediments from different water depths corresponded to water pH values. We thus infer that the CBT for lake sediments may serve as proxy for lake water pH and can be applied to paleoenvironmental reconstruction.

Based on these results, we generated a 280,000-year record of water pH and temperature in Lake Biwa, central Japan, by analysing the methylation index (MBT′) and cyclisation ratio (CBT) of branched tetraethers in sediments from piston and borehole cores to understand the responses of precipitation and air temperature in central Japan to the East Asian monsoon variability on the orbital timescale. Because

water pH in Lake Biwa is determined by phosphorus and alkali cation inputs driven by precipitation and temperature, the record of water pH should indicate changes in precipitation and temperature in central Japan. Comparison with pollen assemblage in a Lake Biwa core suggests that lake water pH was determined by summer temperature in low eccentricity period before 55 ka, while it was determined by summer precipitation in high eccentricity period after 55 ka. From 130 to 55 ka, variation in lake pH (summer precipitation) was lagged behind that in summer temperature by several thousand years. This perspective is consistent with the conclusions of previous studies (Igarashi and Oba, 2006; Yamamoto, 2009) that the temperature variation preceded the precipitation variation in central Japan.

## Acknowledgements

Firstly I would like to thank Associate Professor Dr. Masanobu Yamamoto, who always encouraged and supported my campus and private life. I learned interests and profundities of geology, earth science, paleoclimatology and organic geochemistry.

I would also like to thank Professor Dr. Atsuko Sugimoto, Associate Professor Dr. Tomohisa Irino, Associate Professor Dr. Youhei Yamashita and Associate Professor Dr. Osamu Seki for helpful advices and discussions, and all of the laboratory members for grateful campus life. And I thank Tatsufumi Okino and Keiko Ohnishi (Hokkaido University) for analytical assistance and Ryoma Hayashi (Lake Biwa Museum) for providing valuable information. Additionally, I would also like to thank all of the members of Lake Biwa drilling project, Keiji Takemura (Kyoto University), Akira Hayashida (Doshisha University), Hiroyuki Kitagawa (Nagoya University), and Jun Murase (Nagoya University) for providing samples and helpful discussion. The study was carried out under a Grant-in-Aid for Scientific Research (A) of JSPS no. 19204051 (to M.Y.).

**Contents**

# Chapter 1

# Introduction

## 1.1. Long-term variation in past East Asian monsoon

The East Asian monsoon governs the climate of East Asia (Wang et al., 2003), and East Asian monsoon variability on orbital timescales has been the topic of many studies, which have revealed that it has responded to precession; however, the timing of monsoon variability continues to be debated. Kutzbach (1981) hypothesised that the Asian monsoon responds to insolation changes at low latitudes, which are regulated by precession. According to this hypothesis, the summer monsoon is maximal when Northern Hemisphere summer insolation is maximal in the precession cycle. Indeed, oxygen isotope records from cave stalagmites in China have demonstrated that summer monsoon variability was pronounced at the precession cycle and maximal at July–August precession (e.g., Wang et al., 2001, 2008; Yuan et al., 2004; Dykoski et al., 2005). However, some proxy records are not consistent with this hypothesis. Clemens and Prell (2003) reported that Indian summer monsoon variability showed both precession and obliquity cycles and was maximal at the November perihelion on the precession band. The pollen record in the north-western Pacific off of central Japan shows that the East Asian monsoon has been strongest at the October–November perihelion in precession cycles (Heusser and Morley, 1985; Igarashi and Oba, 2006). Thus, the conclusions have varied according to the proxy record used.

## 1.2. Proxies used for paleoclimate reconstruction in Lake Biwa sediments

Lake sediments provide a good, widely available palaeoclimate archive. Proxies applicable to lake sediments include pollen and diatom fossils, δD of long-chain *n*-alkanes, lignin, biogenic opal, and pigments, among others. In Lake Biwa, sediment cores have been investigated using pollen fossils (Miyoshi et al., 1999; Nakagawa et al., 2008), lignin (Ishiwatari and Uzaki, 1987; Ishiwatari et al., 2009; Ohira et al., 2013), diatom frustules (Kuwae et al., 2004), biogenic opal (Xiao et al., 1997), pigments (Ishiwatari et al., 2009), and δD of long-chain *n*-alkanes (Seki et al., 2012). Although paleoclimate information is available from these proxy records, more records generated by other new proxies are necessary to better understand the response of the East Asian monsoon to orbital forcing.

### 1.3. GDGTs and its applicability for paleoclimatology

Glycerol dialkyl glycerol tetraethers (GDGTs) in natural environments include isoprenoid and branched GDGTs (Appendix 1; Nishihara and Koga, 1987; Sinninghe Damsté et al., 2000). Isoprenoid GDGTs derive from Archaea (De Rosa and Gambacorta, 1988), while the biological sources of branched GDGTs include *Acidobacteria* (Sinninghe Damsté et al., 2000, 2011; Weijers et al., 2006a). These compounds in sediments are used for paleoenvironmental reconstruction in marine and terrestrial realms (Schouten et al., 2002; Weijers et al., 2007a).

Isoprenoid GDGTs have been found in marine sediments (e.g. Schouten et al., 2000), marine suspended particles (e.g. Schouten et al., 2001), marine settling particles (e.g. Wuchter et al., 2006), lake sediments (e.g. Powers et al., 2004) and soils (e.g. Weijers et al., 2006b). Crenarchaeol, an isoprenoid GDGT with one cyclohexane and 4 cyclopentane rings, is thought to derive from Group 1 Crenarchaeota, a phylum of

Archaea (Sinninghe Damsté et al., 2002). The Group 1 Crenarchaeota was subsequently reclassified into a new phylum, Thaumarchaeota (Brochier-Armanet et al., 2008; Spang et al., 2010). Schouten et al. (2002) proposed a paleotemperature proxy, $TEX_{86}$ (tetraether index of tetraethers consisting of 86 carbons), based on the empirical relationship between the relative abundance of isoprenoid GDGTs in seafloor sediments and sea surface temperature. $TEX_{86}$ has also been applied to lake sediments (Powers et al., 2004, 2010). The relative abundance of isoprenoid GDGTs is controlled not only by temperature but also by a contribution from anaerobic methane oxidizing Archaea. Zhang et al. (2011) proposed the methane index (MI) as an indicator of the overprint of the isoprenoid GDGT pool by lipid contributed by archaea mediating the anaerobic oxidation of methane. In soils, *amoA* (encoding a subunit of the key enzyme ammonia monooxygenase) gene abundance of Thaumarchaeota is correlated with crenarchaeol concentration (Leininger et al., 2006), suggesting that ammonia-oxidizing archaea play an important role in contributing the archaeal lipids in soils. The presence of isoprenoid GDGT in soils was reported (Weijers et al., 2006b), but little is known about the detailed distribution of isoprenoid GDGTs in terrestrial environments.

Branched GDGTs were first identified in peat (Sinninghe Damsté et al., 2000) and subsequently found in soil (Weijers et al., 2007a), and marine (Hopmans et al., 2004) and lake sediments (e.g. Sinninghe Damsté et al., 2009; Tierney and Russell, 2009). The stereochemistry of the glycerol moieties of branched GDGTs suggests that they derive from Bacteria rather than Archaea (Weijers et al., 2006a). Their carbon isotope signature suggests a heterotrophic origin (Pancost and Sinninghe Damsté, 2003). Branched GDGT I was recently detected in an *Acidobacterium* (Sinninghe Damsté et al., 2011). Hopmans et al. (2004) found branched GDGTs in marine sediments and proposed the

BIT (branched and isoprenoid tetraether) index as an indicator of the contribution of soil organic matter (OM) to marine environments, because soils contain abundant branched GDGTs. Weijers et al. (2007a) reported that the relative abundance of branched GDGTs in soils reflects soil pH and mean annual air temperature (MAAT). The cyclization ratio of br tetraethers (CBT) correlated with soil pH and the methylation index of br tetraethers (MBT) correlated with both soil pH and MAAT. Based on these empirical relationships, Weijers et al. (2007b) proposed the MBT/CBT paleotemperature index, which they applied to marine sediments from the Congo River fan and obtained reasonable results (Weijers et al., 2007b). Recently, Peterse et al. (2012) improved the relationship among branched GDGT distribution, soil pH and MAAT with additional dataset, and suggested MBT′ instead of MBT. Niemann et al. (2012) applied MBT/CBT index to sediment core in a high Alpine lake in southern Switzerland where GDGTs in catchment soils contribute to, and reasonably reconstructed MAAT. However, the MAAT estimated from the application of MBT/CBT to a marine core from offshore from Norway was much higher than the true value. The higher estimate was interpreted to reflect summer temperature (Rueda et al., 2009). Sinninghe Damsté et al. (2008) also found that the MBT/CBT index afforded higher MAAT for soils from Mt. Kilimanjaro and attributed it to local bias. Tierney and Russell (2009) found that the branched GDGTs in lake sediments differed from those in soils, and suggested in situ production of branched GDGTs in lake water as the cause. The same phenomenon has been reported for a New Zealand lake (Zink et al., 2010), a Scottish lake (Tyler et al., 2010) and a Tibetan salt lake (Wang et al., 2012). Tierney et al. (2010) noted that the correlation between MBT/CBT from sediments and MAAT for 46 lakes in East Africa differed from that of the global soil set. The branched GDGTs in suspended particulate matter from 23 American lakes exhibited a similar regression equation to that for East African lakes (Schoon et al., 2013). These studies demonstrated that the MBT/CBT is useful for paleotemperature estimates for lake sediments, but it is not clear whether or not the branched GDGTs produced in lake water respond to pH and temperature differently from those in soils.

### 1.4. Aims of this study

I have investigated the branched and isoprenoid GDGTs in soils and river and lake sediments from the Lake Biwa basin to clarify (i) spatial and depth variation in branched and isoprenoid GDGTs in soils, (ii) the source of GDGTs in river and lake sediments and (iii) the response of MBT and CBT to pH and temperature in lake environments. Based on these results, we examined branched GDGTs in sediments from borehole BIW08-B and piston core BIW07-6 in Lake Biwa, central Japan, to reconstruct lake water pH and temperature during the last 280,000 years. We then evaluated the variability of the East Asian summer and winter monsoons based on estimated summer precipitation and winter lake water temperature.

## Chapter 2

## Materials and methods

### 2.1. Environmental setting of Lake Biwa basin

Lake Biwa is located at an altitude of 84 m in central Japan and is surrounded by mountains ca. 1,000 m high. It is the largest lake in Japan, with an area of 674 $km^2$ and a watershed area of 3,850 $km^2$ (Fig. 1). More than 118 rivers flow into it and the Seta River discharges from it. The climate of the area is affected by the East Asian monsoon (Yoshino, 1965, 1978); summer monsoon brings warm and humid conditions, whereas the winter monsoon brings snowfall in the northern part of the area and dryness in the southern part.

The MAAT is 14.7 °C at Hikone Meteorological Observatory (87.3 m) and 6.3 °C at Mount Ibuki Weather Station (1,375.8 m), respectively (Japan Meteorological Agency, available at http://www.jma.go.jp/jma/index.html). Water temperature and pH data were obtained from the Lake Biwa Environmental Research Institute (http://www.pref.shiga.lg.jp/biwako/koai/hakusyo/index.html).

### 2.2. Samples

#### 2.2.1. Soils

Soil samples (0–30 cm, 5 cm interval) were collected in August/September 2009 at a total of 25 sites between 86 and 1,149 m above sea level; 5 sites were from Mt. Ibuki, 12 the Ane River drainage area and 8 from the Oku-Biwako area (Table 1 and Fig. 1). Soil samples were kept at 0 °C during sampling and freeze-dried in the laboratory.

The MAAT at each sampling site was calculated from its altitude via a lapse rate model developed from the relationship between MAAT and the altitude at the nearby observation sites (4 sites). The average root mean square error of this lapse rate model is 0.22 °C.

### 2.2.2. River sediments

Four river sediment samples were taken from two sites in the Ane River with a shovel in August/September 2009 (Fig. 1). Site 1 was the sandbank in the river, and samples 1-1 and 1-2 were composed mainly of coarse and fine sand, respectively (Table 2). At site 2, sediments were sampled from a stagnant backwater in the river. Samples 2-1 and 2-2 comprised black fine sand and homogeneous black silt, respectively.

### 2.2.3. Lake Biwa surface sediments

Lake surface sediments were retrieved with a gravity corer and an Ekman-Birge sampler from June–October 1997 (Murase and Sakamoto, 2000; Table 3). Seven surface sediments were taken from the offshore transect Echi River estuary at intervals of ca. 2–3 km. One additional sample was from the Ane River estuary (Fig. 1). Along the Echi River estuary transect, sediments at sites 671 and 716 were medium sand and silt, respectively, and all other sediments were clay (Table 3). Water temperature and pH were obtained from the Lake Biwa Environmental Research Institute (http://www.pref.shiga.lg.jp/biwako/koai/hakusyo/index.html).

### 2.2.4. Cores BIW07-6 and BIW08-B

Piston core BIW07-6 (18.42 m long) was taken from the central part of Lake Biwa (35°13′59.02″N, 136°02′51.89″E; water depth of 55 m) in 2007 (Fig. 1; Takemura et al., 2010). The sediments in the core consisted of homogenous dark-grey silty clay (Fig. 2). The age–depth model for core BIW07-6 was generated from six well-dated widespread ash layers and 13 accelerator mass spectrometry (AMS) $^{14}C$ age of plant wood fossils analyzed at three AMS facilities during the past decade; the Center for Chronological Research at Nagoya University (Laboratory code; NUTA2, Nakamura et al., 2000, 2004), the W.M. Keck Carbon Cycle Accelerator Mass Spectrometry Laboratory (UCIAMS, Southon et al., 2004a, b) and the Korean Institute of Geoscience and Mineral Resources (KIGAM, Hong et al., 2010) (Table 4,). The $^{14}C$ ages were converted to calendar ages using the IntCal13 dataset (Reimer et al., 2013).The average sedimentation rate was found to be 0.4 m/ky (Fig. 3). The sediment was stored at 4°C for 0.5 years. Then, 137 samples (1-cm thick) were collected from 0.30 m (0.6 ka) to 18.29 m (46 ka) and immediately freeze-dried. The average sampling interval was ~0.3 ky.

Borehole core BIW08-B (100.3-m long) was collected from its site (35°13′41.15″N, 136°03′21.19″E; water depth of 53) in 2008 (Fig. 1). The sediments consisted of dark-grey massive silty clay from 0 to 89 m, sandy silt containing abundant sand and plant debris from 89 to 99 m, and dark-grey massive silty clay from 99 to 100.3 m (Fig. 2; Takemura et al., 2010). The age–depth model for core BIW08-B was generated from 17 dated widespread ash layers, two AMS $^{14}C$ age of plant wood fossils analyzed at the Korean Institute of Geoscience and Mineral Resources (KIGAM, Hong et al., 2010) (Table 5), and nine dated Anhysteretic Remanet Magnetization (ARM) events. The $^{14}C$ age were converted to calendar ages using the IntCal13 dataset (Reimer et al., 2013). The ARM events were correlated with those detected in core BIW07-6 (Hayashida et al., 2007). The average sedimentation rate was found to be 0.3 m/ky (Fig. 3). The sediment was stored at 4°C for 0.5 years. Then, 152 samples (2.5-cm thick) were collected from 13 m (43 ka) to 88 m (280 ka), and the samples were immediately freeze-dried. The average sampling interval was ~1.9 ky.

2.3. Analytical methods

2.3.1. pH measurement

Soil and river sediment samples were freeze-dried and sieved at 2 mm. The pH values of the soils and river sediments were measured in a soil/water mixture of 1/2.5 (w/w) with a pH meter (pH BOY-P2, Shindengen Electronic MFG. CO., LTD, Japan).

*2.3.2. Lipid extraction and separation*

Lipids were extracted (3×) from a freeze-dried sample using a DIONEX ASE-200 at 100 °C and 1000 psi for 10 min with 11 ml $CH_2Cl_2/CH_3OH$ (6:4 v/v) and concentrated. The extract was separated into four fractions using column chromatography ($SiO_2$ with 5% distilled water; column of 5.5 mm inner diameter and 45 mm length): F1 (hydrocarbons) with 3 ml *n*-hexane; F2 (aromatic hydrocarbons) with 3 ml hexane/toluene (3:1 v/v); F3 (ketones) with 4 ml toluene; F4 (polar compounds) with 3 ml toluene/$CH_3OH$ (3:1 v/v).

2.3.3. GDGT analysis

An aliquot of F4 was dissolved in hexane/propan-2-ol (99:1 v/v) and filtered. The GDGTs were analyzed using high performance liquid chromatography-mass spectrometry (HPLC-MS) with a Shimadzu SIL-20AD system connected to a Bruker Daltonics micrOTOF-HS time-of-flight mass spectrometer. A Prevail Cyano column

(2.1 × 150 mm, 3 μm; Alltech) at 30 °C was used, following the methods set out by Hopmans et al. (2000) and Schouten et al. (2007). The conditions were: flow rate 0.2 ml/min, isocratic with 99% hexane and 1% propan-2-ol (5 min) followed by a linear gradient to 1.8% propan-2-ol over 45 min. Detection was achieved using atmospheric pressure chemical ionization (APCI) MS in positive ion mode. The spectrometer was run in full scan mode (*m/z* 500–1,500). Compounds were assigned from comparison of mass spectra and retention times with GDGT standards (from the main phospholipids of *Thermoplasma acidophilum* via acid hydrolysis) and values from a previous study (Hopmans et al., 2000). Quantification was achieved by integrating the summed peak areas in the $(M+H)^+$ and $(M+H+1)^+$ chromatograms and comparing them with the peak area from an internal standard $C_{46}$ glycerol trialkyl glycerol tetraether (GTGT; Patwardhan and Thompson, 1999) in the $(M+H)^+$ ion chromatogram, according to the method set out by Huguet et al. (2006). The correction value for the ionization efficiency between GDGTs and the internal standard was obtained by comparing the peak areas from *T. acidophilum*-derived mixed GDGTs with that from $C_{46}$ GTGT. The standard deviation of a replicate analysis was 3.0% of the concentration for each compound.

*2.3.4. Calculations of GDGT proxies*

$TEX_{86}$ was calculated from the concentrations of GDGT-1, GDGT-2 and GDGT-3, plus a regioisomer of crenarchaeol using the following equation (Eq. 1; Schouten et al., 2002):

$TEX_{86}$ = ([GDGT-2] + [GDGT-3] + [crenarchaeol regioisomer])/([GDGT-1] +

$$[GDGT\text{-}2] + [GDGT\text{-}3] + [crenarchaeol\ regioisomer]) \quad \text{(Eq. 1)}$$

Temperature values were calculated according to the following equations based on core top calibrations of global marine sediments (Eq. 2; Kim et al., 2010) and lake sediments (Eq. 3; Powers et al., 2010):

$$T = 81.5 \times TEX_{86} - 26.6 \quad \text{(Eq. 2)}$$

$$T = 55.2 \times TEX_{86} - 14.0 \quad \text{(Eq. 3)}$$

where T = temperature (°C). The analytical accuracy was 0.45 °C in our laboratory. The BIT index (Eq. 4) was calculated as per Hopmans et al. (2004):

$$BIT = ([GDGT\ I] + [GDGT\ II] + [GDGT\ III])/([GDGT\ I] + [GDGT\ II] + [GDGT\ III] + [crenarchaeol]) \quad \text{(Eq. 4)}$$

The methane index (MI; Eq. 5) was calculated as per Zhang et al. (2011):

$$MI = ([GDGT\text{-}1] + [GDGT\text{-}2] + [GDGT\text{-}3])/([GDGT\text{-}1] + [GDGT\text{-}2] + [GDGT\text{-}3] + [crenarchaeol] + [crenarchaeol\ regioisomer]) \quad \text{(Eq. 5)}$$

CBT (Eq. 6) and MBT′ (Eq. 7) were calculated as per Weijers et al. (2007a) and Peterse et al. (2012):

$$CBT = -\log([GDGT\ Ib] + [GDGT\ IIb])/([GDGT\ I] + [GDGT\ II]) \quad \text{(Eq. 6)}$$

$$MBT' = ([GDGT\ I] + [GDGT\ Ib] + [GDGT\ Ic])/([GDGT\ I] + [GDGT\ Ib] + [GDGT\ Ic] + [GDGT\ II] + [GDGT\ IIb] + [GDGT\ IIc] + [GDGT\ III]) \quad \text{(Eq. 7)}$$

The pH (Eq. 8) and MAAT (Eq. 9) were calculated according to the following based on a global soil dataset (Peterse et al., 2012):

$$pH = 7.90 – 1.97 \times CBT \quad \text{(Eq. 8)}$$

$$MAAT = 0.81 – 5.67 \times CBT + 31.0 + MBT' \quad \text{(Eq. 9)}$$

The pH and MAAT were also calculated according to the following equations based on an African lake sediment dataset (Tierney et al., 2010; Eqs. 10 and 11):

$$pH = 10.32 – 3.03 \times CBT \quad \text{(Eq. 10)}$$

$$MAAT = 11.84 – 9.32 \times CBT + 32.54 \times MBT' \quad \text{(Eq. 11)}$$

The analytical accuracy of CBT and MBT′ was 0.015 and 0.006, respectively, in this study.

## Chapter 3

## Branched and isoprenoid glycerol dialkyl glycerol tetraethers in soils and lake/river sediments in Lake Biwa basin and implications for MBT/CBT proxies

Source of GDGTs in river and lake sediments were determined by comparing the distribution of GDGTs in soils, river and lake sediments to clarify spatial and depth variation in branched and isoprenoid GDGT.

### 3.1. Results

#### 3.1.1. Soils

##### 3.1.1.1. Soil type

A typical soil sequence (Table 1) from the surface to subsurface included an O layer in the top with litter, an A layer, consisting of dark brown soil (brown forest soil), and a B layer, consisting of light brownish mineral soil (brown forest soil). The O layer (max. thickness 5 cm) developed in the forest sites where old trees (mainly cedar) were present, whereas it was absent from the forest sites where young trees were present. The boundary between the A and B layers was clear, and the depth of the boundary varied from 5–30 cm (Table 1).

##### 3.1.1.2. Soil pH

The pH ranged from 3.3–8.0 in the surface soils (0–5 cm) (Fig. 4a). The pH in the O layer was variable, with a minimum in the A layer and increasing toward the B layer (Fig. 5a).

3.1.1.3. GDGTs in surface soils

The concentration of total isoprenoid GDGTs and total branched GDGTs ranged from 0.0088–4.3 and from 0.76–40 μg/g, respectively (Fig. 4b and 4c). The branched GDGTs contributed 69.1–99.7% to the total GDGTs.

The distribution of isoprenoid GDGTs revealed that the average relative abundances of GDGT-0, GDGT-1 to -3 and crenarchaeol in soils were 24, 28 and 45%, respectively. $TEX_{86}$ varied from 0.18–0.89 (Fig. 4d), which corresponds to temperatures from –12 to 46 °C based on the marine core-top calibration of Kim et al. (2010). MI ranged from 0.20–0.87 (Fig. 4e). Among the branched GDGTs, GDGT I was most abundant (avg. 63%), followed by GDGT II (23%), GDGT Ib (5%), GDGT III (4%) and GDGT IIb (3%). BIT ranged from 0.75–1.00 and exceeded 0.9 at most sites (Fig. 4f). CBT ranged from 0.28–2.77 (Fig. 4g) and MBT′ from 0.19–0.89 (Fig. 4h).

3.1.1.4. Depth variation of GDGTs

The depth profiles of the GDGT concentrations varied by site (Fig. 6). A typical sequence appeared at site 6 (Fig. 5a and 5b); here, the branched GDGTs were most abundant in the surface O layer and decreased with depth. Isoprenoid GDGTs increased with depth and decreased after the maximum. The maximum concentration of crenarchaeol (5–10 cm) occurred at shallower depth (Fig. 7a) than the maximum concentration of other isoprenoid GDGTs (15–20 cm). This typical profile was partially displayed at the other sites. The upper half was observed at sites 5, 7, 10 and 15, the lower half at sites 3, 9, 12, 18, 19 and 20, and the middle part at sites 4, 11, 22, 25 and 26 (Fig. 6).

The values of $TEX_{86}$ ranged from 0.1–0.8 (Fig. 5b). It was highly variable in the top layer (0–5 cm) but converged to values between 0.6 (22 °C) and 0.8 (39 °C) below this depth (Fig. 5b). MI values ranged from 0.20–1.00 and increased with depth (Fig. 5c). The BIT index ranged from 0.79–1.00 (Fig. 5d); it was > 0.9 for most samples and did not change significantly with depth. At site 12, exceptionally, it increased with depth. CBT values decreased with depth (Fig. 5e), the reverse of the increase in soil pH (Fig. 5a and 5e). Maximum MBT′ values were observed around the O/A boundary and decreased below this depth (Fig. 5f).

3.1.2. River sediments

The measured pH of Ane River sediments ranged from 5.8–7.2, higher than the values for the surface soils (Fig. 4a). in the same catchment area (3.6−6.6).

The concentration of isoprenoid GDGTs ranged from 0.015–0.91 μg/g (Fig. 4b). The total concentration was higher in finer sediments than in coarse sediments (Fig. 4b). The average relative abundance of crenarchaeol, GDGT-0, GDGT-1 and GDGT-2 was 43%, 31%, 10% and 10%, respectively. $TEX_{86}$ values ranged from 0.47–0.57 (Fig. 4d), corresponding to a temperature range of 16–21 °C based on the marine core top calibration of Kim et al. (2010). MI values ranged from 0.32–0.42 (Fig. 4e).

The concentration of branched GDGTs ranged from 0.052–6.8 μg/g and the values were higher in fine sediments than in coarse sediments (Fig. 4c). The average relative abundances of GDGT I, GDGT II, and GDGT III were 33%, 37% and 17%, respectively. BIT values ranged from 0.86–0.94 and were higher for finer sediments (Fig. 4f), as were CBT values (0.50–1.19; Fig. 4g); these values were within the range for the surface soil values in the same catchment (Fig. 4g). MBT′ values ranged from 0.38–0.40 (Fig. 4h) and were lower than those in the soils in the same catchment (0.61−0.87).

### 3.1.3. Lake sediments

The total concentration of isoprenoid GDGTs ranged from 0.064–2.2 μg/g and was higher in finer sediments (Fig. 8a). Among isoprenoid GDGTs, GDGT-0 was the most abundant (38–74%) and increased toward the coast (Fig. 8c). Crenarchaeol was the second most abundant (18–52%) and increased toward offshore sites. $TEX_{86}$ values ranged from 0.32–0.52 and corresponded to a temperature ranges of 0–16 °C and 6–16 °C based on marine (Kim et al., 2010) and lake core-top (Powers et al., 2010) calibrations, respectively (Fig. 8e). MI values ranged from 0.13–0.44 and were higher for shallower sites (Fig. 8f). The total concentration of branched GDGTs ranged from 0.30–4.4 μg/g and was higher in finer sediments (Fig. 8b). The relative abundance of GDGT I, GDGT II, and GDGT III was 14–37%, 27–34% and 13–34%, respectively, followed by GDGT IIb (ca. 12%) and GDGT Ib (7%). The others were < 5% (Fig. 8d). BIT values ranged from 0.79–0.95 and were lower in deeper sites (Fig. 8g). CBT values ranged from 0.28–0.71 and were lower in finer sediments (Fig. 8h). MBT′ values ranged from 0.23–0.45 and were higher in coarser sediments (Fig. 8i).

## 3.2. Discussion

### 3.2.1. Depth variation of GDGTs in soils

The maximum concentration of branched GDGTs appeared in the O layer and decreased with depth (Fig. 6). Active decomposition of OM occurred in litter layer, because heterotrophs obtain energy from the decomposition of plant remains. The producers of branched GDGTs are heterotrophs (Pancost and Sinninghe Damsté, 2003), and they produce more branched GDGTs in the O layer. The relative abundance of branched GDGTs changed with depth. Compounds Ib and IIb increased with depth and other compounds with one or two pentane rings also increased (as seen at site 6 in Fig. 7b). This finding suggests that branched GDGTs in deeper soils were not a remnant of those produced in surface layers, but were produced in situ in the subsurface soil.

In contrast to branched GDGTs, the crenarchaeol concentration was highest in the upper part of the A layer and the concentration of other isoprenoid GDGTs was maximal around the lower part of the A layer or the upper part of the B layer (Fig. 6). Crenarchaeol is assumed to be specific to Thaumarchaeota (Sinninghe Damsté et al., 2002; Schouten et al., 2013). Microbial studies have shown that members of group 1 Crenarchaeota (Thaumarchaeota) are the dominant archaeal taxon in soils (Bates et al., 2011) and can be found at deeper soil depths (Hansel et al., 2008; Hartmann et al., 2009), and the ratio of Archaea: Bacteria increases with soil depth (Kemnitz et al., 2007). Thaumarchaeota include autotrophic nitrifiers that obtain energy via ammonia oxidation (Könneke et al., 2005; Park et al., 2010; Jung et al., 2011; Kim et al., 2012) and possibly heterotrophs (Biddle et al., 2006; Lloyd et al., 2013). We did not measure the ammonia concentration in brown forest soils, but it is generally high around the O/A boundary (Ohta and Kumada, 1978). Abundant ammonia would support the production of Thaumarchaeota in the upper A layer. Other isoprenoid GDGTs, i.e. GDGT-0 to -3 are not only produced by Thaumarchaeota but also by some Euryarchaeota. In particular, anaerobic methane-oxidizing Archaea, ANME-1, produce GDGT-0 to GDGT-3 (e.g. Pancost et al., 2001; Wakeham et al., 2003; Blumenberg et al., 2004; Liu et al., 2011; Schouten et al., 2013). The increase in GDGT-0 to -3 around the A/B boundary suggests a contribution from Euryarchaeota. The function of the Euryarchaeota in subsurface soils is unclear. Further microbial studies are needed to clarify the behavior of

Euryarchaeota in subsurface soil sequences.

3.2.2. Relationship between MBT′/CBT and soil pH/MAAT

CBT values decreased with depth, corresponding to an increase in soil pH (Figs. 5a and 5e). A negative correlation was observed between CBT and soil pH. This tendency has been reported by Weijers et al. (2007a). CBT in 0–5 cm surface soils had the following relationship with soil pH (Eq. 12):

$$\mathrm{CBT} = -\,0.4805 \times \mathrm{pH} + 3.7979 \ (r^2\ 0.69,\ \mathrm{n} = 25) \qquad \text{(Eq. 12)}$$

CBT in all samples had the following relationship:

$$\mathrm{CBT} = -\,0.4748 \times \mathrm{pH} + 3.5828 \ (r^2\ 0.51,\ \mathrm{n} = 81) \qquad \text{(Eq. 13)}$$

These relationships between CBT and soil pH are consistent with those of the global soil sample set published by Peterse et al. (2012).

Maximum MBT′ values appeared in the O and A layers (Fig. 5f). No significant relationship was observed between MBT′ and MAAT, because the range of MAAT (6.5 °C) in our sample set was not large enough to evaluate the correlation with MBT′. Instead, we found a significant correlation between MBT′ and soil pH ($r^2$ 0.72, n = 81). The relationship between MBT’/CBT and MAAT is expressed as:

$$\mathrm{MBT}' = -\,0.133 \times \mathrm{pH} + 0.0154 \times \mathrm{MAAT} + 1.19 \ (r^2\ 0.77,\ \mathrm{n} = 25) \qquad \text{(Eq. 14)}$$

This equation may be converted to:

$$\text{MBT}' = 0.2186 \times \text{CBT} + 0.0379 \times \text{MAAT} - 0.0487 \; (r^2\ 0.68, \text{n} = 25) \qquad \text{(Eq. 15)}$$

This regression equation is similar to that published by Peterse et al. (2012). The depth variation in MBT′/CBT-based temperature increased with depth by a maximum of 6.5 °C (Fig. 5g). Recently, Huguet et al. (2013) reported that tree roots and their surfaces contain branched GDGTs that had different MBT/CBT values from those of the surrounding soils. Because we sieved the soil samples to remove roots, it is less likely that the GDGTs in roots affected changes in MBT′/CBT in our samples. The downward increase in MBT′/CBT-based temperature is thus likely to reflect the addition of newly produced branched GDGTs in subsurface soils. Generally, pH increases and free oxygen decreases with depth in soil sequences. This change in microenvironment results in a microbial community gradient, producing branched GDGTs with different composition. As a result, MBT′ and CBT are altered in the burial process and the estimated pH and MAAT values are biased.

3.2.3. Sources of GDGTs in river and Lake Biwa surface sediments

On the ternary plot for branched GDGTs, crenarchaeol, and GDGT-0, most soils contain more branched GDGTs than river and lake sediments, although some soils have a similar composition to river and lake sediments (Fig. 9a). In contrast, the ternary diagram for crenarchaeol, GDGT-0 and GDGT-1 to -3 distinguishes soils and river sediments from lake sediments (Fig. 9b). Soils and river sediments are richer in

GDGT-1 to -3 than lake sediments (Fig. 9b). The preferential degradation or fractionation of GDGTs during transportation cannot be excluded for the interpretation of this phenomenon, but we suggest that difference in the source organisms are more likely to explain it. The GDGT composition of soils and river sediments suggests two distinct archaeal sources: Euryarchaeota with GDGT-0 and GDGT-1 to -3, but no crenarchaeol (Source E1 in Fig. 9b), and Thaumarchaeota with abundant crenarchaeol (Source T in Fig. 9b). The GDGT composition of lake sediments adds one more archaeal source: lacustrine Euryarchaeota with abundant GDGT-0 (Source E2 in Fig. 9b). Shallower lake sediments are richer in GDGT-0, suggesting that the contribution from source E2 is more important than in shallower sediments.

The CBT- MBT′ plot indicates that most soils have higher MBT′ than river and lake sediments (Fig. 10). The soils from the Mt. Ibuki area are exceptional and have a similar composition to lake and river sediments (Fig. 10). The limestone area of Mt. Ibuki is so small that the GDGTs produced in the area would not contribute significantly to the lake sediments. Thus, the difference in branched GDGTs between soils and the surface sediments from Lake Biwa suggests that most of the branched GDGTs in the lake sediments were not derived from soils, but were produced within the lake. However, the relatively higher MBT′ values in coastal sediments suggest that they might be affected by a contribution from soil GDGTs to some extent. It is still not clear whether branched GDGTs were produced in the lake water or surface sediments. Further studies on the intact GDGTs are necessary to understand the production of branched GDGTs in Lake Biwa.

#### 3.2.4. MBT′/CBT index for lake sediments

Lake Biwa is a monomictic lake, its water stratifies from spring to autumn and mixes in winter, which is controlled by air temperature. The modern measured temperature of surface water in Lake Biwa has an annual average of 16.7°C and is lowest (~7.5°C) in winter and highest in (~27.9°C) in summer, whereas the temperature of bottom water at a depth of 80 m ranges from 7.0 to 7.7°C with an annual average of ~7.3°C (Fig. 9b; off Imadzu: 35°23.68′N, 136°07.95′E; data from the Lake Biwa Environmental Research Institute, http://www.pref.shiga.lg.jp/biwako/koai/hakusyo/index.html). The measured pH value in the surface water of Lake Biwa has an annual average of 8.1 and is lowest (~7.6) in winter and highest (~8.9) in summer, whereas the pH of the bottom water at a depth of 80 m ranges from 7.2 to 7.7 with an average value of ~7.4 (Fig. 11a; off Imadzu: 35°23.68′N, 136°07.95′E; data from the Lake Biwa Environmental Research Institute, http://www.pref.shiga.lg.jp/biwako/koai/hakusyo/index.html).

In Lake Biwa, its water pH depends on the geology of the drainage basin, evaporation, the photosynthesis of phytoplankton and submerged plants, the respiration of organisms, and the decomposition of OM by microbes (Wetzel, 2001). In volcanic regions, lake water receives strong mineral acids, particularly sulphuric acid, which decreases pH to less than 4 (Wetzel, 2001). There is, however, no active volcano in the Lake Biwa watershed. Thus, this factor is not important for pH of Lake Biwa water. In contrast, $Ca^{2+}$ supplied from limestone increases lake water pH (Wetzel, 2001). In the Lake Biwa drainage basin, limestone is exposed only in the Mt. Ibuki area, and its contribution toward controlling lake water pH should be minor. Evaporation of lake water increases water pH (Wetzel, 2001), but pollen records in Lake Biwa cores suggest moist environments throughout the last 430 ky (Miyoshi et al., 1999), so evaporation has not been a factor controlling lake water pH. Consumption of $CO_2$ by the photosynthesis of phytoplankton and submerged plants increases lake water pH (e.g., Talling, 1976). On the other hand, regeneration of $CO_2$ by the respiration of organisms and degradation of OM by microbes decreases lake water pH (Wetzel, 2001). Actually, a tripling of the concentration of chlorophyll from winter to spring in Lake Biwa increases lake water pH by 0.85 (data from the Lake Biwa Environmental Research Institute, http://www.pref.shiga.lg.jp/biwako/koai/hakusyo/index.html). These observations suggest that photosynthesis in the lake water is the major factor controlling water pH in Lake Biwa.

Temperature and pH were calculated by applying the MBT′/CBT index to Lake Biwa surface sediments using Biwa (this study; Eqs. 12 and 14) and global soil (Peterse et al., 2012) and lake (Tierney et al., 2010) calibrations. The estimated pH values in clay sediments were 7.2, 7.3 and 9.3 according to Biwa soil, global soil calibrations and global lake calibrations, respectively (Fig. 11a). The estimated temperature in clay sediments were 5.6 °C, 6.3 °C and 16.2 °C according to Biwa soil, global soil calibrations and global lake calibrations, respectively (Fig. 11b). The pH and temperature estimated using Lake Biwa and global soil calibrations were closer to the measured winter pH and temperature, whereas those estimated using the global lake calibration were very different from the measured pH and temperature. Furthermore, the reconstructed water pH and temperature estimated using soil calibrations have gradients with water depth and correspond to those of bottom water (Fig. 11). Together, these findings suggest that the MBT′/CBT index in Lake Biwa sediments reflect water pH and temperature, and soil calibration is applicable to their reconstruction.

### 3.3. Conclusions

The GDGTs in soils showed depth variations in branched and isoprenoid GDGT concentrations with depth. Branched GDGTs were abundant in the top layer and decreased with depth, while the maximum concentration of isoprenoid GDGTs occurred in subsurface soil. These findings suggest that different microbial communities developed in the subsurface soil sequence.

The relationship between MBT′/CBT and pH/MAAT in Lake Biwa basin soils was consistent with those for global soils (Peterse et al., 2012). The MBT′/CBT values in Lake Biwa sediments differed from those in soils from its watershed, suggesting that the branched GDGTs in the lake sediments did not originate from soil GDGTs but were produced in the lake environment. The CBT and MBT′ values in surface sediments in the lake corresponded to lake water pH and temperature. The MBT′/CBT index may thus be useful for the estimation of paleo-pH and paleotemperature in Lake Biwa.

## Chapter 4

## Water pH and temperature in Lake Biwa from MBT′/CBT indices during the last 280,000 years

Based on the results of Chapter 3, paleo-pH and paleotemperature of the lake water were estimated by analyzing GDGTs in the cores BIW07-6 and BIW08-B (Fig. 1).

### 4.1. Results

The concentrations of isoprenoid and branched GDGTs varied between 0.01 and 2.55 and between 0.05 and 12.58 μg/g, respectively (Fig. 12). CBT-based pH ranged from 6.0 to 7.6 (Fig. 12). The measured pH value in the surface water of Lake Biwa has an annual average of 8.1 and is lowest (~7.6) in winter and highest (~8.8) in summer, whereas the pH of the bottom water at a depth of 59 m ranges from 7.2 to 7.7 with an average value of ~7.5 (off Minami-Hira: 35°11′39″N, 135°59′39″E; data from the Lake Biwa Environmental Research Institute, http://www.pref.shiga.lg.jp/biwako/koai/hakusyo/index.html). On the other hand, the measured pH of surface soils in the drainage basin ranged from 3.3 to 8.0 with an average of 5.0 (Fig. 4a), which are lower than those in lake water. The CBT-based pH values of the core sediments are lower than those in the present lake water. CBT-based pH was maximal at 279, 249, 210, 160, 133, 117, 78, 45, 25 and 6 ka and minimal at 264, 220, 178, 149, 123, 95, 52, 29 and 17 ka. MBT′/CBT-based temperature ranged from 4 to 11°C and was lower during glacials and higher during interglacials (Fig. 12). The modern measured temperature of surface water in Lake Biwa has an annual average of 16.9°C and is lowest (~7.6°C) in winter and highest in (~27.9°C) in summer, whereas the temperature of bottom water at a depth of 59 m ranges from 7.2 to 8.2°C with an annual average of ~7.7°C (off Minami-Hira; data from the Lake Biwa Environmental Research Institute, http://www.pref.shiga.lg.jp/biwako/koai/hakusyo/index.html).

The BIT index ranged from 0.83 to 0.99 (Fig. 12). BIT values exceeded 0.95 in most intervals, but BIT values lower than 0.9 were found at 0–6, 29, 30, 114, 210 and 240 ka (Fig. 12).

## 4.2. Discussion

### 4.2.1. Factor controlling water pH in Lake Biwa

Described in section 3.2.4., photosynthesis in the lake water is the major factor controlling water pH. In Lake Biwa, photosynthesis is mainly controlled by phosphorus concentration in the water (Ishida et al., 1982; Tezuka, 1985). The anthropogenic eutrophication of Lake Biwa induced high primary production, resulting in the increase of the pH of the lake water by more than 1 from 1960s to 1970s (Nakayama, 1981). Phosphorus concentration in the lake is determined by the inflow of phosphorus from the catchment soils, which is govern by precipitation in the watershed (Kunimatsu, 1993). At the present day, the East Asian summer monsoon brings most of annual precipitation to the study area, exceptionally at high elevations in the northern part where snowfall brought by the East Asian winter monsoon is relatively important (http://www.jma.go.jp/jma/index.html). Therefore, summer precipitation in the watershed is a factor that controls photosynthesis and consequently the water pH of the lake. Phosphorus concentration may also be governed by air temperature because the dissolution of silicate depends on temperature in chemical weathering process (White and Blum, 1995). Thus, both higher precipitation and higher temperature potentially increase the inflow of phosphorus to the lake, enhancing primary production, and thus increases the lake water pH. Increases in precipitation and temperature intensify chemical weathering. The chemical weathering increases the inflows of Ca+ and phosphorus to the lake, both increasing lake water pH.

It is not clear whether branched GDGTs are produced in the water column or the sediment surface in Lake Biwa (this study; Ajioka et al., 2014). If branched GDGTs are produced in the water column, the main production depth of branched GDGTs is also unclear. Very recently, Buckles et al. (2014) found high abundance of intact branched GDGTs in the suspended particulates in the oxygen deficient bottom water in Lake Challa and suggested that oxygen deficient environment ($O_2$ <2 mg/L) is a favorable condition for branched GDGT production. In Lake Biwa, such a condition ($O_2$ <2 mg/L) exists the bottom water above sediment surface from autumn to early winter (http://www.pref.shiga.lg.jp/biwako/koai/hakusyo/index.html). It is thus likely that branched GDGTs were produced mainly in the bottom water in Lake Biwa. This is just a speculation by analogy with the case of Lake Calla. Evidence is necessary to test this speculation from the original data of suspended and sinking particles in Lake Biwa,

#### 4.2.2. Changes in lake water pH during the last 280 ky

CBT-based pH during the last 280 ky showed a glacial-interglacial pattern with higher pH in interglacial periods (Fig. 12). Variation pattern in CBT-based pH was consistent with that of *Cryptomeria* pollen abundance and lagged behind that of the Tp value in cores BIW95-4 and Takashima-oki BT in Lake Biwa from 130 ka to 55 ka (Fig. 13; Hayashi et al., 2010a, b). Igarashi and Oba (2006) assumed that the abundance of *Cryptomeria* pollen as a proxy of summer precipitation because the natural distribution of *Cryptomeria* corresponds to the area of precipitation higher than 2000 mm per year. The correspondence between CBT-based pH and *Cryptomeria* pollen abundance indicates that both proxy records are robust records of precipitation.

The pollen temperature index, $T_p$ (= 100 x $T_w$/[$T_c$ + $T_w$], where $T_w$ is the sum of temperate taxa and $T_c$ is the sum of subalpine taxa) is used as a proxy of summer air temperature (Igarashi and Oba, 2006). Igarashi and Oba (2006) reported that variation in the Tp value preceded the abundance of *Cryptomeria* pollen in core MD01-2421 off central Japan in the western North Pacific, indicating that the variation of summer air temperature preceded that of summer precipitation by several thousand years. Yamamoto (2009) interpreted that this time lag was caused the latitudinal shift of the Baiu Front (early summer rain front). Our new record indicates that CBT-based pH was lagged behind the Tp record, implying that summer precipitation was lagged behind summer air temperature, as was already pointed by pollen studies (Igarashi and Oba, 2006; Hayashi et al., 2010a, b).

On the other hands, variation pattern in CBT-based pH was not consistent with that of *Cryptomeria* pollen abundance but with Tp value in core BIW95-4/BT from 55 ka to the present (Fig. 13; Hayashi et al., 2010a, b). This correspondence suggests that the lake water pH was determined by summer temperature rather than summer precipitation in this period. Nakagawa et al. (2008) suggested that the response of the East Asian monsoon to summer insolation was different between low and high eccentricity periods, and that the response was not clear in the low eccentricity (< 0.024) periods. The eccentricity was lower in the period from 55 ka to the present than the period from 130 to 55 ka. We speculate that higher amplitude variation in summer insolation in the latter period induced higher amplitude precipitation variation, which resulted in a condition that precipitation controlled lake water pH. In contrast, lower amplitude variation in the former period induced lower amplitude precipitation variation. Instead, the other climatic forcings such as greenhouse gas forcing were relatively important, and temperature variation was a major factor controlling the variation in lake water pH.

The age uncertainity (2σ values [95% confidence level]) of core BIW08B ranges from 5 to 11 ky in MIS 5 and 6 because of large error of radiogenic ages of tephras (Table 5). However, the pollen composition (Tp and *Cyptomeria* abundance) in core Lake BIW95-4/BT nearby the study site have a consistent variation with that in a marine core MD01-2421 from the offshore of central Japan in the western North Pacific. The age-depth model of core MD01-2421 was established by oxygen isotope stratigraphy using benthic foraminifera isotopes (Oba et al., 2006). Assumed synchronous vegetation change in central Japan, the correspondence of pollen assemblages between MD01-2421 and Lake Biwa cores assures that the uncertainty of the age-depth models of Lake Biwa cores in MIS 5 and 6 is smaller than that indicated by the dating error of each tephras, and the ages of sediments are precise enough to discuss variation on orbital timescales.

With caution of this limitation of age-depth model, comparison with Chinese stalagmite records reveals regional perspective on the East Asian summer monsoon variability. In the period from 55 ka to the present, the variation in CBT-based pH was synchronous with that of $\delta^{18}O$ in stalagmites in China (Fig. 13). This correspondence suggests that summer temperature in central Japan varied synchronously with the $\delta^{18}O$ of the precipitated water in China.

On the other hands, in the period from 143 to 55 ka, the variation in CBT-based pH was lagged behind that of the $\delta^{18}O$ in stalagmites in China by several thousand years

(Fig. 13; Wang et al., 2001, 2008). The mismatch between Japanese precipitation and Chinese stalagmite $\delta^{18}O$ records was already pointed out by Yamamoto (2009) and Clemens et al. (2010). There are two possible interpretations of this phenomenon. First, precipitation in Japan and China during early summer is principally determined by the position of the Baiu Front (an early summer rain front) that develops at the atmospheric boundary between warm moist air masses flowing from the south and cold air masses from the north (Yoshino, 1965). The latitudinal shift of the Baiu Front in response to orbital forcing may have resulted in the difference of response of precipitation between central Japan and China (Yamamoto, 2009). Second, synchronous variations in stalagmite $\delta^{18}O$ from Hulu Cave (Wang et al., 2001) and Sanbao Cave (Wang et al., 2008) in central China, and from Dongge Cave (Yuan et al., 2004) in southern China, suggest that stalagmite $\delta^{18}O$ is not a simple index of local precipitation (Yamamoto, 2009). The negative shift of stalagmite $\delta^{18}O$ from Chinese caves is also synchronous with the rapid rise of air temperature in central Japan at glacial terminations, suggesting that the negative shift of stalagmite $\delta^{18}O$ was partly related to temperature increase in air masses derived from the summer monsoon because heavy rains, which occur more frequently in warmer air mass, induce isotopically lighter water (Yamamoto, 2009). Clemens et al. (2010) showed a different idea that winter precipitation contributed to stalagmite $\delta^{18}O$. This question is still open. Our new result confirms the mismatch between the precipitation records in central Japan and Chinese stalagmite $\delta^{18}O$ records. This is an interesting topic in the Asian monsoon study.

In this study, we assume that the branched GDGTs produced in the lake contributed to sedimentary branched GDGTs in the study site. However, the spike of high CBT (low estimated pH) at 13 ka is exceptionally affected by the contribution of soil GDGTs (Fig.

12). Ohira et al. (2013) reported a spike of abundant lignin at the same layer in core BIW08-B. Because high CBT and low CBT-based pH (3.3 to 8.0 with an average of 5.0; Fig. 4a) in the soils, the high CBT (low estimated pH) at 13 ka associated with high lignin abundance likely reflected the soil GDGT contribution.

#### 4.2.3. Changes in MBT′/CBT -based winter lake water temperature during the last 280 ky

MBT′/CBT-based winter temperature showed a glacial-interglacial pattern (Fig. 12). The variation is consistent with the summer air temperature estimated from the pollen assemblage in Lake Biwa (Nakagawa et al., 2008). However, the MBT′/CBT-based temperatures (3 to 10°C) are more realistic than the pollen-based temperatures (–10 to 5°C; Nakagawa et al., 2008). The winter water temperature in Lake Biwa is controlled by winter cooling (data from the Lake Biwa Environmental Research Institute, http://www.pref.shiga.lg.jp/biwako/koai/hakusyo/index.html, Japan Meteorological Agency; available at http://www.jma.go.jp/jma/index.html) and reflects the intensity of the Asian winter monsoon. The rise of MBT-CBT’ based winter lake water temperature were lagged behind the rise of Tp-based summer air temperature by ~10 ky in Lake Biwa cores (Fig. 13). This suggests warmer summer and colder winter in MIS 5e, and the seasonal temperature variation was larger in this period.

#### 4.2.4. Changes in microbial ecosystem of Lake Biwa during the last 280 ky

BIT index was higher than 0.8 throughout the core (Fig. 12). Because most branched GDGTs are produced in the lake (this study; Ajioka et al., 2014), this high BIT implies that high bacterial production in Lake Biwa. The BIT record indicates negative spikes (< 0.9) at 6–0 ka, 114, 210, and 240 ka, which correspond to the maximal peak of crenarchaeol concentration (Fig. 12). Because crenarchaeol is specific to Thaumarchaeota (Sinninghe Damsté et al., 2002), the production of Thaumarchaota was enhanced in those periods. Although the reason why Thanumarchaotal production was enhanced in the specific periods is not clear, changes in nutrient condition is a likely candidate to cause such an ecological change.

### 4.3. Conclusions

We analysed the MBT′/CBT indices in sediment cores retrieved from Lake Biwa to reconstruct changes in summer precipitation and temperature and winter temperature in central Japan during the last 280 ky. Comparison with pollen assemblage in a Lake Biwa core suggests that lake water pH was determined by summer temperature in low eccentricity period, while it was determined by summer precipitation in high eccentricity period. From 130 to 55 ka, variation in lake pH (summer precipitation) was delayed behind that in summer temperature by several thousand years. Thaumarchaeotal production was enhanced in specific periods in interglacials.

## Chapter 5

## Summary

In this study, branched GDGTs in sediments from borehole BIW08-B and piston core BIW07-6 in Lake Biwa, central Japan, was investigated to reconstruct lake water pH and temperature during the last 280,000 years.

The GDGTs in soils showed depth variations in branched and isoprenoid GDGT concentrations with depth. Branched GDGTs were abundant in the top layer and decreased with depth, while the maximum concentration of isoprenoid GDGTs occurred in subsurface soil. These findings suggest that different microbial communities developed in the subsurface soil sequence.

The relationship between MBT′/CBT and pH/MAAT in Lake Biwa basin soils was consistent with those for global soils (Peterse et al., 2012). The MBT′/CBT values in Lake Biwa sediments differed from those in soils from its watershed, suggesting that the branched GDGTs in the lake sediments did not originate from soil GDGTs but were produced in the lake environment. The CBT and MBT′ values in surface sediments in the lake corresponded to lake water pH and temperature. The MBT′/CBT index may thus be useful for the estimation of paleo-pH and paleotemperature in Lake Biwa.

MBT′/CBT indices were applied to sediment cores retrieved from Lake Biwa to in order to reconstruct changes in summer precipitation and temperature and winter temperature in central Japan during the last 280 ky. Comparison with pollen assemblage in a Lake Biwa core suggests that lake water pH was determined by summer temperature in low eccentricity period, while it was determined by summer precipitation in high eccentricity period. From 130 to 55 ka, variation in lake pH (summer precipitation) was delayed behind summer temperature by several thousand years. Thaumarchaeotal production was enhanced in specific periods in interglacials.

Although CBT has been used for estimating soil pH, this study revealed that the CBT in lake sediments reflects the pH of lake water. Using the CBT as a proxy of lake water pH, changes in lake water pH during the last 280,000 years was successfully reconstructed. The soil pH may have responded summer precipitation and temperature , both are sensitive to summer monsoon variability.

## References

Ajioka, T., Yamamoto, M., and Murase, J., 2014. Branched and isoprenoid glycerol dialkyl glycerol tetraethers in soils and lake/river sediments in Lake Biwa basin and implications for MBT/CBT proxies. Organic Geochemistry 73, 70–82.

Bates, S.T., Berg-Lyons, D., Caporaso, J.G., Walters, W.A., Knight, R., Fierer, N., 2011. Examining the global distribution of dominant archaeal populations in soil. ISME Journal 5, 908–917.

Biddle, J.F., Lipp, J.S., Lever, M.A., Lloyd, K.G., Sorensen, K.B., Anderson, R., Fredricks, H.F., Elvert, M., Kelly, T.J., Schrag, D.P., Sogin, M.L., Brenchley, J.E., Teske, A., House, C.H., Hinrichs, K.U., 2006. Heterotrophic Archaea dominate sedimentary subsurface ecosystems off Peru. Proceedings of the National Academy of Sciences USA 103, 3846–3851.

Blumenberg, M., Seifert, R., Reitner, J., Pape, T., Michaelis, W., 2004. Membrane lipid patterns typify distinct anaerobic methanotrophic consortia. Proceedings of the National Academy of Sciences USA 101, 11111–11116.

Brochier-Armanet, C., Boussau, B., Gribaldo, S., Forterre, P., 2008. Mesophilic Crenarchaeota: proposal for a third archaeal phylum, the Thaumarchaeota. Nature Reviews in Microbiology 6, 245–252.

Buckles, L.K., Weijers, J.W.H., Verschuren, D., Sinninghe Damsté, J.S., 2014. Sources of core and intact branched tetraether membrane lipids in the lacustrine environment: Anatomy of Lake Challa and its catchment, equatorial East Africa. Geochimca et Cosmochimica Acta 140, 106–126.

Clemens, S.C., Prell, W.L., 2003. A 350,000 year summer-monsoon multi-proxy stack from the Own Ridge, Northern Arabian Sea. Marine Geology 201, 35–51.

Clemens, S.C., Prell, W.L., Sun, Y., 2010. Orbital-scale timing and mechanisms driving Late Pleistocene Indo-Asian summer monsoons: Reinterpreting cave speleothem $\delta^{18}O$. Paleoceanography 25, 1–19.

De Rosa, M., Gambacorta, A., 1988. The lipids of archaeabacteria. Progress in Lipid Research 27, 153–175.

Dykoski, C.A., Edwards, R.L., Cheng, H., Yuan, D., Cai, Y., Zhang, M., Lin, Y., Qing, J., An, Z., Revenaugh, J., 2005. A high-resolution, absolute-dated Holocene and deglacial Asian monsoon record from Dongge Cave, China. Earth and Planetary Science Letters 233, 71–86.

Fukuoka, T., Matsui, S., 2002. Stratigraphy of pyroclastic deposits post-dating the AT tephra, Sanbe Volcano. Earth Science (Chikyu Kagaku) 56, 105–122 (in Japanese).

Hansel, C.M., Fendorf, S., Jardine, P.M., Francis, C.A., 2008. Changes in bacterial and archaeal community structure and functional diversity along a geochemically variable soil profile. Applied and Environmental Microbiology 74, 1620–1633.

Hartmann, M., Lee, S., Hallam, S.J., Mohn, W.W., 2009. Bacterial, archaeal and eukaryal community structures throughout soil horizons of harvested and naturally disturbed forest stands. Environmental Microbiology 11, 3045–3062.

Hayashi, R., Takahara, H., Hayashida, A., Takemura, K., 2010a. Millennial-scale vegetation changes during the last 40,000 yr based on a pollen record from Lake Biwa, Japan. Quaternary Research 74, 91–99.

Hayashi, R., Takahara, H., Yoshikawa, S., Inouchi, Y., 2010b. Orbital-scale vegetation variability during MIS6, 5, 4, and 3 based on a pollen record from the Takashima-oki core in Lake Biwa, western Japan. Japanese Journal of Palynology

56, 5–12.

Hayashida, A., Ali, M., Kuniko., Kitagawa H., Torii, M., Takemura, K., 2007. Environmental magnetic record and paleosecular variation data for the last 40 kyrs from the Lake Biwa sediments, central Japan. Earth Planets Space 59, 807–814.

Heusser, L.E., Morley, J.J., 1985. Pollen and radiolarian records from deep-sea core RC14-103: climatic reconstructions of northeast Japan and northwest Pacific for the last 90,000 years. Quaternary Research 24, 60–72.

Hong, W., Park, J.H., Sung, K.S., Woo, H.J., Kim, J.K., Choi, H.W., Kim, G.D., 2010. A new 1 MV AMS facility at KIGAM. Radiocarbon 52, 243–251.

Hopmans, E.C., Schouten, S., Pancost, R., van der Meer, M.T.J., Sinninghe Damsté, J.S., 2000. Analysis of intact tetraether lipids in archaeal cell material and sediments by high performance liquid chromatography/atmospheric pressure chemical ionization mass spectrometry. Rapid Communications in Mass Spectrometry 14, 585–589.

Hopmans, E.C., Weijers, J.W.H., Schefuß, E., Herfort, L., Sinninghe Damsté, J.S., Schouten, S., 2004. A novel proxy for terrestrial organic matter in sediments based on branched and isoprenoid tetraether lipids. Earth and Planetary Science Letters 24, 107–116.

Huguet, C., Hopmans, E.C., Febo-Ayala, W., Thompson, D.H., Sinninghe Damsté, J.S., Schouten, S., 2006. An improved method to determine the absolute abundance of glycerol dibiphytanyl glycerol tetraether lipids. Organic Geochemistry 37, 1036–1041.

Huguet, A., Gocke, M., Derenne, S., Fosse, C., Wiesenberg, G.L.B., 2013. Root-associated branched tetraether sourcemicroorganismsmay reduce estimated paleotemperatures in subsoil. Chemical Geology 356, 1–10.

Igarashi, Y., Oba, T., 2006. Fluctuations of monsoons and insolation in the northwest Pacific during the last 144 kyr from a high resolution pollen analysis of the IMAGES core MD01-2421. Quaternary Science Reviews 25, 1447–1459.

Ishida, Y., Kimura, B., Nakahara, H., adota, H., 1982. Analysis of major nutrient effecting *Uroglena americana* bloom in the northern Lake Biwa, by use of algal bioassay. Bulletin of the Japanese Society of Scientific Fisheries, 48(9), 1281–1287.

Ishiwatari, R., Uzaki, M., 1987. Diagenetic changes of lignin compounds in a more than 0.6 million-year-old lacustrine sediment (Lake Biwa, Japan). Geochimica et. Cosmochimica Acta 51, 321–328.

Ishiwatari, R., Negishi, K., Yoshikawa, H., Yamamoto, S., 2009. Glacial-interglacial productivity and environmental changes in Lake Biwa, Japan: a sediment core study of organic carbon, chlorins and biomarkers. Organic Geochemistry 40, 520–530.

Isomi, H., 1956. Geology of the Ominagahama District. Geological Survey of Japan, Tsukuba, 57pp. (in Japanese).

Jung, M.Y., Park, S.J., Min, D., Kim, J.S., Rijpstra, W.I.C., Sinninghe Damsté, J.S., Kim, G.J., Madsen, E.L., Rhee, S.K., 2011. Enrichment and characterization of an autotrophic ammonia-oxidizing archaeon of mesophilic crenarchaeal group I.1a 54 S. from an agricultural soil. Applied and Environmental Microbiology 77, 8635–8647.

Kemnitz, D., Kolb, S., Conrad, R., 2007. High abundance of Crenarchaeota in a temperate acidic forest soil. Fems Microbiology Ecology 60, 442–448.

Kim, J.-H., van der Meer, J., Schouten, S., Helmke, P., Willmott, V., Sangiorgi, F., Koc, N., Hopmans, E.C., Sinninghe Damste, J.S., 2010. New indices and calibrations derived from the distribution of crenarchaeal isoprenoid tetraether lipids: implications for past sea surface temperature reconstructions. Geochimica et Cosmochimica Acta 74, 4639–4654.

Kim, J.G., Jung, M.Y., Park, S.J., Rijpstra, W.I.C., Sinninghe Damsté, J.S., Madsen, E.L., Min, D., Kim, J.S., Kim, G.J., Rhee, S.K., 2012. Cultivation of an ammoniaoxidizing archaeon of thaumarchaeotal group I.1b from an agricultural soil. Environmental Microbiology 14, 1528–1543.

Kitagawa, H., van der Plicht, J., 1998. Atmospheric radiocarbon calibration to 45,000 yr B.P.: Late Glacial fluctuations and cosmogenic isotope production. Science 279, 1187–1190.

Kitagawa, H., Lim, J., Takemura, K., Hayashida, A., Haraguchi, T., 2010. Radiocarbon content of lignin-enriched fraction in core sediment from Lake Biwa, central Japan. Nuclear Instruments and Methods in Physics Research B 268, 1077–1079.

Könneke, M., de la Torre, A.E., Walker, J.R., Waterbury, J.B., Stahl, D.A., 2005. Isolation of an autotrophic ammonia-oxidizing marine archaeon. Nature 437, 543–546.

Kunimatsu, T., 1993. Part D. The mass inflow from the catchment area to the lake. 1) Characteristics of contamination load in the catchment area. In the 10th anniversary symposium of Lake Biwa Research Institute-Results and future issues of Lake Biwa study. 192–204 (in Japanese).

Kutzbach, J., 1981. Monsoon climate of the Early Holocene: Climate experiment with the Earth’s orbital parameters for 9000 years ago. Science 214, 59–61.

Kuwae, M., Yoshikawa, S., Tsugeki, N., Inouchi, Y., 2004. Reconstruction of a climate record for the past 140 kyr based on diatom valve flux data from Lake Biwa, Japan.

Journal of Paleolimnology 32, 19–39.

Kurimoto, C., Naito, K., Sugiyama, Y., Nakae, S., 1999. Geology of the Tsuruga District. Geological Survey of Japan, Tsukuba, 73pp. (in Japanese).

Leininger, S., Urich, T., Schloter, M., Schwark, L., Qi, J., Nicol, G.W., Prosser, J.I., Schuster, S.C., Schleper, C., 2006. Archaea predominate among ammoniaoxidizing prokaryotes in soils. Nature 442, 806–809.

Liu, X.L., Lipp, J.S., Hinrichs, K.-U., 2011. Distribution of intact and core GDGTs inmarine sediments. Organic Geochemistry 42, 368–375.

Lloyd, K.G., Schreiber, L., Petersen, D.G., Kjeldsen, K.U., Lever, M.A., Steen, A.D., Stepanauskas, R., Richter, M., Kleindienst, S., Lenk, S., Schramm, A., Jorgensen, B.B., 2013. Predominant archaea in marine sediments degrade detrital proteins. Nature 496, 215–218.

Matsumoto, T., Uto, K., Ono, K., Watanabe, K., 1991. K-Ar age determinations for Aso volcanic rocks —concordance with volcanostratigraphy and application to pyroclastic flows—. Abstracts Fall Meet. in 1991, Volcanological Soceity of Japan 73, 1991 (in Japanese).

Miyoshi, N., Fujiki, T., Morita, Y., 1999. Palynology of a 250-m core from Lake Biwa: a 430,000-year record of glacial-interglacial vegetation change in Japan. Review of Palaeobotany and Palynology 104, 267–283.

Murase, J., Sakamoto, M., 2000. Horizontal distribution of carbon and nitrogen and their isotopic compositions in the surface sediment of Lake Biwa. Limnology 1, 177–184.

Nakae, S., Yoshioka, T., Naito, K., 2001. Geology of the Chikubushima District. Geological Survey of Japan, Tsukuba, 71pp. (in Japanese).

Nakagawa, T., Okuda, M., Yonenobu, H., Norio, M., Toshiyuki, F., Gotanda, K., Tarasov, P., Yoshimune, M., Takemura, K., Shoji, N., 2008. Regulation of the monsoon climate by two different orbital rhythms and forcing mechanisms. Geology 36, 491–494.

Nakamura, T., Niu, E., Oda, H., Ikeda, A., Minamia, M., Takahashi, H., Adachi, M., Pals, L., Gottdang, A., Suya, N., 2000. The HVEE Tandetron AMS system at Nagoya University. Nuclear Instruments and Methods in Physics Research B 172, 52–57.

Nakamura, T., Niu, E., Oda, H., Ikeda, A., Minamia, Ohta, T., Oda, T., 2004. High precision $^{14}C$ measurement with the HVEE Tandetron AMS system at Nagoya University. Nuclear Instruments and Methods in Physics Research B 223/224, 124–129.

Nakayama, O., 1981: Current condition of eutrophication and fishery in Lake Biwa. Bulletin of the Japanese Society of Fisheries Oceanography 38, 49–53 (in Japanese).

Niemann, H., Stadnitskaia, A., Wirth, S.B., Gilli, A., Anselmetti, F.S., Sinninghe Damsté, J.S., Schouten, S., Hopmans, E.C., Lehmann, M.F., 2012. Bacterial GDGTs in Holocene sediments and catchment soils of a high Alpine lake: application of the MBT/CBT-paleothermometer. Climate of the Past 8, 889–906, doi:10.5194/cp-8-889-2012.

Nishihara, M., Koga, Y., 1987. Extraction and composition of polar lipids from the archaebacterium, *Methanobacterium thermoautotrophicum*: Effective extraction of tetraether lipids by an acidified solvent. Journal of Biochemistry 101, 997–1005.

Oba, T., Irino, T., Yamamoto, M., Murayama, M., Takamura, A., Aoki, K., 2006.

Paleoceanographic change off central Japan since the last 144,000 years based on high-resolution oxygen and carbon isotope records. Global and Planetary Change 53, 5–20.

Ohta, S., Kumada, K., 1978. Studies on the humus forms of forest soils VI. Mineralization of nitrogen in brown forest soils. Soil Science and Plant Nutrition 24, 41–54.

Ohira, F., Yamamoto, M., Takemura, K., Hayashida, A., 2013. Response of vegetation in central Japan to precession during the last 147,000 years: A lignin record from Lake Biwa core BIW08-B. Quaternary International, in press.

Pancost, R.D., Hopmans, E.C., Sinninghe Damsté, J.S., Medinauth Scientific Party, 2001. Archaeal lipids in Mediterranean cold seeps: molecular proxies for anaerobic methane oxidation. Geochimica et Cosmochimica Acta 65, 1611–1627.

Pancost, R.D., Sinninghe Damsté, J.S., 2003. Carbon isotopic compositions of prokaryotic lipids as tracers of carbon cycling in diverse settings. Chemical Geology 195, 29–58.

Park, B.-J., Park, S.-J., Yoon, D.-N., Schouten, S., Sinninghe Damsté, J.S., Rhee, S.-K., 2010. Cultivation of autotrophic ammonia-oxidizing archaea from marine sediments in co-culture with sulfur-oxidizing bacteria. Applied and Environmental Microbiology 76, 7575–7587.

Patwardhan, A.P., Thompson, D.H., 1999. Efficient synthesis of 40- and 48-membered tetraether macrocyclic bisphosphocholines. Organic Letters 1, 241–243.

Peterse, F., van der Meer, J., Schouten, S., Weijers, J.W.H., Fierer, N., Jackson, R.B., Kim, J.-K., Sinninghe Damsté, J.S., 2012. Revised calibration of the MBT-CBT paleotemperature proxy based on branched tetraether membrane lipids in surface soils. Geochimica et Cosmochimica Acta 96, 215–229.

Powers, L.A., Werne, J.P., Johnson, T.C., Hopmans, E.C., Sinninghe Damsté, J.S., Schouten, S., 2004. Crenarchaeotal lipids in lake sediments: a new paleotemperature proxy for continental paleoclimate reconstruction? Geology 32, 613–616.

Powers, L.P., Werne, J.P., Vanderwoude, A.J., Sinninghe Damsté, J.S., Hopmans, E.C., Schouten, S., 2010. Applicability and calibration of the $TEX_{86}$ paleothermometer in lakes. Organic Geochemistry 41, 404–413.

Reimer, P.J., Bard, E., Bayliss, A., Beck, J.W., Blackwell, P.G., Ramsey, C.B., Buck, C.E., Cheng, H., Edwards, R.L., Friedrich, M., Grootes, P.M., Guilderson, T.P., Haflidason, H., Hajdas, I., Hatte, C., Heaton, T.J., Hoffmann, D.L., Hogg, A.G., Hughen, K.A., Kaiser, K.F., Kromer, B., Manning, S.W., Niu, M., Reimer, R.W., Richards, D.A., Scott, E.M., Southon, J.R., Staff, R.A., Turney, C.S.M., van der Plicht, J., 2013. Intcal13 and Marine13 Radiocarbon Age Calibration Curves 0–50,000 Years Cal Bp. Radiocarbon 55, 1869–1887.

Rueda, G., Rosell-Mele, A., Escala, M., Gyllencreutz, R., Backman, J., 2009. Comparison of instrumental and GDGT-based estimates of sea surface and air temperatures from the Skagerrak. Organic Geochemistry 40, 287–291.

Saito, M., Sawada, J., 2000. Geology of the Yokoyama District. Geological Survey of Japan, Tsukuba, 126pp. (in Japanese).

Schoon, P.L., Kluijver, A., Middelburg, J.J., Downing, J.A., Sinninghe Damsté, J.S., Schouten, S., 2013. Influence of lake water pH and alkalinity on the distribution of core and intact polar branched glycerol dialkyl glycerol tetraethers (GDGTs) in lakes. Organic Geochemistry 60, 72–82.

Schouten, S., Hopmans, E.C., Pancost, R.D., Sinninghe Damsté, J.S., 2000. Widespread occurrence of structurally diverse tetraether membrane lipids: evidence for the ubiquitous presence of low-temperature relatives of hyperthermophiles. Proceedings of the National Academy of Sciences USA 97, 14421–14426.

Schouten, S., Wakeham, S.G., Sinninghe Damsté, J.S., 2001. Anaerobic methane oxidation in euxinic waters of the Black Sea is mediated by archaea. Organic Geochemistry 32, 1277–1281.

Schouten, S., Hopmans, E.C., Schefuß, E., Sinninghe Damsté, J.S., 2002. Distributional variations in marine crenarchaeotal membrane lipids: a new tool for reconstructing ancient sea water temperatures? Earth and Planetary Science Letters 204, 265–274.

Schouten, S., Huguet, C., Hopmans, E.C., Kienhuis, M.V.M., Sinninghe Damsté, J.S., 2007. Analytical methodology for $TEX_{86}$ paleothermometry by high performance liquid chromatography/atmospheric pressure chemical ionization-mass spectrometry. Analytical Chemistry 79, 2940–2944.

Schouten, S., Hopmans, E.C., Sinninghe Damsté, J.S., 2013. The organic geochemistry of glycerol dialkyl glycerol tetraether lipids: A review. Organic Geochemistry 54, 19–61.

Seki, O., Kawamura, K., shiwatari, R., 2012. Assessment of hydrogen isotopic compositions of n-fatty acids as paleoclimate proxies in Lake Biwa sediments. Journal of Quaternary Science 27(9), 884–890.

Sinninghe Damsté, J.S., Hopmans, E.C., Pancost, R.D., Schouten, S., Geenevasen, J.A.J., 2000. Newly discovered non-isoprenoid dialkyl diglycerol tetraether lipids in sediments. Journal of the Chemical Society, Chemical Communications 23, 1683–1684.

Sinninghe Damsté, J.S., Hopmans, E.C., Schouten, S., van Duin, A.C.T., Geenevasen, J.A.J., 2002. Crenarchaeol: the characteristic core glycerol dibiphytanyl glycerol tetraether membrane lipid of cosmopolitan pelagic crenarchaeota. Journal of Lipid Research 43, 1641–1651.

Sinninghe Damsté, J.S., Ossebaar, J., Schouten, S., Verschuren, D., 2008. Altitudinal shifts in the distribution of branched tetraether lipids in soils from Mt. Kilimanjaro (Tanzania): implications for the MBT/CBT continental palaeothermometer. Organic Geochemistry 39, 1072–1076.

Sinninghe Damsté, J.S., Ossebaar, J., Abbas, B., Schouten, S., Verschuren, D., 2009. Fluxes and distribution of tetraether lipids in an equatorial African lake: constraints on the application of the $TEX_{86}$ palaeothermometer and branched tetraether lipids in lacustrine settings. Geochimica et Cosmochimica Acta 73, 4232–4249.

Sinninghe Damsté, J.S., Rijpstra, W.I.C., Hopmans, E.C., Weijers, J.W.H., Foesel, B.U., Overmann, J., Dedysh, S.N., 2011. 13,16-Dimethyl octacosanedioic acid (iso-diabolic acid): a common membrane-spanning lipid of Acidobacteria subdivisions 1 and 3. Applied and Environmental Microbiology 77, 4147–4154.

Southon, J., Santos, G.M., 2004a. Ion source development at KCCAMS, University of California. Radiocarbon 46, 33–39.

Southon, J., Santos, G., Druffel-Rodriguez, K., Druffel, E., Trumbore, S., Xu, X., Griffin, S., Ali., S., Mazon, M., 2004b. The KECK Carbon cycle AMS laboratory, University of California, Irvine: Initial operation and background surprise. Radiocarbon 46, 41–49.

Spang, A., Hatzenpichler, R., Brochier-Armanet, C., Rattei, T., Tischler, P., Spieck, E., Streit, W., Stahl, D.A., Wagner, M., Schleper, C., 2010. Distinct gene set in two different lineages of ammonia-oxidizing archaea supports the phylum Thaumarchaeota. Trends in Microbiology 554, 331–340.

Staff, R.A., Nakagawa, T., Schlolaut, G., Marshall, M.H., Brauer, A., Lamb, H., Bronk Ramsey, C., Bryant, C.L., Brock, F., Kitagawa, H., van der Plicht, J., Payne, R.L., Smith, V.C., Mark, D.F., MacLeod, A., Blockley, S.P.E., Schwenninger, J.L., Tarasov, P., Haraguchi, T., Gotanda, K., Yonenobu, H., Yokoyama, Y., Suigetsu 2006 project members., 2012. The multiple chronological techniques applied to the Lake Suigetsu (SG06) sediment core. Boreas 42, 33–39.

Takemura, K., Iwabe, C., Hayashida, A., Danhara, T., Kitagawa, H., Haraguchi, T., Sato, T., Ishikawa, N., 2010. Stratigraphy of marker tephras and sediments during the past 50,000 years from multiple sites in Lake Biwa, Japan. Daiyonkikenkyu (The Quaternary Research) 49, 147–160 (in Japanese).

Talling, S.J., 1976. The depletion of carbon dioxide from lake water by phytoplankton. The Journal of Ecology 64, 79–121.

Tani, S., Kitagawa, H., Hong, W., Park, J.H., Sung, K., Park, G., 2013. Age determination of the Kawagodaira volcanic eruption in Japan by $^{14}C$ wiggle-matching. Radiocarbon 55, 748–752.

Tezuka, Y., 1985. C:N:P ratios of seston in Lake Biwa as indicators of nutrient deficiency in phytoplankton and decomposition process of hypolimnetic particulate matter. Japanese Journal of Limnology 46, 239–246.

Tierney, J.E., Russell, J.M., 2009. Distributions of branched GDGTs in a tropical lake system: Implications for lacustrine application of the MBT/CBT paleoproxy. Organic Geochemistry 40, 1032–1036.

Tierney, J.E., Russell, J.M., Eggemont, H., Hopmans, E.C., Verschuren, D., Sinninghe

Damsté, J.S., 2010. Environmental controls on branched tetraether lipid distributions in tropical East African lake sediments: a new lacustrine paleothermometer? Geochimica et Cosmochimica Acta 74, 4902–4918.

Tyler, J.J., Nederbragt, A.J., Jones, V.J., Thurow, J.W., 2010. Assessing past temperature and soil pH estimated from bacterial tetraether membrane lipids: evidence from the recent lake sediments of Lochnar, Scotland. Journal of Geophysical Research 115, G01015.

Wakeham, S.G., Lewis, C.A., Hopmans, E.C., Schouten, S., Sinninghe Damsté, J.S., 2003. Archaea mediate anaerobic oxidation of methane in deep euxinic waters of the Black Sea. Geochimica et Cosmochimica Acta 67, 1359–1374.

Wang, Y.J., Cheng, H., Edwards, R.L., An, Z.S., Wu, J.Y., Shen, C.-C., Dorale, J.A., 2001. A high-resolution absolute-dated late Pleistocene monsoon record from Hulu Cave, China. Science 294, 2345–2348.

Wang, G., Clemens, S.C., Liu, P., 2003. Contrasting the Indian and East Asian monsoons: implications on geologic timescales. Marine Geology 201, 5–21.

Wang, Y.J., Cheng, H., Edwards, R.L., Kong, X., Shao, X., Chen, S., Wu, J., Jiang, X., Wang, X., An, Z., 2008. Millennial- and orbital-scale changes in the East Asian monsoon over the past 224,000 years. Nature 451, 1090–1093.

Wang, H., Liu, W., Zhang, C., Wang, Z., Wang, J., Liu, Z., Dong, H., 2012. Distribution of glycerol dialkyl glycerol tetraethers in surface sediments of Lake Qinghai and surrounding soil. Organic Geochemistry 47, 78–87.

Weijers, J.W.H., Schouten, S., Geenevasen, J.A.J., David, O.R.P., Coleman, J., Pancost, R.D., Sinninghe Damste, J.S., 2006a. Membrane lipids of mesophilic anaerobic bacteria thriving in peats have typical archaeal traits. Environmental Microbiology

8, 648–657.

Weijers, J.W.H., Schouten, S., Spaargaren, O.C., Sinninghe Damsté, J.S., 2006b. Occurrence and distribution of tetraether membrane in soils: implications for the use of the BIT index and the $TEX_{86}$ SST proxy. Organic Geochemistry 37, 1680–1693.

Weijers, J.W.H., Schouten, S., van Den Donker, J.C., Hopmans, E.C., Sinninghe Damsté, J.S., 2007a. Environmental controls on bacterial tetraether membrane lipid distribution in soils. Geochimica et Cosmochimica Acta 71, 703–713.

Weijers, J.W.H., Schefuß, E., Schouten, S., Sinninghe Damsté, J.S., 2007b. Coupled thermal and hydrological evolution of tropical Africa over the last deglaciation. Science 315, 1701–1704.

Wetzel, R.G., 2001. Limnology: Lake and River Ecosystems. Third edition, Academic Press, San. Diego, USA, 1006 pp.

White, A.F., Blum, A.E., 1995. Effects of climate on chemical weathering in watersheds. Geochimica et Cosmochimica Acta 59, 1729–1747.

Wuchter, C., Schouten, S., Wakeham, S.G., Sinninghe Damsté, J.S., 2006. Archaeal tetraether membrane lipid fluxes in the northeastern Pacific and the Arabian Sea: implications for $TEX_{86}$ paleothermometry. Paleoceanography 21, PA4208.

Xiao, J., Inouchi, Y., Kumai, H., Yoshikawa, S., Kondo, Y., Liu, T., An, Z., 1997. Biogenic silica record in Lake Biwa of central Japan over the past 145,000 years. Quaternary Research 47, 277–283.

Yamamoto, M., 2009. Response of mid-latitude North Pacific surface temperatures to orbital forcing and linkage to the East Asian summer monsoon and tropical ocean-atmosphere interactions. Journal of Quaternary Science 24, 836–847.

Yoshino, M.M., 1965. Four stages of the rainy season in early summer over East Asia (part I). Journal of the Meteorological Society of Japan 43, 231–245.

Yoshino, M., 1978. Climatology. Taimeidou, Tokyo, 350pp. (in Japanese).

Yuan, D., Cheng, H., Edwards, R.L., Dykoski, C.A., Kelly, M.J., Zhang, M., Qing, J., Lin, Y., Wang, Y., Wu, J., Dorale, J.A., An, Z., Cai, Y., 2004. Timing, duration, and transitions of the last interglacial Asian monsoon. Science 304, 575–578.

Zhang, Y.G., Zhang, C.L., Liu, X.L., Li, L., Hinrichs, K.U., Noakes, J.E., 2011. Methane Index: a tetraether archaeal lipid biomarker indicator for detecting the instability of marine gas hydrates. Earth and Planetary Science Letters 307, 525–534.

Zink, K.-G., Vandergoes, M.J., Mangelsdorf, K., Dieffenbacher-Krall, A.C., Schwark, L., 2010. Application of bacterial glycerol dialkyl glycerol tetraethers (GDGTs) to develop modern and past temperature estimates from New Zealand lakes. Organic Geochemistry 41, 1060–1066.

**Table 1**

Locations, soil types, vegetation, lithology of basement rocks and mean annual air temperatures of soil samples.

| Site No. | Latitude (N) | Longitude (E) | Altitude (m) | Depth (cm) | Soil type[a] | Vegetation | Lithology of basement rock[b] | MAAT[c] (°C) |
|---|---|---|---|---|---|---|---|---|
| 1 | 35°23.56' | 136°13.27' | 86 | 0-5 | O | Cropland | Sand | 14.1 |
| 3 | 35°30.93' | 136°22.23' | 590 | 0-5 | O | Japanese cedar | Granite | 11.1 |
| | | | | 5-20 | A | | | |
| | | | | 20-30 | B | | | |
| 4 | 35°30.40' | 136°22.34' | 714 | 0-5 | O | Japanese cedar | Granite | 10.3 |
| | | | | 5-30 | A | | | |
| 5 | 35°30.38' | 136°22.45' | 773 | 0-5 | O | Japanese cedar | Granite | 9.9 |
| | | | | 5-20 | A | | | |
| | | | | 20-30 | B | | | |
| 6 | 35°31.19' | 136°22.65' | 652 | 0-5 | O | Japanese cedar | Granite | 10.7 |
| | | | | 5-15 | A | | | |
| | | | | 15-30 | B | | | |
| 7 | 35°31.05' | 136°22.17' | 588 | 0-5 | O | Japanese cedar and bamboo | Granite | 11.1 |
| | | | | 5-30 | A | | | |
| 8 | 35°31.02' | 136°22.16' | 579 | 0-5 | A | Rice paddy | Granite | 11.1 |
| 9 | 35°29.82' | 136°21.61' | 534 | 0-15 | A | Mixed trees and grass | Granite | 11.4 |
| | | | | 15-30 | B | | | |
| 10 | 35°29.00' | 136°21.05' | 440 | 0-5 | O | Pine and shrub* | Shale | 12.0 |
| | | | | 5-15 | B | | | |
| 11 | 35°28.28' | 136°20.97' | 344 | 0-5 | O | Japanese cedar | Shale | 12.6 |
| | | | | 5-25 | A | | | |
| 12 | 35°26.99' | 136°21.57' | 283 | 0-20 | A | Japanese cedar and bamboo | Shale | 12.9 |
| 13 | 35°25.55' | 136°25.01' | 1149 | 0-5 | B | Grasses | Limestone | 7.6 |
| 14 | 35°25.15' | 136°25.04' | 986 | 0-5 | O | Grasses | Limestone | 8.6 |
| 15 | 35°25.73' | 136°25.23' | 925 | 0-20 | A | Japanese cedar | Limestone | 9.0 |
| 16 | 35°24.25' | 136°25.49' | 805 | 0-5 | A | Grasses | Sandstone | 9.7 |
| 17 | 35°22.85' | 136°26.13' | 217 | 0-5 | A | Japanese cedar | Chert, slate and sandstone | 13.3 |
| 18 | 35°24.36' | 136°19.81' | 133 | 0-5 | A | Japanese cedar* | Tuff | 13.8 |
| | | | | 5-10 | B | | | |
| 19 | 35°30.83' | 136°09.21' | 107 | 0-15 | A | Japanese cedar and bamboo | Sandstone and shale | 14.0 |
| 20 | 35°30.72' | 136°09.36' | 127 | 0-5 | O | Japanese cedar | Shale | 13.9 |
| | | | | 5-20 | B | | | |
| 21 | 35°30.41' | 136°09.61' | 212 | 0-5 | B | Mixed trees | Sandstone and shale | 13.4 |
| 22 | 35°30.35' | 136°09.19' | 196 | 0-5 | O | Japanese cedar | Shale | 13.5 |
| | | | | 5-20 | A | | | |
| 23 | 35°28.97' | 136°07.47' | 89 | 0-5 | O | Grasses | Greenstone | 14.1 |
| 24 | 35°27.29' | 136°08.99' | 302 | 0-5 | O | Maple | Mudstone | 12.8 |
| 25 | 35°28.60' | 136°08.55' | 297 | 0-15 | A | Broad leaf trees | Greenstone | 12.8 |
| | | | | 15-25 | B | | | |
| 26 | 35°29.17' | 136°09.00' | 360 | 0-5 | O | Japanese cedar | Sandstone | 12.5 |
| | | | | 5-20 | A | | | |

[a] Soil type; O, A and B mean litter layer, organic material-rich dark brown soil layers and organic material-poor yellowish brown soil layers, respectively.

[b] Lithology refers to Isomi (1956), Kurimoto et al. (1999), Saito and Sawada (2000) and Nakae et al. (2001).

[c] Mean annual air temperatures were calculated by the linearly interpolation on altitude between temperatures at two nearby stations.

* These soils are artificially disturbed.

**Table 2**

Locations, lithology, measured sediment pH and mean annual air temperatures of riverine sediments.

| Site No. | Latitude (N) | Longitude (E) | Altitude (m) | Depth (cm) | Lithology | Sediment pH | MAAT (°C) |
|---|---|---|---|---|---|---|---|
| 1-1 | 35°23.54' | 136°13.31' | 84 | 0-5 | Coarse sand | 6.9 | 14.1 |
| 1-2 | | | 84 | 0-5 | Fine sand | 5.8 | 14.1 |
| 2-1 | 35°30.95' | 136°22.04' | 541 | 0-1 | Fine sand | 7.2 | 11.4 |
| 2-2 | | | 541 | 0-1 | Silt | 7.0 | 11.4 |

**Table 3**

Locations, lithologies, mean annual water pH values and water temperatures of Lake Biwa surface sediments.

| Site No. | Latitude (N) | Longitude (E) | Water depth (m) | Depth (cm) | Lithology | Water pH[a] | Water temperature (°C)[a] |
|---|---|---|---|---|---|---|---|
| 521 | 35°23.16' | 136°12.00' | 50.0 | 0-2 | Clay | 7.5 | 7.9 |
| 671 | 35°13.08' | 135°58.14' | 26.2 | 0-2 | Medium sand | 7.7 | 9.8 |
| 676 | 35°13.14' | 135°59.10' | 79.2 | 0-2 | Clay | 7.4 | 7.4 |
| 686 | 35°13.08' | 136°00.84' | 70.0 | 0-2 | Clay | 7.4 | 7.5 |
| 701 | 35°13.14' | 136°02.70' | 55.1 | 0-2 | Clay | 7.5 | 7.8 |
| 706 | 35°13.14' | 136°04.74' | 28.0 | 0-2 | Clay | 7.6 | 9.4 |
| 716 | 35°13.08' | 136°06.24' | 13.3 | 0-2 | Silt | 7.9 | 13.9 |
| 721 | 35°13.32' | 136°08.10' | 9.8 | 0-2 | Clay | 8.1 | 15.4 |

[a] Water pH and temperatures were measured at near station off Imadzu (N35°23.68', E136°07.95').

**Table 4**

Age controls of core BIW07-6

| Depth (m) | Source | $^{14}C$ (BP, 1σ) | | | Model age (cal BP, 2σ) | | | Remarks |
|---|---|---|---|---|---|---|---|---|
| 0.980 | KgP | | | | 3150 | ± | 12 | [1] |
| 1.115 | SOh | 3650 | ± | 30 | 4086 | - | 3887 | [2] |
| 1.450 | K-Ah | | | | 7350 | ± | 80 | [3] |
| 2.501 | U-Oki | | | | 10286 | ± | 45 | [4] |
| 3.510 | $^{14}C$ (wood) | 11855 | ± | 40 | 13844 | - | 13486 | [5] |
| 3.700 | $^{14}C$ (wood) | 12400 | ± | 45 | 14940 | - | 14110 | [6] |
| 4.010 | $^{14}C$ (wood) | 12865 | ± | 45 | 15880 | - | 15000 | [5] |
| 5.380 | $^{14}C$ (wood) | 14510 | ± | 80 | 17940 | - | 17235 | [5] |
| 5.630 | Sakate | | | | 19484 | ± | 112 | [4] |
| 6.130 | $^{14}C$ (wood) | 18050 | ± | 90 | 22005 | - | 21555 | [5] |
| 6.620 | $^{14}C$ (wood) | 19010 | ± | 100 | 23275 | - | 22310 | [5] |
| 7.160 | $^{14}C$ (wood) | 20440 | ± | 110 | 24815 | - | 23955 | [5] |
| 8.530 | $^{14}C$ (wood) | 23760 | ± | 170 | 29160 | - | 28033 | [5] |
| 9.870 | AT | | | | 30009 | ± | 189 | [4] |
| 11.560 | $^{14}C$ (wood) | 27950 | ± | 280 | 32965 | - | 31470 | [6] |
| 12.030 | $^{14}C$ (wood) | 28760 | ± | 320 | 34495 | - | 32265 | [6] |
| 15.360 | $^{14}C$ (wood) | 36530 | ± | 820 | 42970 | - | 40090 | [5] |
| 17.660 | $^{14}C$ (wood) | 41200 | ± | 1500 | 48642 | - | 42855 | [6] |
| 18.340 | $^{14}C$ (wood) | 42570 | ± | 1270 | 49190 | - | 44295 | [6] |

[1] Tani et al. (2013); [2] Fukuoka and Matsui (2002); [3] Kitagawa and van der Plicht (1998); [4] Staff et al. (2012); [5] Kitagawa et al. (2010); [6] Kitagawa et al. (in preparation).

**Table 5**

Age controls of core BIW08-B

| Depth (m) | Source | $^{14}C$ (BP, 1σ) | | | Model age (cal BP, 2σ) | | | Remarks |
|---|---|---|---|---|---|---|---|---|
| 0.00 | Core-top | | | | -57 | ± | 0 | [1] |
| 1.12 | $^{14}C$ (wood) | 1920 | ± | 60 | 1868 | ± | 160 | [1] |
| 2.09 | SOh | 3650 | ± | 30 | 4086 | - | 3887 | [2] |
| 2.18 | $^{14}C$ (wood) | 4720 | ± | 110 | 5408 | ± | 324 | [1] |
| 2.45 | K-Ah | | | | 7350 | ± | 80 | [3] |
| 3.28 | U-Oki | | | | 10286 | ± | 45 | [4] |
| 4.34 | ARM-1 event | | | | 13837 | ± | 103 | [5][6] |
| 4.97 | ARM-2 event | | | | 16586 | ± | 155 | [5][6] |
| 5.63 | Sakate | | | | 19484 | ± | 112 | [4] |
| 6.04 | ARM-3 event | | | | 23181 | ± | 277 | [5][6] |
| 7.61 | DSs (Plinian) | | | | 29247 | ± | 270 | [1] |
| 7.85 | AT | | | | 30009 | ± | 189 | [4] |
| 8.82 | ARM-4 event | | | | 31078 | ± | 442 | [5][6] |
| 9.84 | ARM-6 event | | | | 32720 | ± | 803 | [5][6] |
| 10.58 | ARM-7 event | | | | 34529 | ± | 770 | [5][6] |
| 12.58 | ARM-8 event | | | | 40594 | ± | 1425 | [5][6] |
| 13.32 | SI | | | | 42080 | ± | 1250 | [1] |
| 13.69 | ARM-9 event | | | | 42619 | ± | 1329 | [5][6] |
| 14.83 | ARM-10 event | | | | 44154 | ± | 2028 | [5][6] |
| 23.58 | DNP | | | | 82922 | ± | 10758 | [6] |
| 23.66 | DMP2 | | | | 83039 | ± | 10788 | [6] |
| 26.81 | KTZ | | | | 96715 | ± | 7080 | [6] |
| 27.73 | AsoABCD | | | | 104263 | ± | 5352 | [6] |
| 28.41 | Unnamed tephra | | | | 108098 | ± | 5505 | [6] |
| 34.81 | Unnamed tephra | | | | 114925 | ± | 5544 | [6] |
| 38.99 | Unnamed tephra | | | | 120837 | ± | 7675 | [6] |
| 40.59 | Aso-3b | | | | 123619 | ± | 9005 | [7] |
| 44.67 | Aso2 | | | | 142975 | ± | 9059 | [7] |
| 83.91 | Aso1 | | | | 266000 | ± | 28000 | [7] |

[1] Kitagawa et al. (in preparation); [2] Fukuoka and Matsui (2002); [3] Kitagawa and van der Plicht (1998); [4] Staff et al. (2012); [5] Hayashida et al. (2007); [6] Takemura et al. (in preparation); [7] Matsumoto et al. (1991).

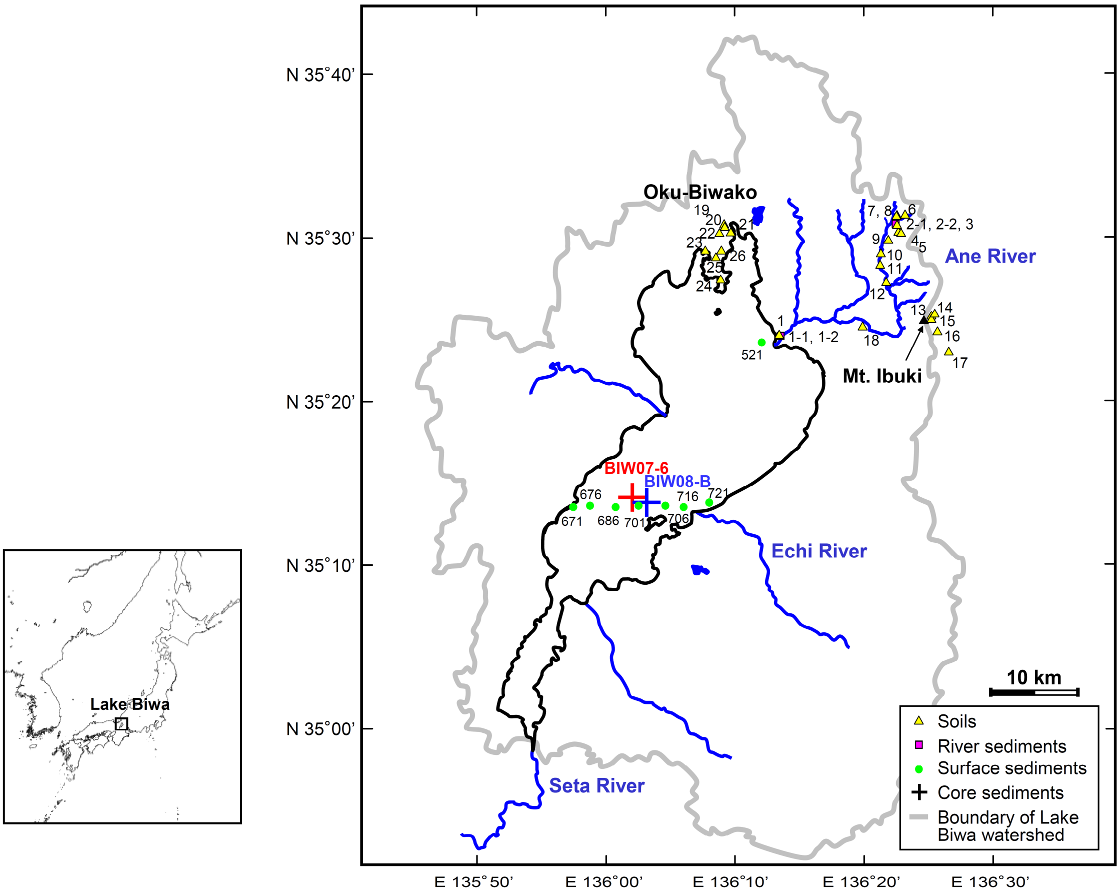


**Fig. 1.** Map showing the sampling sites.

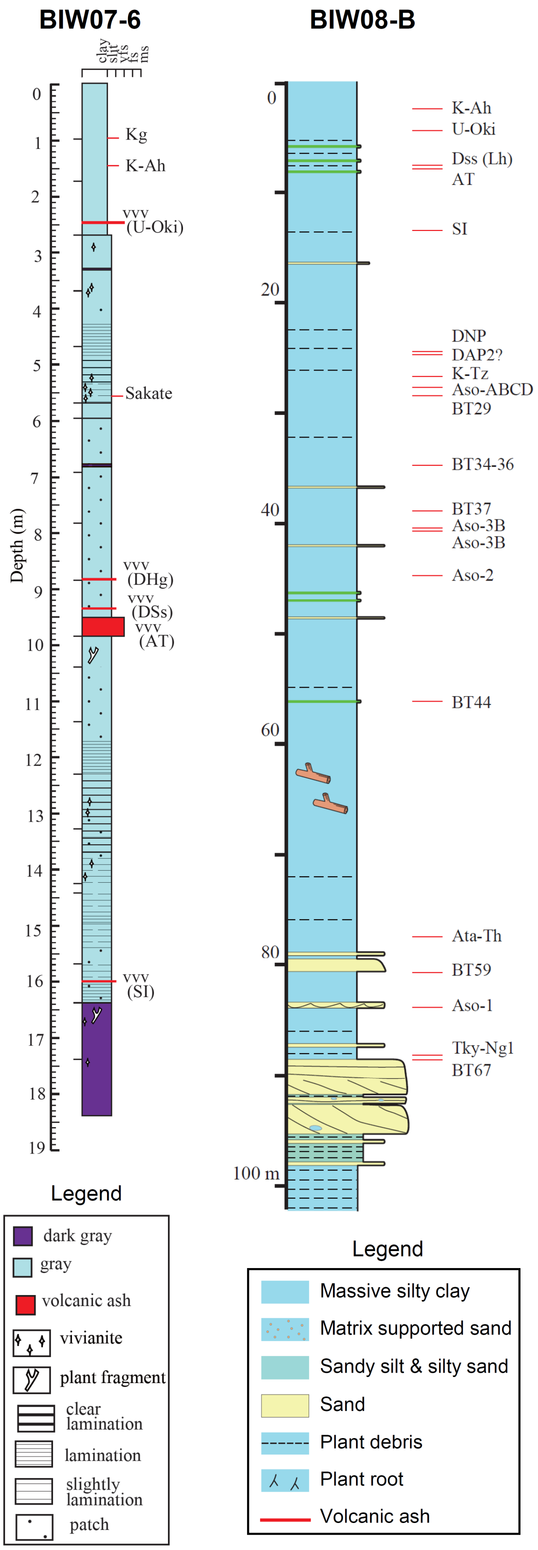


**Fig. 2.** Lithologic columns of (a) core BIW07-6 and (b) borehole core BIW08-B (Takemura et al., 2010).

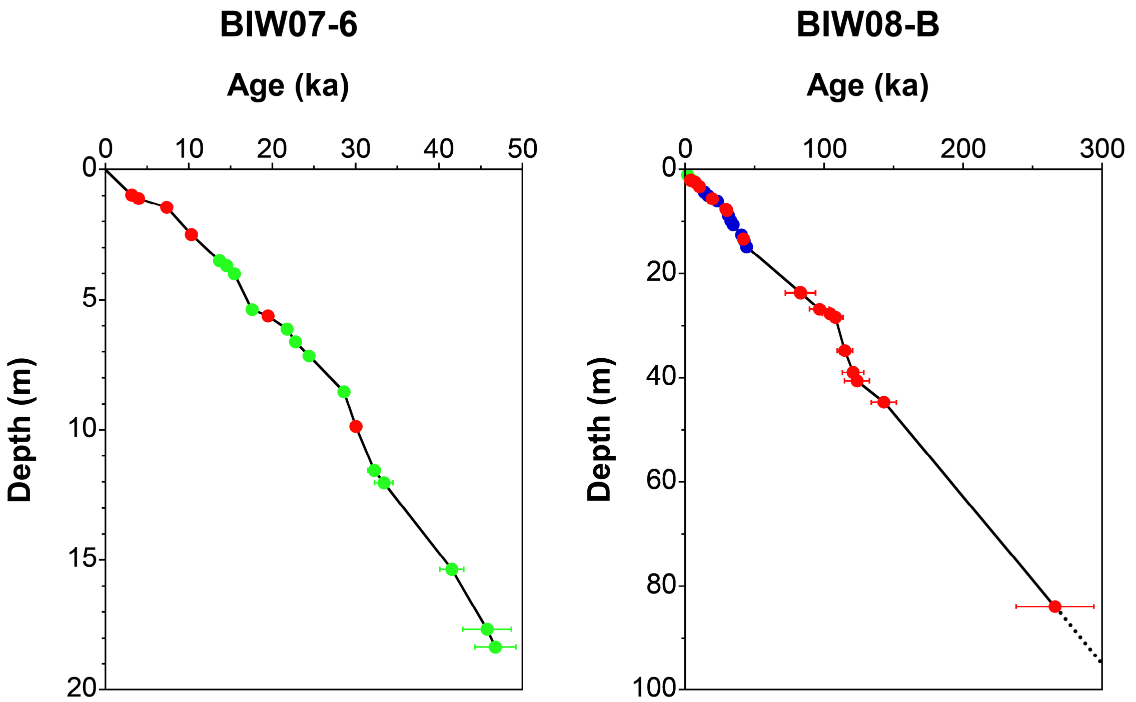


**Fig. 3.** Age–depth models of cores BIW07-6 and BIW08-B. The red, green and blue dots show volcanic ashes, $^{14}C$ of plant debris and total organic carbon, and ARM events, respectively (see Tables 4 and 5). Error bars indicate the 95% confidence intervals (2σ).

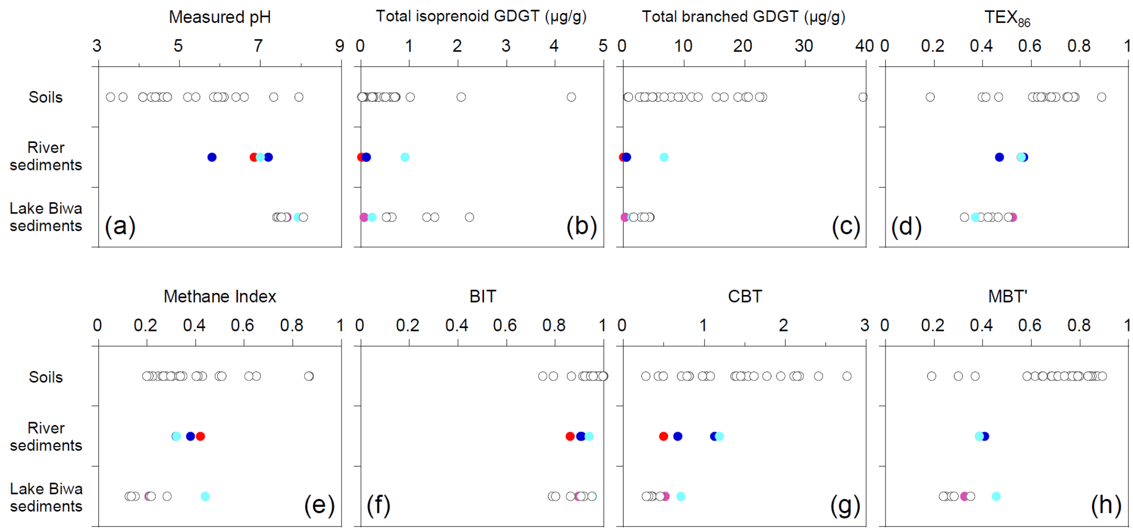


**Fig. 4.** Measured pH (a), concentration of total isoprenoid GDGTs (b) and branched GDGTs (c), $TEX_{86}$ (d), methane index (e), BIT (f), CBT (g) and MBT′ (h) for soils, river sediments and Lake Biwa surface sediments. For river and Lake Biwa surface sediments, the red, purple, blue and sky blue dots indicate coarse, medium, fine sand and silt samples, respectively. The pH values for Lake Biwa surface sediments represent the observed mean annual water pH.

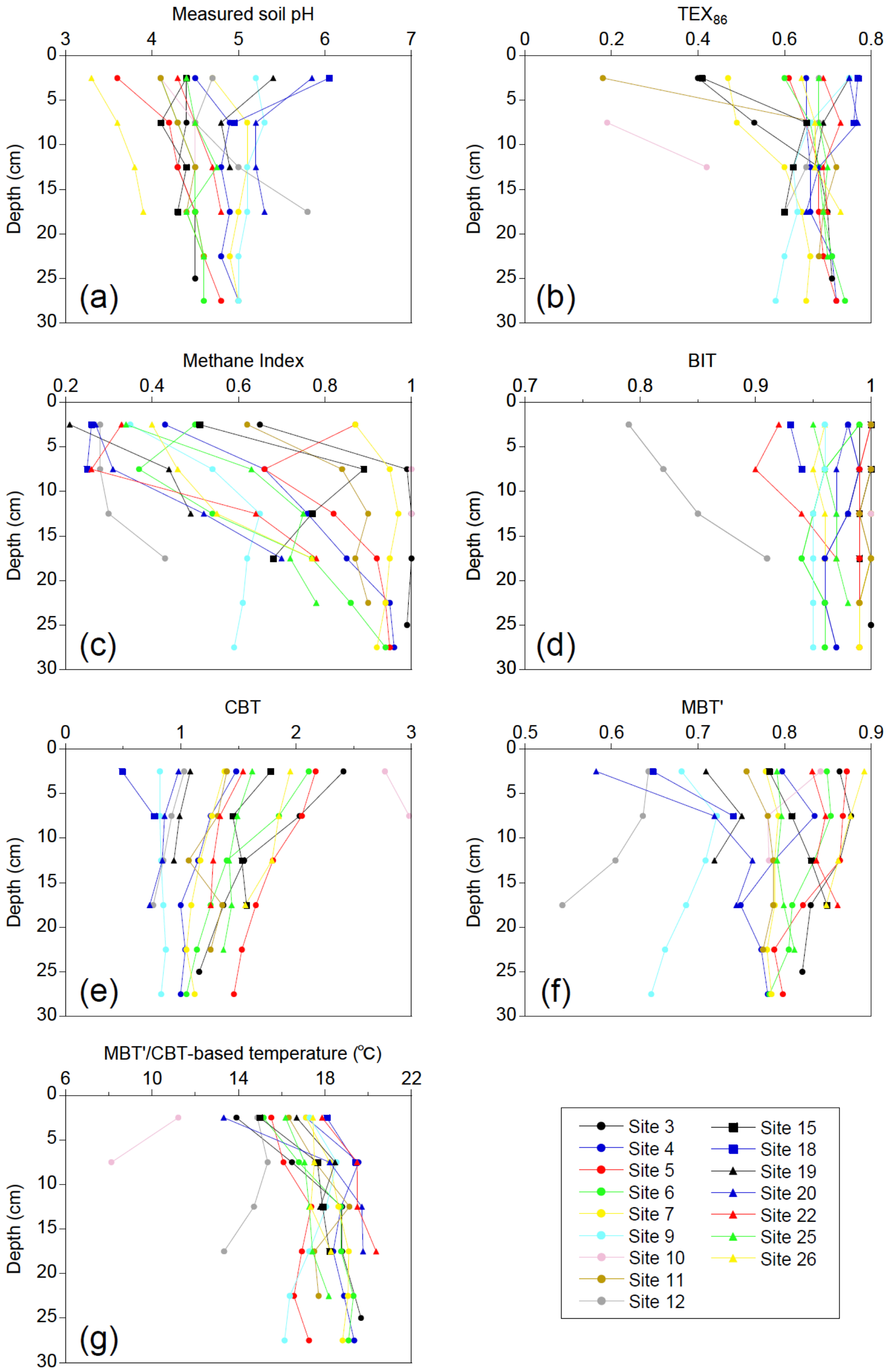


**Fig. 5.** Depth variation in measured soil pH (a), $TEX_{86}$ (b), methane index (c), BIT (d), CBT (e) and MBT′ (f), and estimated temperature based on MBT’/CBT (g) according to the calibration of Peterse et al. (2012).

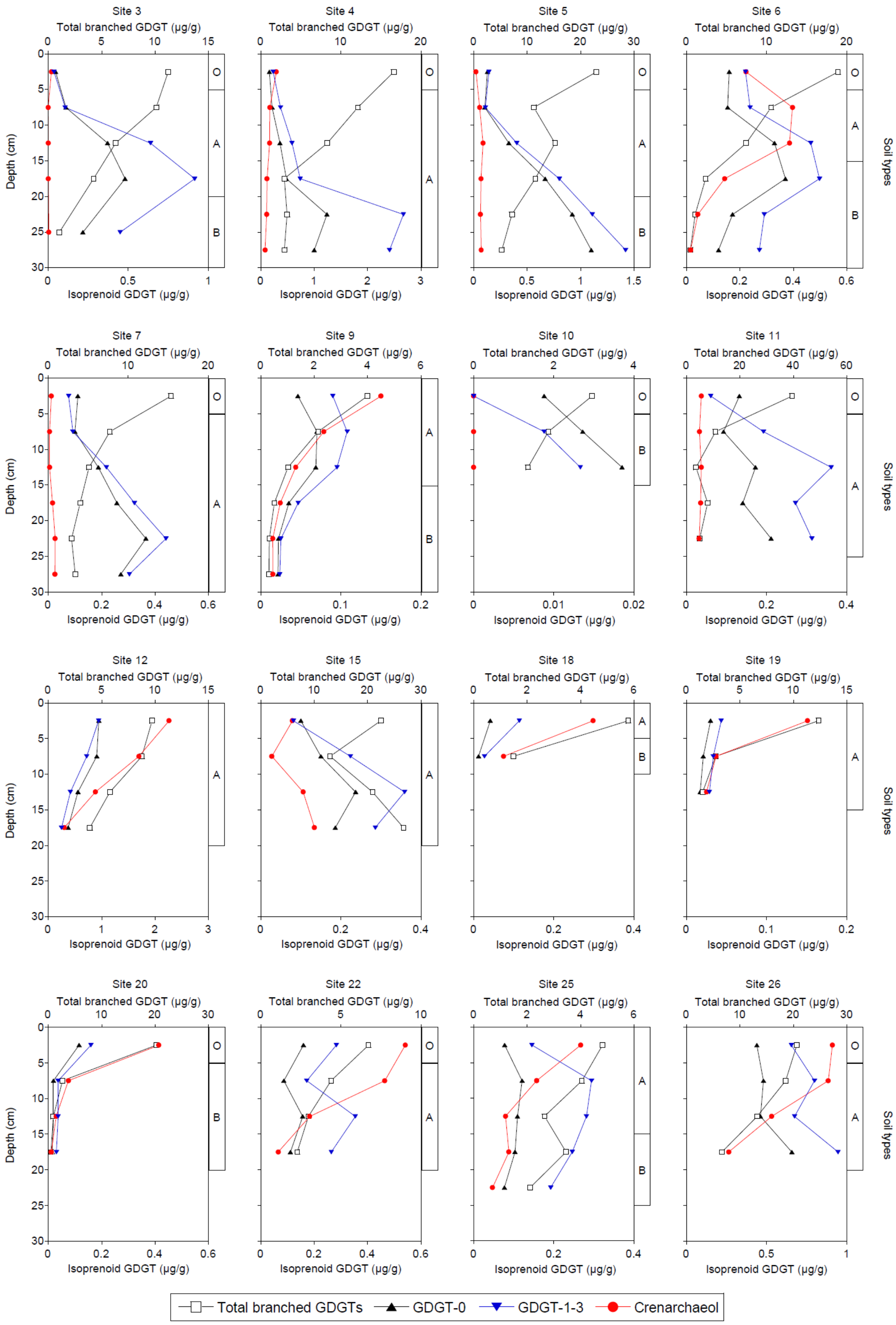


**Fig. 6.** Depth variation in the concentration of total branched GDGTs, GDGT-0, GDGT-1 to -3 and crenarchaeol.

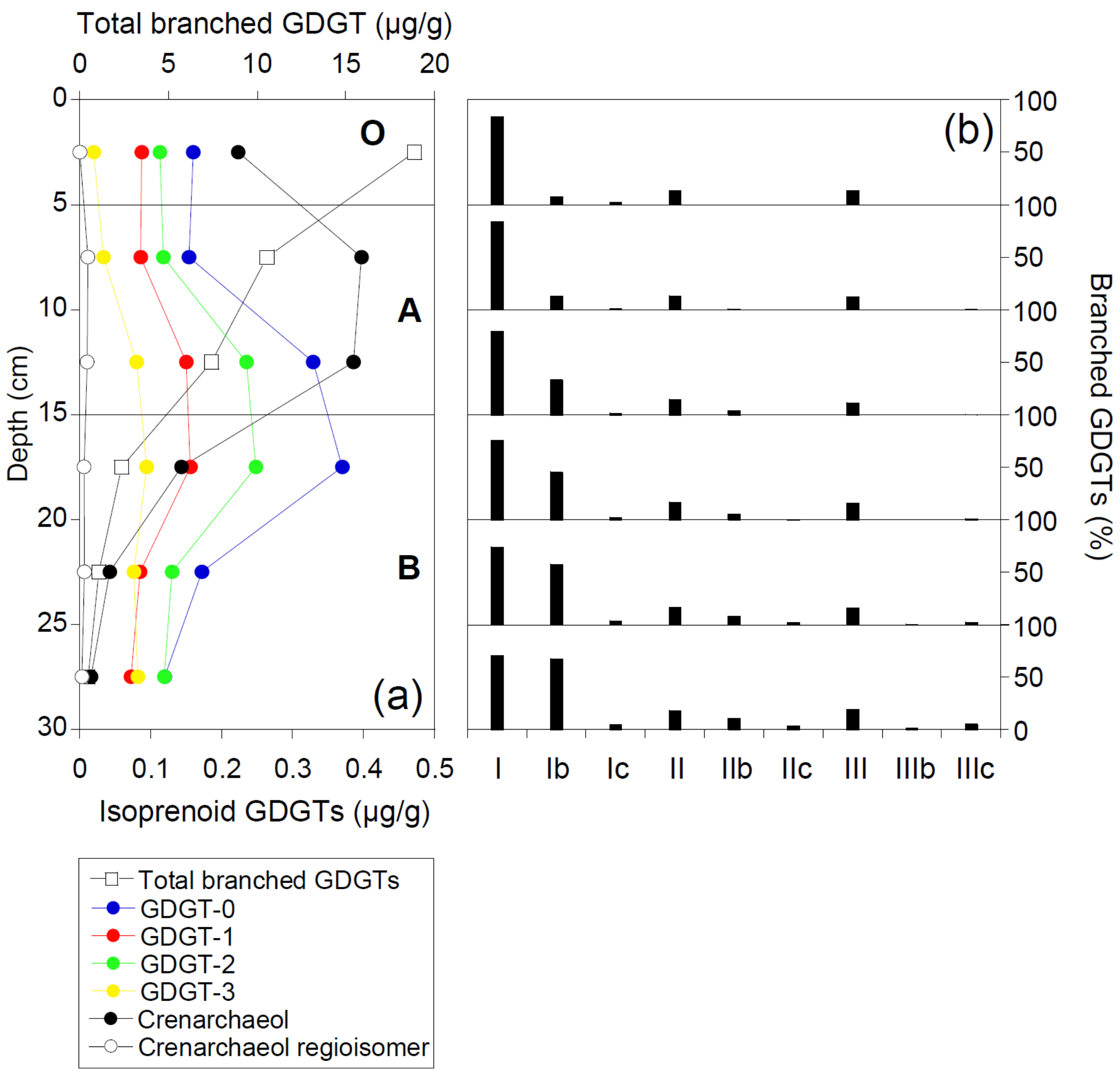


**Fig. 7.** Vertical variation in concentration of total branched GDGTs and isoprenoid GDGTs (a) and relative abundances of branched GDGTs (b) at site 6. Relative abundances of GDGT Ib, Ic, IIb, IIc, III, IIIb and IIIc are multiplied by 10.

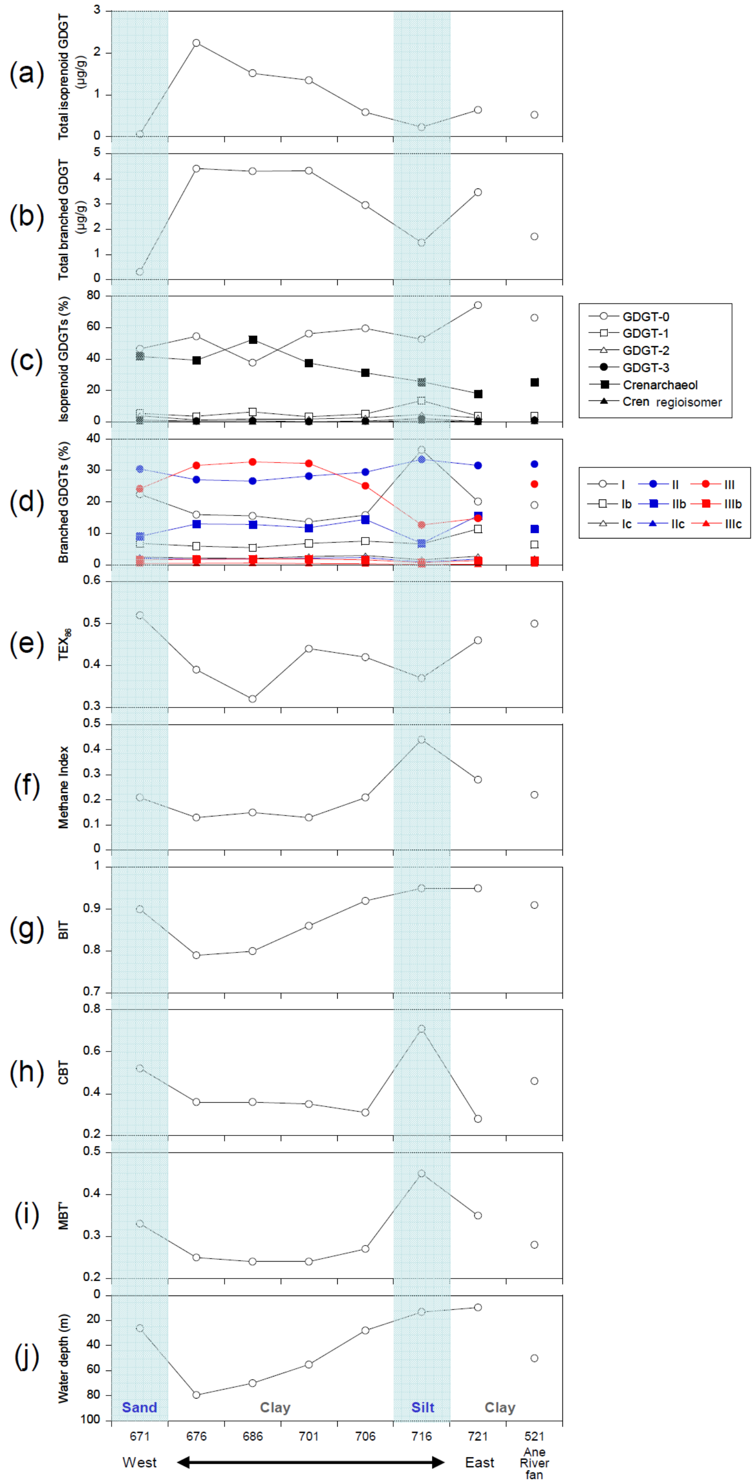


**Fig. 8.** Total iso (a) and br (b) GDGT concentrations, distributions of iso (c) and br (d) GDGTs, $TEX_{86}$ (e), methane index (f), BIT (g), CBT (h), MBT′ (i) and water depth (j) for Lake Biwa surface sediments. Light blue shading indicates sand or silt.

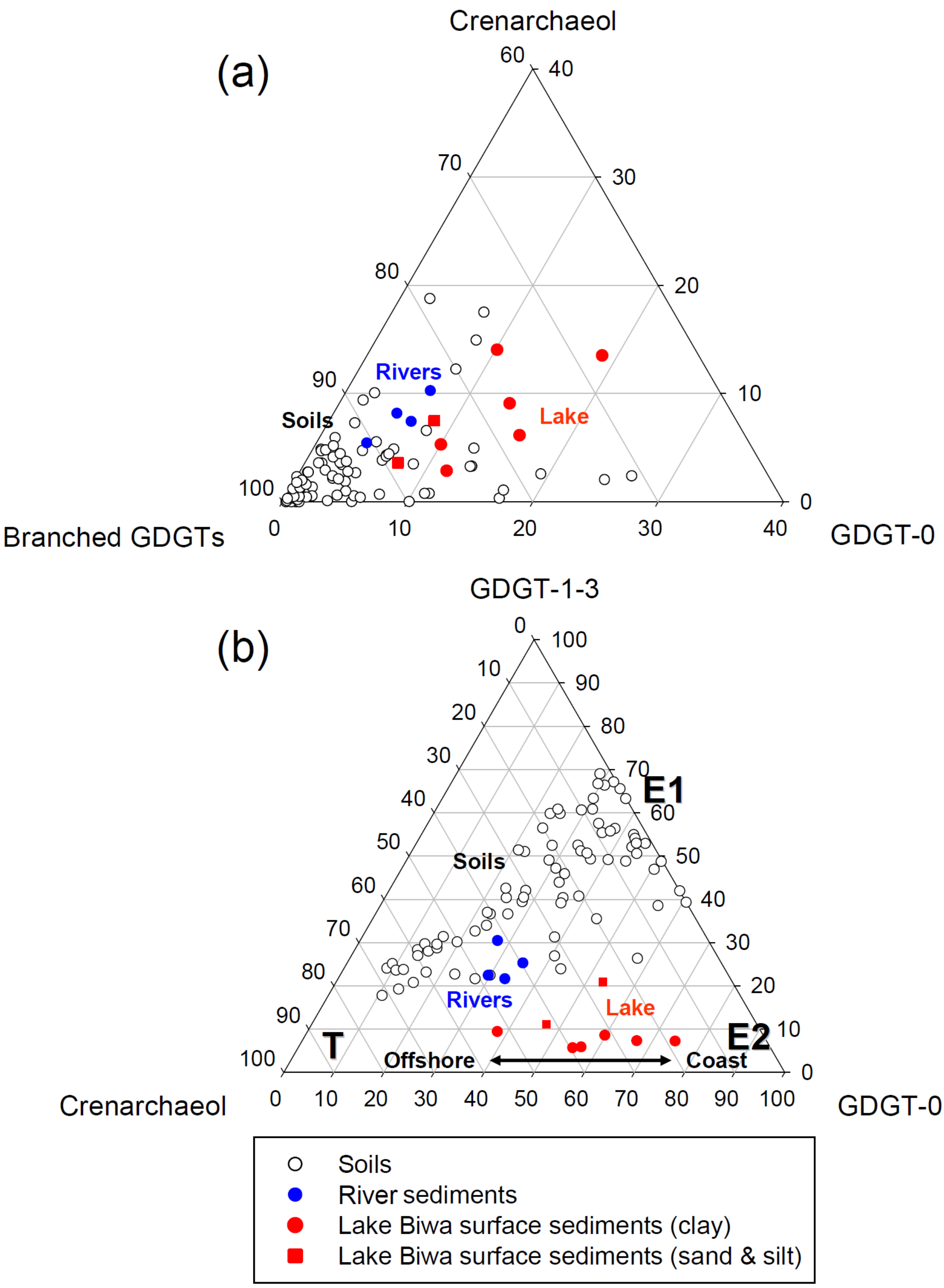


**Fig. 9.** Ternary diagrams indicating relative abundance of crenarchaeol, branched GDGTs and GDGT-0 (a) and GDGT-1 to -3, crenarchaeol and GDGT-0 (b) in soils, river sediments and Lake Biwa surface sediments.

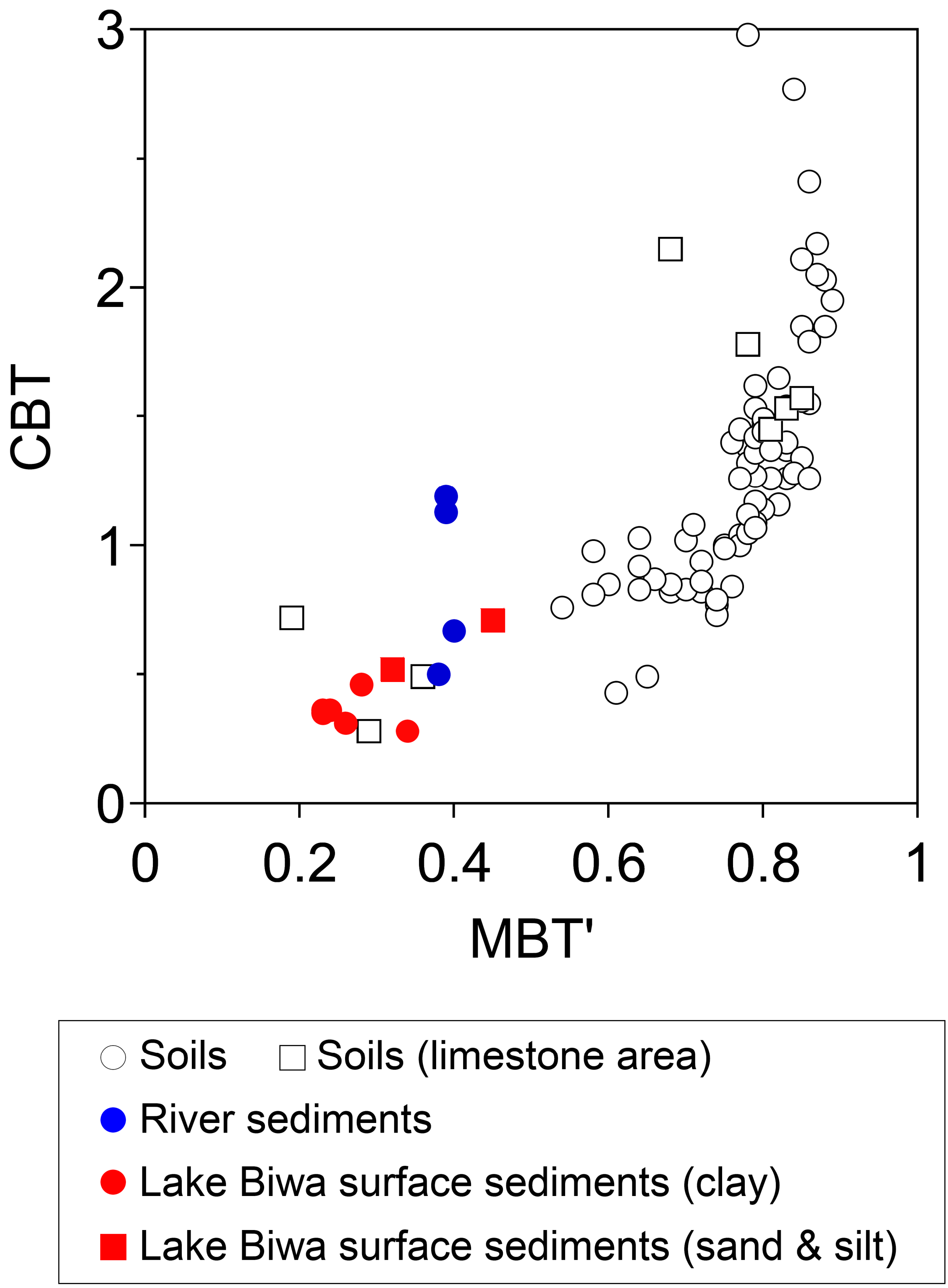


**Fig. 10.** Plots of CBT vs. MBT′ for soils, river sediments and Lake Biwa surface sediments.

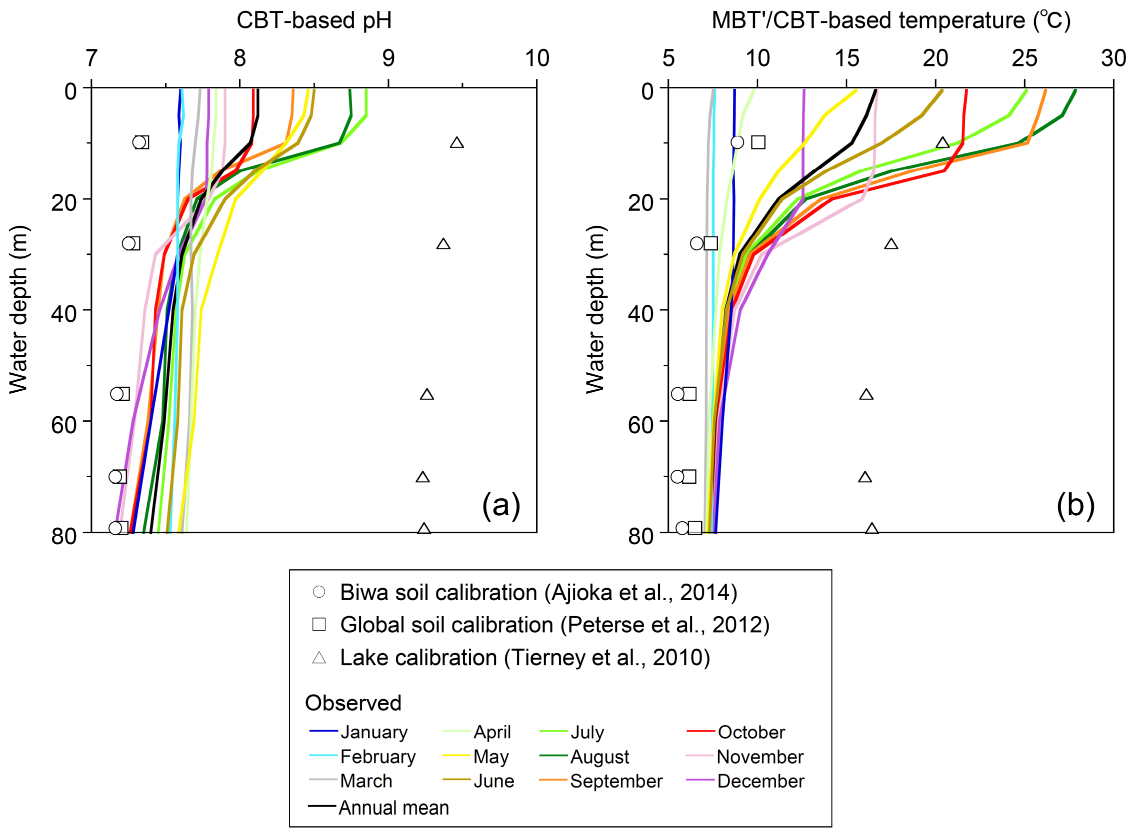


**Fig. 11.** Reconstructed water pH (a) and MBT′/CBT-based temperature (b) in Lake Biwa surface clays. The temperature based on lake calibration was obtained from MBT/CBT rather than MBT′/CBT.

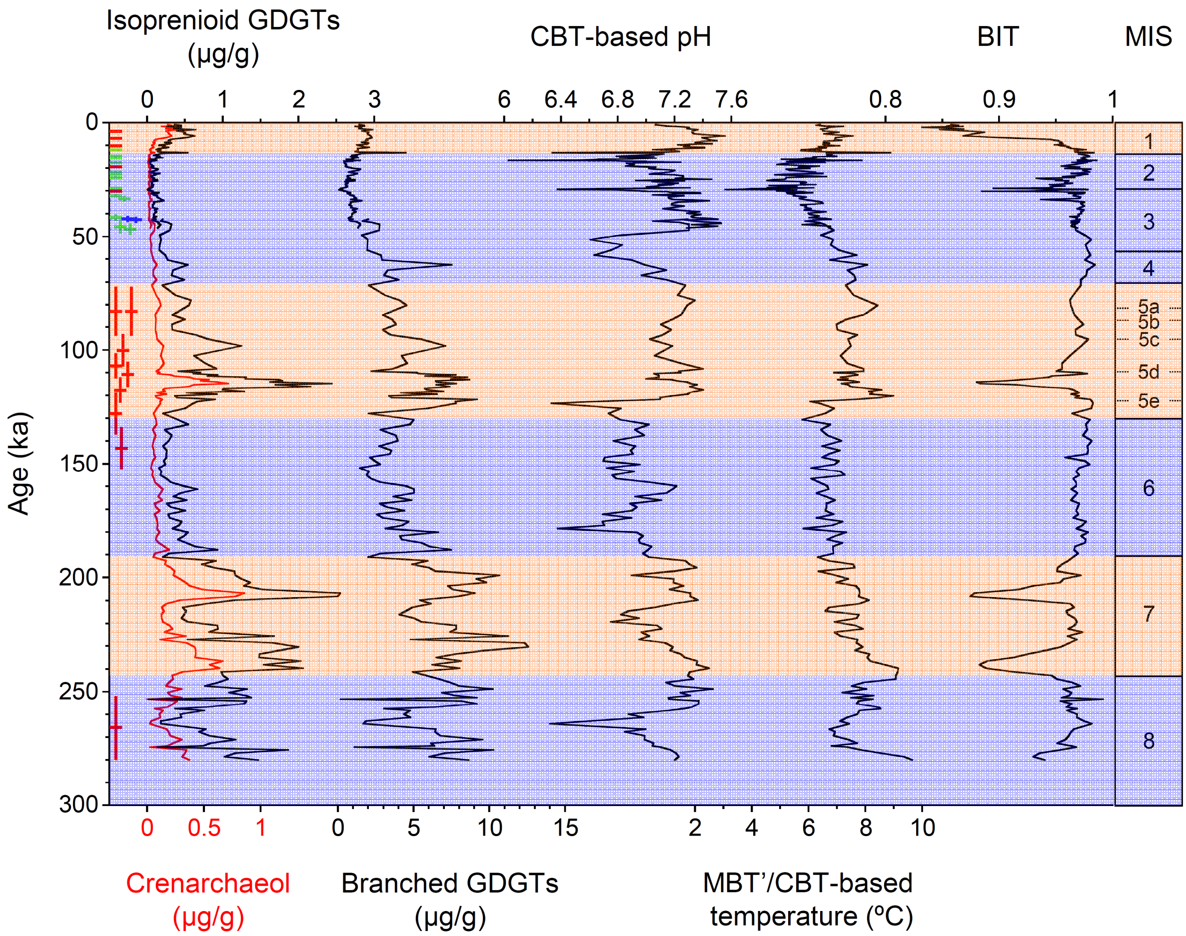


**Fig. 12.** Variations in the concentrations of total isoprenoid and branched GDGTs and crenarchaeol, CBT-based pH, MBT′/CBT-based temperature and BIT in cores BIW07-6 and BIW08-B during the last 280,000 years. Red, blue and green bars indicate age controls with 95% confidence intervals of volcanic ashes, the $^{14}$C of plant debris and total organic carbon, and ARM events, respectively.

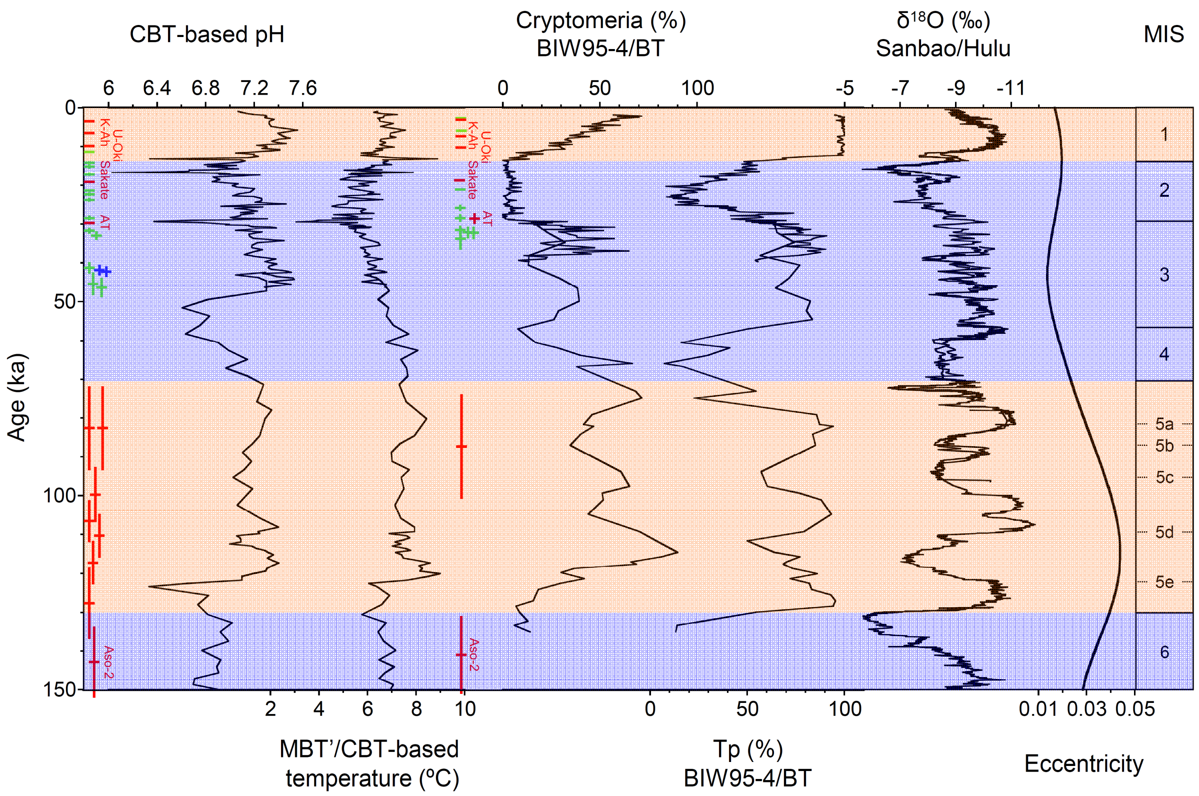


**Fig. 13.** Variations in CBT-based pH and MBT′/CBT-based temperature from cores BIW07-6 and BIW08-B (this study), Tp and *Cryptomeria* (%) from cores BIW95 and Takashima-oki BT in Lake Biwa (Hayashi et al., 2010a and b), the $\delta^{18}O$ of stalagmites in Sanbao and Hulu caves in central China (Wang et al., 2001, 2008), and eccentricity during the last 150,000 years. Red, blue and green bars indicate age controls with 95% confidence intervals of volcanic ashes, the $^{14}C$ of plant debris and total organic carbon, and ARM events, respectively. The names of tephras that appeared commonly in BIW07-6/BIW08-B and BIW95-4/BT are shown in the panel.

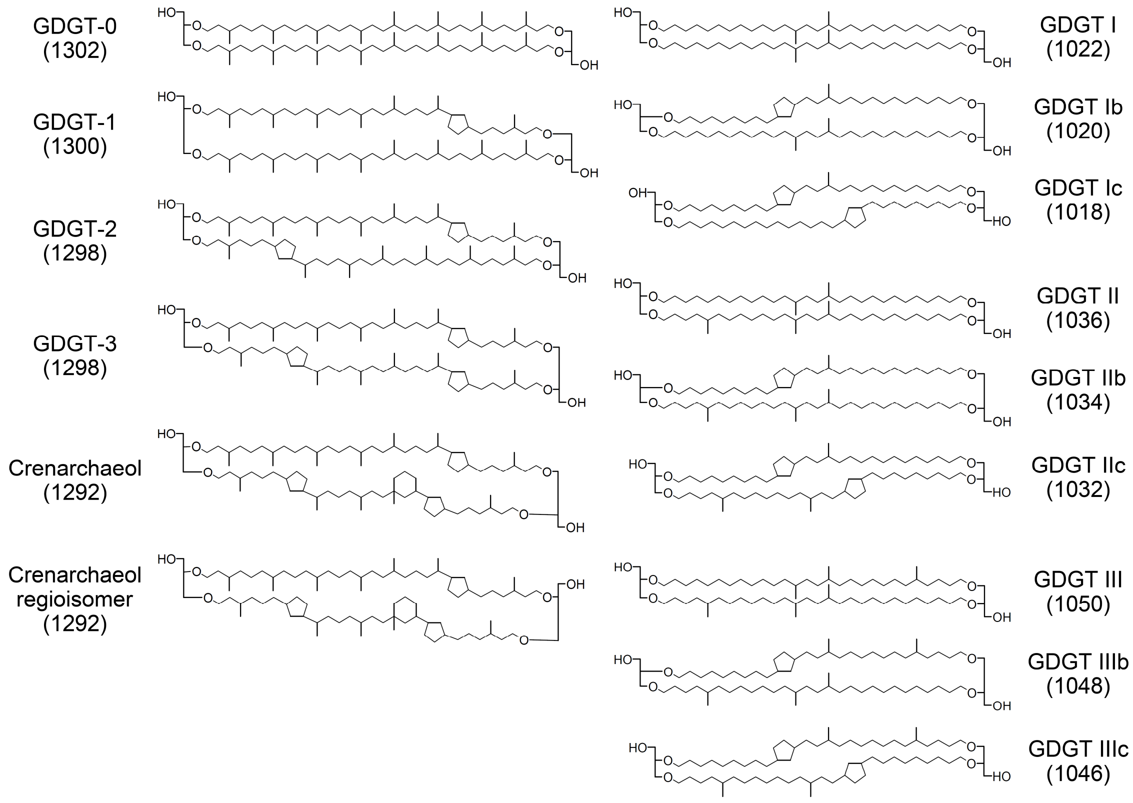


**Appendix 1.** Structures of isoprenoid and branched GDGTs.

Appendix 2. GDGT concentrations, proxy data and estimated pH and temperature for soils.

| Site No. | Depth (cm) | GDGT-0 (ng/g) | GDGT-1 to 3 (ng/g) | Crenarchaeol (ng/g) | Isoprenoid GDGTs (μg/g) | Branched GDGTs (μg/g) | CBT | MBT' | Measured pH | CBT -based pH | MBT'/CBT -based temperature (℃) |
|---|---|---|---|---|---|---|---|---|---|---|---|
| 1-3 | 0-5 | 23 | 64 | 180 | 0.29 | 0.76 | 0.43 | 0.61 | 6.6 | 7.05 | 17.41 |
| 3 | 0-5 | 46 | 37 | 21 | 0.10 | 11.24 | 2.41 | 0.86 | 4.4 | 3.15 | 13.91 |
| | 5-10 | 111 | 106 | 1 | 0.22 | 10.11 | 2.03 | 0.88 | 4.4 | 3.89 | 16.47 |
| | 10-15 | 370 | 639 | 1 | 1.01 | 6.32 | 1.55 | 0.86 | 4.3 | 4.85 | 18.80 |
| | 15-20 | 479 | 914 | 1 | 1.39 | 4.26 | 1.37 | 0.83 | 4.5 | 5.21 | 18.80 |
| | 20-30 | 216 | 449 | 4 | 0.67 | 1.04 | 1.16 | 0.82 | 4.5 | 5.61 | 19.67 |
| 4 | 0-5 | 161 | 232 | 291 | 0.70 | 16.60 | 1.48 | 0.80 | 4.5 | 4.98 | 17.13 |
| | 5-10 | 215 | 371 | 170 | 0.78 | 12.11 | 1.26 | 0.83 | 4.9 | 5.42 | 19.55 |
| | 10-15 | 361 | 584 | 167 | 1.13 | 8.30 | 1.15 | 0.79 | 4.8 | 5.64 | 18.74 |
| | 15-20 | 480 | 740 | 117 | 1.36 | 2.96 | 1.00 | 0.75 | 4.9 | 5.93 | 18.38 |
| | 20-25 | 1245 | 2673 | 112 | 4.05 | 3.31 | 1.04 | 0.77 | 4.8 | 5.85 | 18.89 |
| | 25-30 | 1002 | 2415 | 84 | 3.52 | 2.97 | 1.00 | 0.78 | 5.0 | 5.93 | 19.35 |
| 5 | 0-5 | 128 | 143 | 22 | 0.29 | 22.96 | 2.17 | 0.87 | 3.6 | 3.62 | 15.52 |
| | 5-10 | 104 | 110 | 56 | 0.27 | 11.24 | 2.05 | 0.87 | 4.2 | 3.86 | 16.08 |
| | 10-15 | 329 | 403 | 88 | 0.82 | 15.19 | 1.80 | 0.86 | 4.3 | 4.35 | 17.37 |
| | 15-20 | 668 | 801 | 68 | 1.54 | 11.53 | 1.65 | 0.82 | 4.5 | 4.66 | 16.94 |
| | 20-25 | 921 | 1109 | 63 | 2.10 | 7.14 | 1.53 | 0.79 | 4.6 | 4.89 | 16.57 |
| | 25-30 | 1100 | 1424 | 70 | 2.61 | 5.26 | 1.46 | 0.80 | 4.8 | 5.02 | 17.26 |
| 6 | 0-5 | 160 | 221 | 223 | 0.60 | 18.89 | 2.11 | 0.85 | 4.1 | 3.74 | 15.16 |
| | 5-10 | 154 | 238 | 397 | 0.80 | 10.55 | 1.85 | 0.85 | 4.3 | 4.26 | 16.80 |
| | 10-15 | 329 | 465 | 386 | 1.19 | 7.43 | 1.40 | 0.83 | 4.5 | 5.14 | 18.73 |
| | 15-20 | 370 | 498 | 143 | 1.02 | 2.37 | 1.26 | 0.81 | 4.5 | 5.42 | 18.75 |
| | 20-25 | 172 | 291 | 42 | 0.51 | 1.08 | 1.14 | 0.81 | 4.6 | 5.66 | 19.32 |
| | 25-30 | 120 | 273 | 16 | 0.41 | 0.48 | 1.05 | 0.78 | 4.6 | 5.82 | 19.09 |
| 7 | 0-5 | 111 | 77 | 12 | 0.20 | 15.33 | 1.38 | 0.78 | 4.7 | 5.18 | 17.12 |
| | 5-10 | 100 | 93 | 5 | 0.20 | 7.70 | 1.27 | 0.79 | 5.1 | 5.41 | 18.22 |
| | 10-15 | 188 | 218 | 6 | 0.41 | 5.11 | 1.17 | 0.79 | 5.1 | 5.60 | 18.63 |
| | 15-20 | 257 | 323 | 17 | 0.60 | 3.99 | 1.09 | 0.79 | 5.0 | 5.76 | 19.10 |
| | 20-25 | 366 | 441 | 26 | 0.83 | 2.94 | 1.05 | 0.78 | 4.9 | 5.84 | 19.07 |
| | 25-30 | 272 | 304 | 26 | 0.60 | 3.38 | 1.12 | 0.78 | 5.0 | 5.70 | 18.81 |
| 8 | 0-5 | 280 | 155 | 211 | 0.66 | 3.84 | 1.02 | 0.70 | 5.9 | 5.90 | 16.88 |
| 9 | 0-5 | 46 | 90 | 150 | 0.31 | 3.99 | 0.82 | 0.68 | 5.2 | 6.29 | 17.30 |
| | 5-10 | 70 | 108 | 79 | 0.27 | 2.15 | 0.82 | 0.72 | 5.3 | 6.28 | 18.54 |
| | 10-15 | 69 | 95 | 44 | 0.21 | 1.02 | 0.83 | 0.71 | 5.1 | 6.26 | 18.05 |
| | 15-20 | 35 | 47 | 25 | 0.11 | 0.51 | 0.85 | 0.69 | 5.1 | 6.23 | 17.28 |
| | 20-25 | 22 | 25 | 15 | 0.06 | 0.32 | 0.87 | 0.66 | 5.0 | 6.18 | 16.38 |
| | 25-30 | 22 | 24 | 15 | 0.06 | 0.31 | 0.83 | 0.65 | 5.0 | 6.27 | 16.13 |
| 10 | 0-5 | 9 | 0 | 0 | 0.01 | 2.95 | 2.77 | 0.84 | 4.1 | 2.45 | 11.22 |
| | 5-10 | 14 | 9 | 0 | 0.02 | 1.86 | 2.98 | 0.78 | 4.5 | 2.03 | 8.12 |
| | 10-15 | 18 | 13 | 0 | 0.03 | 1.35 | | 0.78 | 4.5 | | |
| 11 | 0-5 | 132 | 61 | 37 | 0.23 | 39.53 | 1.40 | 0.76 | 4.1 | 5.14 | 16.32 |
| | 5-10 | 92 | 192 | 32 | 0.32 | 10.86 | 1.32 | 0.78 | 4.3 | 5.31 | 17.55 |
| | 10-15 | 172 | 361 | 37 | 0.57 | 3.54 | 1.07 | 0.79 | 4.5 | 5.79 | 19.13 |
| | 15-20 | 140 | 272 | 35 | 0.45 | 7.93 | 1.36 | 0.79 | 4.4 | 5.22 | 17.50 |
| | 20-25 | 211 | 313 | 32 | 0.56 | 4.93 | 1.26 | 0.78 | 4.6 | 5.42 | 17.71 |
| 12 | 0-5 | 949 | 944 | 2264 | 4.34 | 9.71 | 1.03 | 0.64 | 4.7 | 5.86 | 14.88 |
| | 5-10 | 911 | 721 | 1698 | 3.48 | 8.76 | 0.92 | 0.64 | 4.5 | 6.10 | 15.35 |
| | 10-15 | 557 | 417 | 885 | 1.94 | 5.78 | 0.85 | 0.60 | 5.0 | 6.22 | 14.72 |
| | 15-20 | 377 | 250 | 302 | 0.96 | 3.91 | 0.76 | 0.54 | 5.8 | 6.40 | 13.34 |
| 13 | 0-5 | 44 | 99 | 206 | 0.37 | 3.23 | 0.28 | 0.30 | 8.0 | 7.36 | 8.50 |
| 14 | 0-5 | 0 | 0 | 64 | 0.06 | 2.68 | 0.72 | 0.19 | 7.3 | 6.49 | 2.57 |

(Continue to the next page)

| Site No. | Depth (cm) | GDGT-0 (ng/g) | GDGT-1 to 3 (ng/g) | Crenarchaeol (μg/g) | Isoprenoid GDGTs (μg/g) | Branched GDGTs (μg/g) | CBT | MBT' | Measured pH | CBT -based pH | MBT'/CBT -based temperature (℃) |
|---|---|---|---|---|---|---|---|---|---|---|---|
| 15 | 0-5 | 100 | 82 | 79 | 0.26 | 22.47 | 1.78 | 0.78 | 4.4 | 4.40 | 15.00 |
| | 5-10 | 150 | 224 | 28 | 0.40 | 12.98 | 1.45 | 0.81 | 4.1 | 5.04 | 17.65 |
| | 10-15 | 237 | 359 | 106 | 0.70 | 20.92 | 1.53 | 0.83 | 4.4 | 4.89 | 17.90 |
| | 15-20 | 186 | 286 | 134 | 0.61 | 26.70 | 1.57 | 0.85 | 4.3 | 4.80 | 18.21 |
| 16 | 0-5 | 6 | 8 | 25 | 0.04 | 0.88 | 2.15 | 0.68 | 4.6 | 3.67 | 9.83 |
| 17 | 0-5 | 95 | 211 | 405 | 0.72 | 3.52 | 0.49 | 0.37 | 6.1 | 6.93 | 9.42 |
| 18 | 0-5 | 41 | 114 | 298 | 0.48 | 5.78 | 0.49 | 0.65 | 6.1 | 6.93 | 18.09 |
| | 5-10 | 12 | 27 | 74 | 0.12 | 1.49 | 0.77 | 0.74 | 5.0 | 6.38 | 19.40 |
| 19 | 0-5 | 30 | 43 | 151 | 0.24 | 12.36 | 1.08 | 0.71 | 5.4 | 5.78 | 16.69 |
| | 5-10 | 21 | 33 | 37 | 0.10 | 2.74 | 0.99 | 0.75 | 4.8 | 5.95 | 18.47 |
| | 10-15 | 17 | 29 | 25 | 0.08 | 1.52 | 0.94 | 0.72 | 4.9 | 6.05 | 17.78 |
| 20 | 0-5 | 116 | 160 | 414 | 0.72 | 20.22 | 0.98 | 0.58 | 5.9 | 5.97 | 13.32 |
| | 5-10 | 20 | 37 | 76 | 0.14 | 2.68 | 0.86 | 0.72 | 5.2 | 6.21 | 18.23 |
| | 10-15 | 20 | 37 | 30 | 0.09 | 0.97 | 0.84 | 0.76 | 5.2 | 6.25 | 19.71 |
| | 15-20 | 16 | 31 | 12 | 0.06 | 0.52 | 0.73 | 0.74 | 5.3 | 6.47 | 19.77 |
| 21 | 0-5 | 89 | 182 | 402 | 0.70 | 7.88 | 0.81 | 0.58 | 6.4 | 6.30 | 14.25 |
| 22 | 0-5 | 160 | 283 | 541 | 1.02 | 6.72 | 1.54 | 0.83 | 4.3 | 4.86 | 17.86 |
| | 5-10 | 87 | 172 | 464 | 0.74 | 4.39 | 1.34 | 0.85 | 4.5 | 5.26 | 19.49 |
| | 10-15 | 157 | 354 | 183 | 0.71 | 2.97 | 1.28 | 0.84 | 4.7 | 5.38 | 19.50 |
| | 15-20 | 111 | 264 | 66 | 0.45 | 2.28 | 1.26 | 0.86 | 4.8 | 5.42 | 20.37 |
| 23 | 0-5 | 25 | 41 | 166 | 0.23 | 9.09 | 0.79 | 0.74 | 6.0 | 6.35 | 19.14 |
| 24 | 0-5 | 13 | 0 | 15 | 0.03 | 4.89 | 1.45 | 0.77 | 4.7 | 5.04 | 16.42 |
| 25 | 0-5 | 77 | 145 | 267 | 0.51 | 4.82 | 1.62 | 0.79 | 4.4 | 4.71 | 16.17 |
| | 5-10 | 121 | 294 | 157 | 0.59 | 4.05 | 1.49 | 0.80 | 4.5 | 4.96 | 17.05 |
| | 10-15 | 109 | 281 | 79 | 0.48 | 2.65 | 1.42 | 0.79 | 4.8 | 5.09 | 17.27 |
| | 15-20 | 103 | 246 | 88 | 0.45 | 3.46 | 1.44 | 0.80 | 4.4 | 5.06 | 17.42 |
| | 20-25 | 77 | 192 | 47 | 0.32 | 2.11 | 1.37 | 0.81 | 4.6 | 5.19 | 18.17 |
| 26 | 0-5 | 439 | 654 | 910 | 2.06 | 20.62 | 1.95 | 0.89 | 3.3 | 4.06 | 17.44 |
| | 5-10 | 480 | 799 | 884 | 2.22 | 18.56 | 1.85 | 0.88 | 3.6 | 4.26 | 17.50 |
| | 10-15 | 461 | 674 | 531 | 1.70 | 13.20 | 1.79 | 0.86 | 3.8 | 4.36 | 17.35 |
| | 15-20 | 657 | 945 | 264 | 1.89 | 6.61 | 1.56 | 0.85 | 3.9 | 4.84 | 18.28 |

Appendix 3. GDGT concentrations, proxy data and estimated pH and temperature for river sediments.

| Site No. | Depth (cm) | GDGT-0 (ng/g) | GDGT-1 to 3 (ng/g) | Crenarchaeol (ng/g) | Isoprenoid GDGTs (μg/g) | Branched GDGTs (μg/g) | CBT | MBT' | Measured pH | CBT -based pH | MBT'/CBT -based temperature (℃) |
|---|---|---|---|---|---|---|---|---|---|---|---|
| 1-1 | 0-5 | 4 | 5 | 6 | 0.02 | 0.05 | 0.50 | 0.39 | 6.9 | 6.92 | 9.98 |
| 1-2 | 0-5 | 39 | 28 | 44 | 0.11 | 0.51 | 0.67 | 0.41 | 5.8 | 6.57 | 9.64 |
| | | | | | | | | | | | |
| 2-1 | 0-1 | 31 | 24 | 50 | 0.10 | 0.53 | 1.13 | 0.39 | 7.2 | 5.67 | 6.33 |
| 2-2 | 0-1 | 301 | 195 | 406 | 0.91 | 6.76 | 1.19 | 0.39 | 7.0 | 5.56 | 6.01 |

Appendix 4-1. GDGT concentrations, proxy data for lake surface sediments.

| Site No. | Water Depth (cm) | GDGT-0 (ng/g) | GDGT-1 to 3 (ng/g) | Crenarchaeol (ng/g) | Isoprenoid GDGTs (μg/g) | Branched GDGTs (μg/g) | BIT | MI | $TEX_{86}$ | $TEX_{86}^{L}$ | $TEX_{86}^{H}$ |
|---|---|---|---|---|---|---|---|---|---|---|---|
| 671 | 26.2 | 30 | 7 | 27 | 0.06 | 0.30 | 0.90 | 0.21 | 0.52 | -0.42 | -0.28 |
| 676 | 79.2 | 1223 | 127 | 881 | 2.24 | 4.41 | 0.79 | 0.13 | 0.39 | -0.63 | -0.41 |
| 686 | 70.0 | 574 | 143 | 798 | 1.52 | 4.31 | 0.80 | 0.15 | 0.32 | -0.69 | -0.49 |
| 701 | 55.1 | 762 | 79 | 509 | 1.35 | 4.33 | 0.86 | 0.13 | 0.44 | -0.46 | -0.36 |
| 706 | 28.0 | 350 | 50 | 185 | 0.59 | 2.96 | 0.92 | 0.21 | 0.42 | -0.50 | -0.38 |
| 716 | 13.3 | 122 | 48 | 59 | 0.23 | 1.46 | 0.95 | 0.44 | 0.37 | -0.63 | -0.43 |
| 721 | 9.8 | 475 | 46 | 116 | 0.64 | 3.47 | 0.95 | 0.28 | 0.46 | -0.41 | -0.34 |
| 521 | 50.0 | 347 | 38 | 134 | 0.52 | 1.71 | 0.91 | 0.22 | 0.50 | -0.53 | -0.30 |

Appendix 4-2. GDGT proxy data and estimated pH and temperature for lake surface sediments.

| Site No. | Water Depth (cm) | CBT | MBT' | CBT-based pH | | | MBT'/CBT-based temperature (℃) | | |
|---|---|---|---|---|---|---|---|---|---|
| | | | | Ajioka et al. (2014) | Peterse et al. (2012) | Tierney et al. (2010) | Ajioka et al. (2014) | Peterse et al. (2012) | Tierney et al. (2010) |
| 671 | 26.2 | 0.52 | 0.33 | 6.82 | 6.87 | 8.74 | 6.87 | 7.94 | 17.3 |
| 676 | 79.2 | 0.36 | 0.25 | 7.16 | 7.20 | 9.24 | 5.78 | 6.49 | 16.4 |
| 686 | 70.0 | 0.36 | 0.24 | 7.16 | 7.19 | 9.23 | 5.50 | 6.16 | 16.0 |
| 701 | 55.1 | 0.35 | 0.24 | 7.17 | 7.21 | 9.26 | 5.52 | 6.18 | 16.1 |
| 706 | 28.0 | 0.31 | 0.27 | 7.25 | 7.28 | 9.37 | 6.58 | 7.38 | 17.5 |
| 716 | 13.3 | 0.71 | 0.45 | 6.42 | 6.49 | 8.16 | 9.17 | 10.86 | 19.9 |
| 721 | 9.8 | 0.28 | 0.35 | 7.32 | 7.34 | 9.46 | 8.87 | 10.04 | 20.4 |
| 521 | 50.0 | 0.46 | 0.28 | 6.95 | 7.00 | 8.93 | 6.05 | 6.91 | 16.5 |

Appendix 5. GDGT concentrations, proxy data and estimated pH and temperature for BIW07-6.

| Sample No. | Top depth (m) | Mid depth (m) | Age (ka) | Crenarchaeol (μg/g) | Isoprenoid GDGTs (μg/g) | Branched GDGTs (μg/g) | CBT | MBT' | BIT | CBT -based pH | MBT'/CBT -based temperature (℃) |
|---|---|---|---|---|---|---|---|---|---|---|---|
| 30 | 0.30 | 0.295 | 0.909 | 0.18 | 0.36 | 1.40 | 0.40 | 0.28 | 0.86 | 7.07 | 6.41 |
| 38 | 0.38 | 0.375 | 1.170 | 0.21 | 0.44 | 1.73 | 0.39 | 0.27 | 0.86 | 7.10 | 6.26 |
| 46 | 0.46 | 0.455 | 1.432 | 0.22 | 0.45 | 1.74 | 0.37 | 0.28 | 0.85 | 7.14 | 6.58 |
| 55 | 0.55 | 0.545 | 1.727 | 0.13 | 0.26 | 1.14 | 0.34 | 0.30 | 0.87 | 7.20 | 7.23 |
| 63 | 0.63 | 0.625 | 1.988 | 0.23 | 0.45 | 1.56 | 0.29 | 0.27 | 0.83 | 7.29 | 6.72 |
| 71 | 0.71 | 0.705 | 2.250 | 0.18 | 0.35 | 1.40 | 0.29 | 0.27 | 0.85 | 7.30 | 6.66 |
| 80 | 0.80 | 0.795 | 2.545 | 0.16 | 0.35 | 1.39 | 0.30 | 0.27 | 0.86 | 7.28 | 6.65 |
| 88 | 0.88 | 0.875 | 2.807 | 0.19 | 0.44 | 1.78 | 0.28 | 0.26 | 0.87 | 7.31 | 6.42 |
| 96 | 0.96 | 0.955 | 3.068 | 0.29 | 0.65 | 2.29 | 0.26 | 0.25 | 0.85 | 7.36 | 6.50 |
| 105 | 1.05 | 1.045 | 3.547 | 0.17 | 0.39 | 1.59 | 0.28 | 0.26 | 0.87 | 7.32 | 6.51 |
| 113 | 1.13 | 1.125 | 4.075 | 0.18 | 0.51 | 2.03 | 0.28 | 0.28 | 0.89 | 7.32 | 7.06 |
| 121 | 1.21 | 1.205 | 4.881 | 0.19 | 0.49 | 1.94 | 0.27 | 0.26 | 0.88 | 7.34 | 6.53 |
| 130 | 1.30 | 1.295 | 5.788 | 0.22 | 0.63 | 2.15 | 0.17 | 0.27 | 0.87 | 7.56 | 7.56 |
| 138 | 1.38 | 1.375 | 6.594 | 0.17 | 0.52 | 2.25 | 0.24 | 0.27 | 0.90 | 7.39 | 6.94 |
| 146 | 1.46 | 1.455 | 7.364 | 0.07 | 0.31 | 1.88 | 0.22 | 0.26 | 0.95 | 7.44 | 6.92 |
| 155 | 1.55 | 1.545 | 7.615 | 0.07 | 0.29 | 1.97 | 0.21 | 0.27 | 0.95 | 7.46 | 7.17 |
| 163 | 1.63 | 1.625 | 7.839 | 0.06 | 0.28 | 1.83 | 0.20 | 0.26 | 0.95 | 7.50 | 6.92 |
| 171 | 1.71 | 1.705 | 8.062 | 0.07 | 0.31 | 1.90 | 0.24 | 0.25 | 0.95 | 7.40 | 6.56 |
| 191 | 1.91 | 1.905 | 8.621 | 0.05 | 0.23 | 1.55 | 0.27 | 0.26 | 0.96 | 7.35 | 6.52 |
| 199 | 1.99 | 1.985 | 8.845 | 0.07 | 0.32 | 2.04 | 0.26 | 0.26 | 0.95 | 7.37 | 6.71 |
| 205 | 2.05 | 2.045 | 9.012 | 0.06 | 0.25 | 1.77 | 0.24 | 0.26 | 0.96 | 7.40 | 6.73 |
| 213 | 2.13 | 2.125 | 9.236 | 0.06 | 0.30 | 1.98 | 0.21 | 0.25 | 0.96 | 7.46 | 6.65 |
| 221 | 2.21 | 2.205 | 9.459 | 0.06 | 0.26 | 1.85 | 0.28 | 0.26 | 0.96 | 7.31 | 6.51 |
| 230 | 2.30 | 2.295 | 9.711 | 0.05 | 0.18 | 1.26 | 0.33 | 0.27 | 0.95 | 7.22 | 6.59 |
| 238 | 2.38 | 2.375 | 9.934 | 0.04 | 0.16 | 1.37 | 0.29 | 0.27 | 0.96 | 7.30 | 6.79 |
| 246 | 2.46 | 2.455 | 10.158 | 0.05 | 0.24 | 1.47 | 0.29 | 0.28 | 0.95 | 7.30 | 7.10 |
| 255 | 2.55 | 2.545 | 10.435 | 0.05 | 0.20 | 1.66 | 0.31 | 0.26 | 0.96 | 7.26 | 6.35 |
| 263 | 2.63 | 2.625 | 10.704 | 0.06 | 0.29 | 2.06 | 0.24 | 0.25 | 0.96 | 7.41 | 6.62 |
| 271 | 2.71 | 2.705 | 10.973 | 0.05 | 0.24 | 1.77 | 0.24 | 0.25 | 0.96 | 7.41 | 6.60 |
| 280 | 2.76 | 2.755 | 11.141 | 0.04 | 0.17 | 1.30 | 0.29 | 0.25 | 0.96 | 7.30 | 6.26 |
| 288 | 2.84 | 2.835 | 11.410 | 0.03 | 0.15 | 1.35 | 0.34 | 0.27 | 0.97 | 7.19 | 6.31 |
| 296 | 2.92 | 2.915 | 11.680 | 0.02 | 0.12 | 1.29 | 0.41 | 0.26 | 0.98 | 7.05 | 5.74 |
| 305 | 3.01 | 3.005 | 11.983 | 0.03 | 0.18 | 1.35 | 0.34 | 0.27 | 0.97 | 7.20 | 6.44 |
| 313 | 3.09 | 3.085 | 12.252 | 0.03 | 0.18 | 1.32 | 0.34 | 0.24 | 0.97 | 7.20 | 5.72 |
| 321 | 3.17 | 3.165 | 12.521 | 0.03 | 0.14 | 1.14 | 0.32 | 0.26 | 0.97 | 7.23 | 6.33 |
| 330 | 3.26 | 3.255 | 12.824 | 0.03 | 0.19 | 1.38 | 0.37 | 0.30 | 0.97 | 7.14 | 7.07 |
| 338 | 3.34 | 3.335 | 13.093 | 0.06 | 0.53 | 4.48 | 0.75 | 0.45 | 0.98 | 6.34 | 8.88 |
| 346 | 3.42 | 3.415 | 13.362 | 0.03 | 0.19 | 1.52 | 0.39 | 0.29 | 0.97 | 7.09 | 6.64 |
| 355 | 3.51 | 3.505 | 13.666 | 0.03 | 0.16 | 1.45 | 0.37 | 0.29 | 0.97 | 7.12 | 6.85 |
| 363 | 3.59 | 3.585 | 13.966 | 0.02 | 0.13 | 1.23 | 0.40 | 0.29 | 0.97 | 7.07 | 6.65 |
| 371 | 3.67 | 3.665 | 14.267 | 0.02 | 0.09 | 0.90 | 0.46 | 0.30 | 0.98 | 6.95 | 6.66 |
| 380 | 3.76 | 3.755 | 14.582 | 0.02 | 0.17 | 1.26 | 0.54 | 0.33 | 0.98 | 6.79 | 6.98 |
| 388 | 3.84 | 3.835 | 14.830 | 0.01 | 0.13 | 0.83 | 0.41 | 0.27 | 0.98 | 7.05 | 6.15 |
| 396 | 3.92 | 3.915 | 15.078 | 0.02 | 0.14 | 1.22 | 0.52 | 0.30 | 0.97 | 6.81 | 6.28 |
| 405 | 4.01 | 4.005 | 15.355 | 0.03 | 0.21 | 1.37 | 0.45 | 0.28 | 0.97 | 6.98 | 6.09 |
| 413 | 4.09 | 4.085 | 15.497 | 0.02 | 0.12 | 1.07 | 0.45 | 0.27 | 0.97 | 6.97 | 5.91 |
| 421 | 4.17 | 4.165 | 15.632 | 0.02 | 0.11 | 0.92 | 0.40 | 0.27 | 0.98 | 7.07 | 6.06 |
| 430 | 4.26 | 4.255 | 15.784 | 0.02 | 0.12 | 1.03 | 0.47 | 0.27 | 0.97 | 6.92 | 5.62 |
| 438 | 4.34 | 4.335 | 15.919 | 0.02 | 0.09 | 0.76 | 0.48 | 0.31 | 0.97 | 6.90 | 6.59 |
| 446 | 4.42 | 4.415 | 16.054 | 0.01 | 0.04 | 0.54 | 0.60 | 0.27 | 0.97 | 6.66 | 5.04 |
| 455 | 4.51 | 4.505 | 16.206 | 0.01 | 0.07 | 0.64 | 0.60 | 0.30 | 0.97 | 6.66 | 5.63 |
| 463 | 4.59 | 4.585 | 16.342 | 0.02 | 0.11 | 1.05 | 0.60 | 0.30 | 0.98 | 6.66 | 5.81 |
| 471 | 4.67 | 4.665 | 16.477 | 0.01 | 0.06 | 0.58 | 0.66 | 0.34 | 0.97 | 6.52 | 6.39 |
| 480 | 4.75 | 4.745 | 16.612 | 0.02 | 0.13 | 1.46 | 0.90 | 0.45 | 0.99 | 6.03 | 7.87 |
| 488 | 4.83 | 4.825 | 16.747 | 0.02 | 0.11 | 0.75 | 0.54 | 0.32 | 0.97 | 6.78 | 6.62 |
| 496 | 4.91 | 4.905 | 16.882 | 0.01 | 0.04 | 0.40 | 0.50 | 0.26 | 0.97 | 6.87 | 5.34 |
| 505 | 5.00 | 4.995 | 17.034 | 0.01 | 0.05 | 0.99 | 0.43 | 0.29 | 0.98 | 7.00 | 6.55 |
| 513 | 5.08 | 5.075 | 17.169 | 0.01 | 0.03 | 0.44 | 0.48 | 0.25 | 0.97 | 6.91 | 5.23 |
| 521 | 5.16 | 5.155 | 17.304 | 0.01 | 0.04 | 0.42 | 0.32 | 0.24 | 0.97 | 7.25 | 5.69 |
| 530 | 5.25 | 5.245 | 17.456 | 0.01 | 0.05 | 0.45 | 0.37 | 0.24 | 0.96 | 7.14 | 5.62 |
| 538 | 5.33 | 5.325 | 17.591 | 0.01 | 0.04 | 0.40 | 0.39 | 0.29 | 0.98 | 7.09 | 6.59 |
| 546 | 5.41 | 5.405 | 17.859 | 0.01 | 0.04 | 0.46 | 0.50 | 0.26 | 0.97 | 6.86 | 5.31 |
| 555 | 5.50 | 5.495 | 18.509 | 0.02 | 0.05 | 0.56 | 0.47 | 0.24 | 0.97 | 6.92 | 4.88 |
| 563 | 5.58 | 5.575 | 19.086 | 0.02 | 0.08 | 0.49 | 0.51 | 0.30 | 0.95 | 6.85 | 6.39 |
| 571 | 5.66 | 5.655 | 19.603 | 0.01 | 0.06 | 0.64 | 0.40 | 0.25 | 0.97 | 7.07 | 5.64 |

(Continue to the next page)

| Sample No. | Top depth (m) | Mid depth (m) | Age （ka） | Crenarchaeol (μg/g) | Isoprenoid GDGTs (μg/g) | Branched GDGTs (μg/g) | CBT | MBT' | BIT | CBT -based pH | MBT'/CBT -based temperature (℃) |
|---|---|---|---|---|---|---|---|---|---|---|---|
| 580 | 5.76 | 5.755 | 20.080 | 0.04 | 0.10 | 1.08 | 0.43 | 0.27 | 0.96 | 7.02 | 6.05 |
| 588 | 5.84 | 5.835 | 20.461 | 0.02 | 0.14 | 1.49 | 0.41 | 0.24 | 0.98 | 7.06 | 5.21 |
| 596 | 5.92 | 5.915 | 20.843 | 0.03 | 0.12 | 1.35 | 0.34 | 0.23 | 0.97 | 7.20 | 5.32 |
| 613 | 6.11 | 6.105 | 21.749 | 0.01 | 0.04 | 0.70 | 0.35 | 0.27 | 0.98 | 7.17 | 6.25 |
| 630 | 6.28 | 6.275 | 22.171 | 0.03 | 0.11 | 1.18 | 0.40 | 0.27 | 0.97 | 7.08 | 6.02 |
| 638 | 6.36 | 6.355 | 22.338 | 0.04 | 0.17 | 1.28 | 0.40 | 0.29 | 0.96 | 7.06 | 6.50 |
| 655 | 6.53 | 6.525 | 22.692 | 0.02 | 0.09 | 1.08 | 0.42 | 0.24 | 0.98 | 7.02 | 5.15 |
| 663 | 6.61 | 6.605 | 22.858 | 0.02 | 0.12 | 1.05 | 0.34 | 0.21 | 0.97 | 7.20 | 4.80 |
| 680 | 6.78 | 6.775 | 23.392 | 0.01 | 0.05 | 0.65 | 0.31 | 0.24 | 0.97 | 7.26 | 5.70 |
| 688 | 6.86 | 6.855 | 23.651 | 0.02 | 0.06 | 0.62 | 0.31 | 0.27 | 0.96 | 7.26 | 6.64 |
| 705 | 6.99 | 6.985 | 24.073 | 0.02 | 0.07 | 0.70 | 0.31 | 0.22 | 0.97 | 7.25 | 5.22 |
| 714 | 7.08 | 7.075 | 24.364 | 0.04 | 0.10 | 0.81 | 0.34 | 0.22 | 0.93 | 7.21 | 5.21 |
| 730 | 7.24 | 7.235 | 24.813 | 0.02 | 0.07 | 0.54 | 0.21 | 0.19 | 0.94 | 7.46 | 5.17 |
| 738 | 7.32 | 7.315 | 25.003 | 0.04 | 0.13 | 1.12 | 0.36 | 0.21 | 0.96 | 7.15 | 4.78 |
| 755 | 7.49 | 7.485 | 25.405 | 0.02 | 0.08 | 0.53 | 0.47 | 0.23 | 0.95 | 6.93 | 4.53 |
| 763 | 7.57 | 7.565 | 25.595 | 0.03 | 0.14 | 1.12 | 0.30 | 0.20 | 0.96 | 7.27 | 4.72 |
| 780 | 7.74 | 7.735 | 25.997 | 0.01 | 0.06 | 0.45 | 0.42 | 0.26 | 0.96 | 7.04 | 5.78 |
| 788 | 7.82 | 7.815 | 26.186 | 0.02 | 0.07 | 0.68 | 0.37 | 0.26 | 0.96 | 7.13 | 5.93 |
| 805 | 7.92 | 7.915 | 26.423 | 0.02 | 0.07 | 0.52 | 0.35 | 0.25 | 0.96 | 7.18 | 5.80 |
| 813 | 8.00 | 7.995 | 26.613 | 0.02 | 0.06 | 0.65 | 0.33 | 0.24 | 0.96 | 7.23 | 5.71 |
| 830 | 8.17 | 8.165 | 27.015 | 0.02 | 0.06 | 0.48 | 0.39 | 0.26 | 0.95 | 7.09 | 5.78 |
| 838 | 8.25 | 8.245 | 27.204 | 0.02 | 0.08 | 0.54 | 0.34 | 0.26 | 0.94 | 7.19 | 6.26 |
| 855 | 8.42 | 8.415 | 27.607 | 0.02 | 0.06 | 0.53 | 0.39 | 0.21 | 0.95 | 7.09 | 4.61 |
| 863 | 8.50 | 8.495 | 27.796 | 0.02 | 0.06 | 0.64 | 0.39 | 0.24 | 0.96 | 7.09 | 5.31 |
| 880 | 8.67 | 8.665 | 28.090 | 0.02 | 0.07 | 0.60 | 0.42 | 0.25 | 0.95 | 7.04 | 5.58 |
| 888 | 8.75 | 8.745 | 28.218 | 0.03 | 0.08 | 0.62 | 0.43 | 0.24 | 0.95 | 7.00 | 5.20 |
| 905 | 8.92 | 8.915 | 28.489 | 0.02 | 0.05 | 0.43 | 0.42 | 0.22 | 0.95 | 7.03 | 4.55 |
| 913 | 9.00 | 8.995 | 28.616 | 0.02 | 0.06 | 0.42 | 0.29 | 0.25 | 0.94 | 7.31 | 6.18 |
| 920 | 9.17 | 9.165 | 28.887 | 0.02 | 0.03 | 0.19 | 0.44 | 0.25 | 0.89 | 6.98 | 5.22 |
| 938 | 9.25 | 9.245 | 29.014 | 0.02 | 0.04 | 0.27 | 0.58 | 0.23 | 0.92 | 6.69 | 3.99 |
| 955 | 9.42 | 9.415 | 29.285 | 0.00 | 0.02 | 0.14 | 0.74 | 0.25 | 0.97 | 6.37 | 3.71 |
| 963 | 9.50 | 9.495 | 29.413 | 0.01 | 0.04 | 0.30 | 0.71 | 0.22 | 0.98 | 6.42 | 3.07 |
| 971 | 9.58 | 9.575 | 29.540 | 0.00 | 0.01 | 0.05 | 0.54 | 0.28 | 0.96 | 6.77 | 5.58 |
| 1005 | 9.92 | 9.915 | 30.058 | 0.03 | 0.07 | 0.51 | 0.44 | 0.23 | 0.93 | 6.99 | 4.87 |
| 1013 | 10.00 | 9.995 | 30.144 | 0.04 | 0.08 | 0.38 | 0.45 | 0.25 | 0.88 | 6.96 | 5.22 |
| 1030 | 10.17 | 10.165 | 30.325 | 0.02 | 0.08 | 0.64 | 0.36 | 0.25 | 0.95 | 7.15 | 5.77 |
| 1046 | 10.33 | 10.325 | 30.495 | 0.01 | 0.07 | 0.63 | 0.35 | 0.25 | 0.97 | 7.17 | 5.92 |
| 1061 | 10.48 | 10.475 | 30.655 | 0.01 | 0.07 | 0.70 | 0.34 | 0.22 | 0.97 | 7.19 | 5.23 |
| 1069 | 10.55 | 10.545 | 30.730 | 0.01 | 0.16 | 0.86 | 0.28 | 0.24 | 0.98 | 7.33 | 6.15 |
| 1086 | 10.72 | 10.715 | 30.911 | 0.02 | 0.11 | 0.71 | 0.25 | 0.24 | 0.97 | 7.38 | 6.06 |
| 1095 | 10.81 | 10.805 | 31.007 | 0.02 | 0.14 | 0.81 | 0.25 | 0.21 | 0.96 | 7.38 | 5.50 |
| 1111 | 10.97 | 10.965 | 31.178 | 0.01 | 0.05 | 0.64 | 0.33 | 0.22 | 0.97 | 7.22 | 5.25 |
| 1136 | 11.22 | 11.215 | 31.444 | 0.02 | 0.09 | 0.85 | 0.35 | 0.24 | 0.97 | 7.17 | 5.51 |
| 1161 | 11.45 | 11.445 | 31.690 | 0.02 | 0.08 | 0.78 | 0.41 | 0.25 | 0.97 | 7.05 | 5.50 |
| 1186 | 11.70 | 11.695 | 32.105 | 0.03 | 0.14 | 1.03 | 0.31 | 0.23 | 0.96 | 7.26 | 5.46 |
| 1211 | 11.95 | 11.945 | 32.656 | 0.02 | 0.13 | 1.09 | 0.36 | 0.25 | 0.97 | 7.16 | 5.92 |
| 1236 | 12.20 | 12.195 | 33.245 | 0.03 | 0.17 | 1.24 | 0.36 | 0.24 | 0.97 | 7.16 | 5.67 |
| 1261 | 12.38 | 12.375 | 33.682 | 0.04 | 0.19 | 0.85 | 0.34 | 0.25 | 0.94 | 7.19 | 5.83 |
| 1286 | 12.63 | 12.625 | 34.290 | 0.04 | 0.22 | 1.59 | 0.22 | 0.23 | 0.96 | 7.44 | 6.15 |
| 1311 | 12.88 | 12.875 | 34.899 | 0.02 | 0.09 | 0.84 | 0.33 | 0.27 | 0.98 | 7.23 | 6.45 |
| 1336 | 13.13 | 13.125 | 35.507 | 0.02 | 0.10 | 0.87 | 0.35 | 0.27 | 0.97 | 7.18 | 6.52 |
| 1361 | 13.35 | 13.345 | 36.042 | 0.01 | 0.07 | 0.74 | 0.35 | 0.24 | 0.97 | 7.18 | 5.71 |
| 1386 | 13.60 | 13.595 | 36.650 | 0.02 | 0.08 | 0.92 | 0.31 | 0.24 | 0.98 | 7.27 | 5.91 |
| 1411 | 13.85 | 13.845 | 37.258 | 0.02 | 0.07 | 0.86 | 0.34 | 0.25 | 0.97 | 7.19 | 5.88 |
| 1436 | 14.10 | 14.095 | 37.866 | 0.03 | 0.14 | 1.28 | 0.38 | 0.26 | 0.97 | 7.12 | 6.10 |
| 1461 | 14.33 | 14.325 | 38.425 | 0.02 | 0.09 | 0.97 | 0.33 | 0.25 | 0.97 | 7.22 | 5.86 |
| 1486 | 14.58 | 14.575 | 39.033 | 0.02 | 0.12 | 1.20 | 0.25 | 0.26 | 0.97 | 7.38 | 6.62 |
| 1511 | 14.83 | 14.825 | 39.641 | 0.02 | 0.10 | 0.99 | 0.30 | 0.24 | 0.97 | 7.29 | 5.99 |
| 1536 | 15.08 | 15.075 | 40.250 | 0.02 | 0.09 | 0.91 | 0.25 | 0.24 | 0.97 | 7.38 | 6.06 |
| 1561 | 15.33 | 15.325 | 40.858 | 0.02 | 0.09 | 0.93 | 0.28 | 0.25 | 0.97 | 7.32 | 6.37 |
| 1586 | 15.55 | 15.545 | 41.221 | 0.03 | 0.12 | 0.92 | 0.28 | 0.25 | 0.96 | 7.32 | 6.29 |
| 1611 | 15.80 | 15.795 | 41.600 | 0.02 | 0.08 | 0.73 | 0.27 | 0.24 | 0.97 | 7.34 | 6.02 |
| 1636 | 16.05 | 16.045 | 41.978 | 0.02 | 0.09 | 0.68 | 0.22 | 0.25 | 0.97 | 7.45 | 6.59 |
| 1661 | 16.30 | 16.295 | 42.357 | 0.02 | 0.12 | 1.01 | 0.19 | 0.25 | 0.97 | 7.51 | 6.79 |
| 1686 | 16.54 | 16.535 | 42.721 | 0.02 | 0.07 | 0.74 | 0.30 | 0.25 | 0.97 | 7.27 | 6.15 |
| 1711 | 16.79 | 16.785 | 43.100 | 0.02 | 0.11 | 0.87 | 0.27 | 0.24 | 0.96 | 7.34 | 6.11 |

(Continue to the next page)

| Sample No. | Top depth (m) | Mid depth (m) | Age（ka） | Crenarchaeol (μg/g) | Isoprenoid GDGTs (μg/g) | Branched GDGTs (μg/g) | CBT | MBT' | BIT | CBT -based pH | MBT'/CBT -based temperature (℃) |
|---|---|---|---|---|---|---|---|---|---|---|---|
| 1736 | 17.04 | 17.035 | 43.479 | 0.03 | 0.13 | 1.21 | 0.25 | 0.24 | 0.97 | 7.38 | 6.17 |
| 1761 | 17.29 | 17.285 | 43.858 | 0.04 | 0.16 | 1.37 | 0.18 | 0.23 | 0.96 | 7.52 | 6.37 |
| 1786 | 17.54 | 17.535 | 44.237 | 0.03 | 0.14 | 1.44 | 0.18 | 0.24 | 0.97 | 7.53 | 6.48 |
| 1811 | 17.79 | 17.785 | 44.787 | 0.04 | 0.18 | 1.50 | 0.28 | 0.23 | 0.96 | 7.32 | 5.78 |
| 1836 | 18.04 | 18.035 | 45.495 | 0.03 | 0.16 | 1.38 | 0.19 | 0.25 | 0.96 | 7.50 | 6.77 |
| 1861 | 18.29 | 18.285 | 46.204 | 0.03 | 0.14 | 1.31 | 0.30 | 0.27 | 0.97 | 7.28 | 6.71 |

Appendix 6. GDGT concentrations, proxy data and estimated pH and temperature for BIW08-B.

| Sample No. | Top depth (m) | Mid depth (m) | Age (ka) | Crenarchaeol (μg/g) | Isoprenoid GDGTs (μg/g) | Branched GDGTs (μg/g) | CBT | MBT' | BIT | CBT -based pH | MBT'/CBT -based temperature (℃) |
|---|---|---|---|---|---|---|---|---|---|---|---|
| 8-1 8 | 13.495 | 13.5075 | 42.353 | 0.04 | 0.21 | 2.01 | 0.29 | 0.26 | 0.97 | 7.29 | 6.58 |
| 8-1 28 | 13.995 | 14.0075 | 43.047 | 0.04 | 0.18 | 1.61 | 0.41 | 0.26 | 0.97 | 7.05 | 5.87 |
| 8-2 12 | 14.480 | 14.4925 | 43.700 | 0.05 | 0.27 | 2.21 | 0.32 | 0.26 | 0.97 | 7.23 | 6.33 |
| 8-2 30 | 14.930 | 14.9425 | 44.652 | 0.07 | 0.32 | 2.76 | 0.29 | 0.26 | 0.97 | 7.30 | 6.56 |
| 9-1 7 | 15.495 | 15.5075 | 47.156 | 0.06 | 0.30 | 2.72 | 0.29 | 0.28 | 0.97 | 7.30 | 6.90 |
| 9-1 27 | 15.995 | 16.0075 | 49.371 | 0.03 | 0.17 | 1.58 | 0.52 | 0.31 | 0.98 | 6.82 | 6.43 |
| 9-2 18 | 16.490 | 16.5025 | 51.564 | 0.03 | 0.18 | 1.96 | 0.62 | 0.35 | 0.98 | 6.61 | 6.86 |
| 9-2 37 | 16.965 | 16.9775 | 53.669 | 0.04 | 0.17 | 1.95 | 0.52 | 0.32 | 0.98 | 6.83 | 6.78 |
| 10-1 16 | 17.490 | 17.5025 | 55.995 | 0.03 | 0.16 | 1.93 | 0.55 | 0.34 | 0.98 | 6.75 | 7.06 |
| 10-1 36 | 17.990 | 18.0025 | 58.210 | 0.04 | 0.24 | 2.84 | 0.61 | 0.38 | 0.98 | 6.64 | 7.69 |
| 10-2 19 | 18.475 | 18.4875 | 60.359 | 0.06 | 0.27 | 2.92 | 0.48 | 0.31 | 0.98 | 6.90 | 6.75 |
| 10-2 38 | 18.950 | 18.9625 | 62.464 | 0.09 | 0.54 | 7.53 | 0.44 | 0.35 | 0.98 | 6.99 | 8.08 |
| 11-1 6 | 19.490 | 19.5025 | 64.856 | 0.05 | 0.34 | 3.29 | 0.37 | 0.31 | 0.98 | 7.14 | 7.37 |
| 11-1 26 | 19.990 | 20.0025 | 67.071 | 0.05 | 0.32 | 3.05 | 0.45 | 0.34 | 0.98 | 6.96 | 7.61 |
| 11-2 18 | 20.450 | 20.4625 | 69.110 | 0.08 | 0.49 | 4.01 | 0.37 | 0.32 | 0.97 | 7.14 | 7.66 |
| 11-2 38 | 20.950 | 20.9625 | 71.325 | 0.04 | 0.20 | 2.04 | 0.30 | 0.29 | 0.97 | 7.28 | 7.30 |
| 12-1 15 | 21.970 | 21.9825 | 75.844 | 0.08 | 0.37 | 3.11 | 0.33 | 0.31 | 0.97 | 7.22 | 7.59 |
| 12-2 14 | 22.450 | 22.4625 | 77.971 | 0.11 | 0.58 | 4.06 | 0.27 | 0.31 | 0.96 | 7.34 | 8.00 |
| 12-2 34 | 22.950 | 22.9625 | 80.186 | 0.12 | 0.55 | 4.54 | 0.30 | 0.34 | 0.96 | 7.29 | 8.42 |
| 13-1 19 | 23.985 | 23.9975 | 84.504 | 0.07 | 0.33 | 2.95 | 0.32 | 0.32 | 0.97 | 7.24 | 7.92 |
| 13-2 14 | 24.465 | 24.4775 | 86.588 | 0.08 | 0.50 | 3.58 | 0.35 | 0.30 | 0.97 | 7.19 | 7.33 |
| 13-2 34 | 24.965 | 24.9775 | 88.759 | 0.07 | 0.33 | 3.85 | 0.38 | 0.30 | 0.97 | 7.10 | 6.97 |
| 14-1 2 | 25.510 | 25.5225 | 91.125 | 0.07 | 0.33 | 2.96 | 0.35 | 0.29 | 0.97 | 7.18 | 7.01 |
| 14-1 22 | 26.010 | 26.0225 | 93.296 | 0.08 | 0.64 | 3.49 | 0.38 | 0.33 | 0.97 | 7.12 | 7.71 |
| 14-2 14 | 26.470 | 26.4825 | 95.293 | 0.09 | 0.81 | 5.49 | 0.42 | 0.32 | 0.98 | 7.03 | 7.38 |
| 14-2 34 | 26.970 | 26.9825 | 98.130 | 0.14 | 1.25 | 7.11 | 0.35 | 0.31 | 0.97 | 7.18 | 7.50 |
| 15-1 10 | 27.495 | 27.5075 | 102.438 | 0.12 | 0.62 | 4.19 | 0.41 | 0.31 | 0.96 | 7.06 | 7.12 |
| 15-1 30 | 27.995 | 28.0075 | 105.828 | 0.15 | 0.77 | 4.57 | 0.31 | 0.30 | 0.96 | 7.25 | 7.37 |
| 15-2 15 | 28.475 | 28.4875 | 108.181 | 0.11 | 0.92 | 3.63 | 0.24 | 0.30 | 0.96 | 7.40 | 7.93 |
| 16-1 14 | 29.475 | 29.4875 | 109.247 | 0.08 | 0.41 | 2.22 | 0.32 | 0.32 | 0.95 | 7.23 | 7.94 |
| 16-1 34 | 29.975 | 29.9875 | 109.781 | 0.11 | 0.70 | 5.17 | 0.32 | 0.28 | 0.97 | 7.24 | 6.89 |
| 16-2 17 | 30.470 | 30.4825 | 110.309 | 0.09 | 0.61 | 5.36 | 0.41 | 0.33 | 0.98 | 7.05 | 7.60 |
| 16-2 37 | 30.970 | 30.9825 | 110.842 | 0.21 | 0.93 | 7.80 | 0.39 | 0.33 | 0.96 | 7.08 | 7.73 |
| 17-1 10 | 31.480 | 31.4925 | 111.386 | 0.24 | 0.80 | 5.76 | 0.39 | 0.32 | 0.95 | 7.09 | 7.46 |
| 17-1 30 | 31.980 | 31.9925 | 111.920 | 0.37 | 1.30 | 8.54 | 0.39 | 0.31 | 0.94 | 7.09 | 7.13 |
| 17-2 15 | 32.460 | 32.4725 | 112.432 | 0.42 | 1.29 | 7.45 | 0.44 | 0.33 | 0.93 | 7.00 | 7.39 |
| 17-2 35 | 32.960 | 32.9725 | 112.965 | 0.55 | 1.74 | 8.69 | 0.35 | 0.29 | 0.92 | 7.18 | 7.02 |
| 18-1 9 | 33.480 | 33.4925 | 113.520 | 0.47 | 1.79 | 6.45 | 0.33 | 0.31 | 0.91 | 7.21 | 7.55 |
| 18-1 29 | 33.980 | 33.9925 | 114.053 | 0.61 | 1.62 | 6.54 | 0.30 | 0.31 | 0.88 | 7.29 | 7.77 |
| 18-2 14 | 34.450 | 34.4625 | 114.554 | 0.72 | 2.44 | 7.83 | 0.29 | 0.28 | 0.88 | 7.31 | 7.15 |
| 18-2 34 | 34.950 | 34.9625 | 115.141 | 0.41 | 1.69 | 6.49 | 0.26 | 0.29 | 0.92 | 7.36 | 7.40 |
| 19-1 11 | 35.570 | 35.5825 | 116.018 | 0.36 | 2.16 | 7.39 | 0.29 | 0.30 | 0.93 | 7.31 | 7.47 |
| 19-1 31 | 36.070 | 36.0825 | 116.725 | 0.16 | 1.02 | 5.71 | 0.27 | 0.32 | 0.96 | 7.35 | 8.09 |
| 19-2 14 | 36.470 | 36.4825 | 117.291 | 0.14 | 1.00 | 5.90 | 0.24 | 0.33 | 0.97 | 7.40 | 8.58 |
| 19-2 34 | 36.970 | 36.9825 | 117.998 | 0.16 | 1.28 | 6.97 | 0.27 | 0.32 | 0.97 | 7.35 | 8.12 |
| 20-1 14 | 37.480 | 37.4925 | 118.719 | 0.09 | 0.52 | 4.13 | 0.29 | 0.33 | 0.97 | 7.30 | 8.25 |
| 20-1 34 | 37.980 | 37.9925 | 119.426 | 0.17 | 0.92 | 6.54 | 0.29 | 0.32 | 0.96 | 7.29 | 8.15 |
| 20-2 19 | 38.460 | 38.4725 | 120.105 | 0.07 | 0.37 | 3.37 | 0.34 | 0.37 | 0.97 | 7.19 | 8.98 |
| 20-2 39 | 38.960 | 38.9725 | 120.812 | 0.09 | 0.40 | 3.56 | 0.39 | 0.36 | 0.97 | 7.10 | 8.50 |
| 21-1 19 | 39.490 | 39.5025 | 121.728 | 0.14 | 0.90 | 9.19 | 0.39 | 0.33 | 0.98 | 7.10 | 7.64 |
| 21-2 16 | 39.990 | 40.0025 | 122.597 | 0.11 | 0.67 | 7.75 | 0.60 | 0.31 | 0.98 | 6.65 | 6.06 |
| 21-2 35 | 40.465 | 40.4775 | 123.423 | 0.12 | 0.61 | 7.82 | 0.75 | 0.36 | 0.98 | 6.33 | 6.39 |
| 22-2 2 | 40.990 | 41.0025 | 125.576 | 0.09 | 0.50 | 5.93 | 0.52 | 0.33 | 0.98 | 6.82 | 6.90 |
| 22-2 22 | 41.490 | 41.5025 | 127.948 | 0.06 | 0.21 | 2.01 | 0.56 | 0.32 | 0.96 | 6.74 | 6.57 |
| 23 21 | 42.040 | 42.0525 | 130.557 | 0.08 | 0.41 | 5.02 | 0.52 | 0.28 | 0.98 | 6.82 | 5.76 |
| 24 4 | 42.485 | 42.4975 | 132.668 | 0.09 | 0.55 | 4.75 | 0.43 | 0.30 | 0.98 | 7.02 | 6.76 |
| 24 24 | 42.985 | 42.9975 | 135.040 | 0.05 | 0.23 | 2.79 | 0.47 | 0.30 | 0.98 | 6.92 | 6.43 |
| 25 7 | 43.490 | 43.5025 | 137.436 | 0.08 | 0.33 | 3.83 | 0.44 | 0.30 | 0.97 | 6.99 | 6.67 |
| 25 27 | 43.990 | 44.0025 | 139.808 | 0.06 | 0.29 | 3.97 | 0.55 | 0.34 | 0.98 | 6.77 | 7.17 |
| 26 7 | 44.500 | 44.5125 | 142.228 | 0.05 | 0.21 | 2.72 | 0.47 | 0.30 | 0.98 | 6.92 | 6.47 |
| 26 27 | 45.000 | 45.0125 | 144.049 | 0.06 | 0.26 | 3.52 | 0.49 | 0.33 | 0.98 | 6.89 | 7.10 |
| 27 15 | 45.490 | 45.5025 | 145.585 | 0.06 | 0.26 | 3.45 | 0.48 | 0.31 | 0.98 | 6.91 | 6.72 |
| 27 34 | 45.965 | 45.9775 | 147.074 | 0.07 | 0.25 | 2.12 | 0.57 | 0.32 | 0.96 | 6.71 | 6.47 |
| 28 17 | 46.480 | 46.4925 | 148.689 | 0.05 | 0.22 | 2.45 | 0.58 | 0.35 | 0.98 | 6.69 | 7.07 |
| 29 4 | 46.980 | 46.9925 | 150.256 | 0.04 | 0.24 | 2.81 | 0.46 | 0.31 | 0.98 | 6.96 | 6.91 |

(Continue to the next page)

| Sample No. | Top depth (m) | Mid depth (m) | Age (ka) | Crenarchaeol (μg/g) | Isoprenoid GDGTs (μg/g) | Branched GDGTs (μg/g) | CBT | MBT' | BIT | CBT -based pH | MBT'/CBT -based temperature (℃) |
|---|---|---|---|---|---|---|---|---|---|---|---|
| 29 24 | 47.480 | 47.4925 | 151.824 | 0.04 | 0.16 | 1.46 | 0.57 | 0.31 | 0.97 | 6.72 | 6.09 |
| 30 4 | 47.995 | 48.0075 | 153.439 | 0.05 | 0.19 | 2.06 | 0.48 | 0.33 | 0.97 | 6.92 | 7.13 |
| 30 24 | 48.495 | 48.5075 | 155.006 | 0.04 | 0.18 | 1.89 | 0.55 | 0.35 | 0.97 | 6.76 | 7.28 |
| 31 12 | 48.995 | 49.0075 | 156.574 | 0.06 | 0.26 | 2.18 | 0.54 | 0.30 | 0.97 | 6.79 | 6.09 |
| 31 32 | 49.495 | 49.5075 | 158.141 | 0.07 | 0.31 | 2.82 | 0.42 | 0.28 | 0.97 | 7.02 | 6.36 |
| 32 15 | 49.990 | 50.0025 | 159.693 | 0.11 | 0.48 | 4.49 | 0.33 | 0.28 | 0.97 | 7.21 | 6.65 |
| 32 34 | 50.465 | 50.4775 | 161.183 | 0.14 | 0.67 | 5.04 | 0.35 | 0.28 | 0.96 | 7.18 | 6.70 |
| 33 19 | 50.980 | 50.9925 | 162.797 | 0.12 | 0.44 | 5.03 | 0.37 | 0.27 | 0.97 | 7.14 | 6.27 |
| 34 4 | 51.485 | 51.4975 | 164.381 | 0.10 | 0.35 | 3.65 | 0.47 | 0.31 | 0.97 | 6.92 | 6.61 |
| 34 23 | 51.985 | 51.9975 | 165.948 | 0.14 | 0.53 | 4.85 | 0.38 | 0.30 | 0.96 | 7.11 | 6.93 |
| 36 4 | 52.480 | 52.4925 | 167.500 | 0.07 | 0.26 | 2.76 | 0.49 | 0.31 | 0.97 | 6.89 | 6.63 |
| 36 24 | 52.980 | 52.9925 | 169.068 | 0.08 | 0.31 | 3.24 | 0.47 | 0.30 | 0.97 | 6.94 | 6.63 |
| 37 4 | 53.465 | 53.4775 | 170.588 | 0.11 | 0.51 | 4.41 | 0.48 | 0.31 | 0.97 | 6.90 | 6.59 |
| 37 24 | 53.965 | 53.9775 | 172.156 | 0.06 | 0.28 | 2.57 | 0.58 | 0.34 | 0.97 | 6.69 | 6.88 |
| 38 2 | 54.480 | 54.4925 | 173.770 | 0.08 | 0.30 | 2.97 | 0.48 | 0.29 | 0.97 | 6.90 | 6.26 |
| 38 22 | 54.980 | 54.9925 | 175.338 | 0.09 | 0.45 | 4.68 | 0.58 | 0.35 | 0.98 | 6.69 | 7.20 |
| 39 4 | 55.485 | 55.4975 | 176.921 | 0.09 | 0.42 | 4.23 | 0.58 | 0.34 | 0.97 | 6.70 | 6.82 |
| 39 24 | 55.985 | 55.9975 | 178.489 | 0.09 | 0.34 | 3.14 | 0.73 | 0.33 | 0.97 | 6.38 | 5.80 |
| 40 2 | 56.490 | 56.5025 | 180.072 | 0.11 | 0.54 | 6.63 | 0.47 | 0.33 | 0.98 | 6.93 | 7.32 |
| 40 22 | 56.990 | 57.0025 | 181.640 | 0.09 | 0.49 | 4.08 | 0.45 | 0.31 | 0.97 | 6.98 | 6.94 |
| 41 5 | 57.460 | 57.4725 | 183.113 | 0.08 | 0.41 | 4.22 | 0.46 | 0.30 | 0.98 | 6.95 | 6.65 |
| 41 25 | 57.960 | 57.9725 | 184.681 | 0.10 | 0.52 | 5.52 | 0.46 | 0.32 | 0.98 | 6.95 | 7.19 |
| 42 4 | 58.475 | 58.4875 | 186.296 | 0.15 | 0.63 | 6.05 | 0.42 | 0.30 | 0.97 | 7.04 | 6.86 |
| 42 24 | 58.975 | 58.9875 | 187.863 | 0.19 | 0.93 | 7.47 | 0.43 | 0.30 | 0.97 | 7.01 | 6.86 |
| 43 4 | 59.500 | 59.5125 | 189.509 | 0.07 | 0.29 | 2.83 | 0.44 | 0.31 | 0.97 | 6.98 | 6.87 |
| 43 24 | 60.000 | 60.0125 | 191.077 | 0.05 | 0.21 | 1.99 | 0.43 | 0.28 | 0.97 | 7.02 | 6.31 |
| 44 4 | 60.510 | 60.5225 | 192.676 | 0.17 | 0.91 | 5.94 | 0.30 | 0.27 | 0.96 | 7.28 | 6.71 |
| 44 24 | 61.010 | 61.0225 | 194.243 | 0.16 | 0.72 | 4.91 | 0.29 | 0.30 | 0.96 | 7.30 | 7.57 |
| 45 4 | 61.455 | 61.4675 | 195.638 | 0.21 | 0.89 | 6.01 | 0.26 | 0.30 | 0.95 | 7.36 | 7.63 |
| 45 24 | 61.955 | 61.9675 | 197.206 | 0.24 | 1.15 | 6.43 | 0.34 | 0.27 | 0.95 | 7.20 | 6.35 |
| 46 4 | 62.505 | 62.5175 | 198.930 | 0.23 | 1.16 | 10.68 | 0.48 | 0.32 | 0.97 | 6.90 | 6.94 |
| 46 24 | 63.005 | 63.0175 | 200.498 | 0.29 | 1.24 | 9.14 | 0.34 | 0.31 | 0.96 | 7.19 | 7.40 |
| 47 4 | 63.485 | 63.4975 | 202.003 | 0.34 | 1.36 | 9.82 | 0.34 | 0.29 | 0.95 | 7.19 | 6.97 |
| 47 24 | 63.985 | 63.9975 | 203.570 | 0.38 | 1.28 | 7.26 | 0.31 | 0.31 | 0.93 | 7.26 | 7.65 |
| 48 2 | 64.475 | 64.4875 | 205.107 | 0.48 | 1.53 | 7.59 | 0.36 | 0.32 | 0.92 | 7.16 | 7.78 |
| 48 22 | 64.975 | 64.9875 | 206.674 | 0.85 | 2.55 | 9.04 | 0.28 | 0.31 | 0.88 | 7.31 | 7.80 |
| 49 4 | 65.435 | 65.4475 | 208.116 | 0.77 | 2.52 | 7.92 | 0.28 | 0.31 | 0.87 | 7.31 | 7.76 |
| 49 24 | 65.935 | 65.9475 | 209.684 | 0.30 | 1.16 | 5.41 | 0.26 | 0.32 | 0.93 | 7.36 | 8.13 |
| 50 4 | 66.475 | 66.4875 | 211.377 | 0.17 | 0.78 | 6.14 | 0.34 | 0.32 | 0.96 | 7.19 | 7.79 |
| 50 24 | 66.975 | 66.9875 | 212.945 | 0.13 | 0.47 | 4.92 | 0.41 | 0.29 | 0.97 | 7.06 | 6.73 |
| 51 4 | 67.475 | 67.4875 | 214.512 | 0.15 | 0.51 | 4.48 | 0.50 | 0.31 | 0.96 | 6.87 | 6.59 |
| 51 24 | 67.975 | 67.9875 | 216.080 | 0.13 | 0.49 | 4.04 | 0.52 | 0.36 | 0.96 | 6.82 | 7.76 |
| 52 5 | 68.470 | 68.4825 | 217.632 | 0.13 | 0.46 | 5.04 | 0.46 | 0.34 | 0.97 | 6.95 | 7.70 |
| 52 25 | 68.970 | 68.9825 | 219.199 | 0.14 | 0.54 | 5.51 | 0.56 | 0.33 | 0.97 | 6.75 | 6.91 |
| 53 5 | 69.510 | 69.5225 | 220.892 | 0.20 | 0.93 | 7.82 | 0.40 | 0.33 | 0.97 | 7.08 | 7.64 |
| 53 25 | 70.010 | 70.0225 | 222.460 | 0.22 | 0.94 | 7.83 | 0.38 | 0.33 | 0.96 | 7.11 | 7.91 |
| 54 5 | 70.500 | 70.5125 | 223.996 | 0.15 | 0.82 | 7.38 | 0.45 | 0.31 | 0.97 | 6.97 | 6.91 |
| 54 25 | 71.000 | 71.0125 | 225.564 | 0.34 | 1.68 | 11.23 | 0.42 | 0.31 | 0.96 | 7.02 | 7.13 |
| 55 6 | 71.495 | 71.5075 | 227.116 | 0.12 | 0.53 | 4.79 | 0.46 | 0.34 | 0.97 | 6.95 | 7.73 |
| 55 26 | 71.955 | 71.9675 | 228.558 | 0.35 | 1.65 | 12.32 | 0.37 | 0.32 | 0.96 | 7.13 | 7.68 |
| 56 6 | 72.525 | 72.5375 | 230.345 | 0.42 | 2.00 | 12.58 | 0.34 | 0.33 | 0.95 | 7.19 | 7.90 |
| 56 26 | 73.025 | 73.0375 | 231.913 | 0.43 | 1.75 | 9.78 | 0.35 | 0.32 | 0.94 | 7.17 | 7.63 |
| 57 6 | 73.525 | 73.5375 | 233.480 | 0.43 | 1.48 | 7.74 | 0.32 | 0.33 | 0.93 | 7.24 | 8.14 |
| 57 26 | 74.025 | 74.0375 | 235.048 | 0.42 | 1.48 | 6.49 | 0.30 | 0.32 | 0.91 | 7.27 | 8.06 |
| 58 6 | 74.505 | 74.5175 | 236.553 | 0.67 | 2.03 | 8.15 | 0.26 | 0.32 | 0.89 | 7.36 | 8.17 |
| 58 26 | 75.005 | 75.0175 | 238.120 | 0.55 | 1.54 | 6.22 | 0.26 | 0.34 | 0.88 | 7.35 | 8.68 |
| 59 6 | 75.515 | 75.5275 | 239.719 | 0.64 | 2.06 | 8.03 | 0.22 | 0.35 | 0.89 | 7.44 | 9.16 |
| 59 26 | 76.015 | 76.0275 | 241.287 | 0.31 | 0.98 | 4.93 | 0.29 | 0.36 | 0.91 | 7.31 | 9.13 |
| 60 6 | 76.505 | 76.5175 | 242.823 | 0.22 | 1.00 | 5.83 | 0.29 | 0.36 | 0.95 | 7.29 | 9.08 |
| 60 26 | 77.005 | 77.0175 | 244.391 | 0.23 | 1.07 | 6.69 | 0.27 | 0.36 | 0.95 | 7.33 | 9.07 |
| 61 2 | 77.475 | 77.4875 | 245.864 | 0.19 | 0.94 | 7.40 | 0.37 | 0.33 | 0.96 | 7.14 | 7.95 |
| 61 22 | 77.975 | 77.9875 | 247.432 | 0.16 | 0.76 | 8.01 | 0.34 | 0.31 | 0.97 | 7.20 | 7.51 |
| 62 2 | 78.405 | 78.4175 | 248.780 | 0.30 | 1.32 | 10.24 | 0.21 | 0.30 | 0.96 | 7.47 | 8.03 |
| 62 22 | 78.905 | 78.9175 | 250.348 | 0.18 | 1.08 | 6.87 | 0.32 | 0.29 | 0.96 | 7.24 | 7.17 |
| 62 39 | 79.330 | 79.3425 | 251.680 | 0.21 | 1.30 | 7.75 | 0.29 | 0.33 | 0.96 | 7.31 | 8.29 |
| 64 3 | 79.600 | 79.6125 | 252.527 | 0.31 | 1.37 | 9.16 | 0.36 | 0.31 | 0.95 | 7.16 | 7.50 |

(Continue to the next page)

| Sample No. | Top depth (m) | Mid depth (m) | Age （ka） | Crenarchaeol (μg/g) | Isoprenoid GDGTs (μg/g) | Branched GDGTs (μg/g) | CBT | MBT' | BIT | CBT -based pH | MBT'/CBT -based temperature (℃) |
|---|---|---|---|---|---|---|---|---|---|---|---|
| 64 13 | 79.815 | 79.8275 | 253.201 | 0.00 | 0.02 | 0.18 | 0.36 | 0.34 | 0.99 | 7.16 | 8.26 |
| 64 23 | 80.065 | 80.0775 | 253.984 | 0.27 | 1.32 | 8.13 | 0.26 | 0.30 | 0.95 | 7.37 | 7.77 |
| 65 3 | 80.480 | 80.4925 | 255.285 | 0.23 | 1.28 | 9.16 | 0.26 | 0.30 | 0.96 | 7.37 | 7.69 |
| 65 23 | 80.980 | 80.9925 | 256.853 | 0.18 | 0.77 | 6.34 | 0.28 | 0.33 | 0.96 | 7.32 | 8.45 |
| 65 31 | 81.180 | 81.1925 | 257.480 | 0.07 | 0.37 | 3.04 | 0.31 | 0.34 | 0.97 | 7.26 | 8.53 |
| 66 3 | 81.455 | 81.4675 | 258.342 | 0.14 | 0.76 | 4.76 | 0.36 | 0.32 | 0.96 | 7.16 | 7.79 |
| 66 23 | 81.955 | 81.9675 | 259.910 | 0.11 | 0.44 | 4.38 | 0.49 | 0.35 | 0.97 | 6.88 | 7.72 |
| 67 2 | 82.415 | 82.4275 | 261.352 | 0.12 | 0.45 | 4.78 | 0.44 | 0.33 | 0.97 | 6.98 | 7.35 |
| 67 22 | 82.915 | 82.9275 | 262.920 | 0.04 | 0.19 | 1.86 | 0.63 | 0.36 | 0.97 | 6.60 | 7.11 |
| 67 38 | 83.315 | 83.3275 | 264.174 | 0.03 | 0.18 | 1.68 | 0.76 | 0.40 | 0.98 | 6.32 | 7.43 |
| 68 27 | 84.050 | 84.0625 | 266.478 | 0.17 | 0.78 | 6.45 | 0.44 | 0.30 | 0.97 | 7.00 | 6.73 |
| 69 5 | 84.450 | 84.4625 | 267.732 | 0.19 | 0.69 | 6.40 | 0.51 | 0.32 | 0.96 | 6.85 | 6.93 |
| 69 25 | 84.950 | 84.9625 | 269.300 | 0.20 | 0.82 | 6.75 | 0.44 | 0.31 | 0.96 | 6.99 | 6.88 |
| 70 4 | 85.510 | 85.5225 | 271.055 | 0.31 | 1.17 | 9.55 | 0.44 | 0.33 | 0.96 | 6.99 | 7.40 |
| 70 24 | 86.010 | 86.0225 | 272.623 | 0.23 | 0.83 | 6.13 | 0.41 | 0.33 | 0.95 | 7.05 | 7.71 |
| 71 2 | 86.425 | 86.4375 | 273.924 | 0.18 | 0.74 | 6.37 | 0.41 | 0.30 | 0.96 | 7.04 | 6.80 |
| 71 8 | 86.575 | 86.5875 | 274.394 | 0.03 | 0.13 | 1.07 | 0.39 | 0.32 | 0.97 | 7.10 | 7.38 |
| 71 22 | 86.925 | 86.9375 | 275.492 | 0.35 | 1.86 | 10.25 | 0.35 | 0.33 | 0.95 | 7.17 | 7.84 |
| 72 2 | 87.425 | 87.4375 | 277.059 | 0.33 | 1.16 | 7.07 | 0.33 | 0.35 | 0.94 | 7.21 | 8.54 |
| 72 22 | 87.925 | 87.9375 | 278.627 | 0.31 | 1.02 | 6.03 | 0.33 | 0.38 | 0.93 | 7.23 | 9.36 |
| 73 9 | 88.370 | 88.3825 | 280.022 | 0.37 | 1.47 | 8.62 | 0.34 | 0.39 | 0.94 | 7.20 | 9.65 |